

UNCLASSIFIED

AD NUMBER

AD845570

LIMITATION CHANGES

TO:

Approved for public release; distribution is unlimited. Document partially illegible.

FROM:

Distribution authorized to DoD only;
Administrative/Operational Use; JAN 1968. Other requests shall be referred to Army Weapons Command, Attn: AMSWE, Rock Island, IL 61201. Document partially illegible.

AUTHORITY

USAARDC ltr, 23 Feb 1978

THIS PAGE IS UNCLASSIFIED

THIS REPORT HAS BEEN DELIMITED
AND CLEARED FOR PUBLIC RELEASE
UNDER DOD DIRECTIVE 5200.20 AND
NO RESTRICTIONS ARE IMPOSED UPON
ITS USE AND DISCLOSURE.

DISTRIBUTION STATEMENT A

APPROVED FOR PUBLIC RELEASE;
DISTRIBUTION UNLIMITED.



Corporation

FINAL REPORT

MODERN CASELESS RIFLE STUDY

CONTRACT NO. DAAF01-67-C-0724

Report No. EK-5188

Date: January, 1968

Prepared by: G. R. Christ

Approved by: H. A. Wilkening

STATEMENT #4 UNCLASSIFIED

This document is outside the Department of Defense must have prior approval of AAI AAI AAI

*Att: AAI 11/15/68
K. R. Wilkins 11/12/68*

**Best
Available
Copy**



Corporation



AAI 5.56 MM CASELESS RIFLE

1968-1970



TABLE OF CONTENTS

	<u>Page</u>
I. INTRODUCTION - - - - -	1.01
II. WEAPON CONCEPT - - - - -	2.01
A. General - - - - -	2.01
B. Action - - - - -	2.01
C. Breech Seal - - - - -	2.08
D. Extraction and Ejection - - - - -	2.08
E. Magazine - - - - -	2.08
F. Trigger Mechanism - - - - -	2.15
G. Stock, Sights, and Ancillary Equipment - - - - -	2.18
III. TEST RESULTS - - - - -	3.01
A. Description of Test Program - - - - -	3.01
B. Description of Test Results - - - - -	3.05
1. Sealing - - - - -	3.05
2. Ignition - - - - -	3.07
3. Rate-of-Fire - - - - -	3.12
4. Extraction and Ejection - - - - -	3.14
5. Erosion - - - - -	3.14
6. Cook-off - - - - -	3.15
7. Automatic Feeding - - - - -	3.15
C. Firing Records - - - - -	3.18
IV. HUMAN FACTORS ENGINEERING - - - - -	4.01
V. CONCLUSION - - - - -	5.01

TABLE OF CONTENTS (Cont'd)

	<u>Page</u>
Appendix "A" - - - - -	A.01
A. Interior Ballistics - - - - -	A.02
B. Chamber Heating - - - - -	A.09
C. Ammunition/Weapon Interface - - - - -	A.20
D. Cycle Analysis - - - - -	A.31
E. Stress Analysis - - - - -	A.44
F. Weight Analysis - - - - -	A.66

LIST OF ILLUSTRATIONS AND TABLES

<u>Figure</u>		<u>Page</u>
2-1	Assembly Drawing	2.02
2-2	Assembled Test Fixture	2.03
2-3	Artist's Concept of Caseless Rifle	2.04
2-4	Specifications for AAI Caseless Rifle	2.05
2-5	Firing Sequence	2.06
2-6	Sequence of Operation	2.07
2-7	Bolt and Firing Pin Seals	2.09
2-8	Assembled Bolt, Firing Pin and Seals	2.10
2-9	Disassembled Bolt, Firing Pin and Seals	2.11
2-10	Compressed Air Extractor	2.12
2-11	Compressed Air Extractor	2.13
2-12	20-Round Magazine	2.14
2-13	Magazine Concepts	2.16
2-14	Trigger Mechanism	2.17
2-15	SPIW Stock	2.19
2-16	Rifle Sight	2.20
2-17	Bipod	2.22
3-1	Disassembled Test Fixture	3.02
3-2	Cartridge Assembly	3.03
3-3	"Mann" Barrel	3.04
3-4	Tapered Bolt Seal	3.06
3-5	Actual Firing Pin Time-Displacement Curve	3.13
3-6	Magazine	3.17
4-1	Firing Mock-up, Prone Position	4.02
4-2	Firing Mock-up, Standing Position	4.03
A-1	Theoretical Effect of Adding WC Blank Propellant	A.07
A-2	Actual Result of Adding WC Blank Propellant	A.08
A-3	Chamber Temperature vs. Heat Sink Weight	A.18



Corporation

LIST OF ILLUSTRATIONS AND TABLES (Cont'd)

<u>Figure</u>		<u>Page</u>
A-4	Firing Pin Obturator	A.21
A-5	Typical Pressure-Time Curve	A.32
A-6	Displacement-Time Curve	A.41
A-7	Rate vs Firing Pin Weight	A.43
A-8	Gun Barrel Stress Level	A.61
A-9	Center of Gravity of Weapon	A.67

<u>Table</u>		
3-1	Effect of Firing Pin Variation on Ignition	3.09
3-2	Cook-off Temperature Determination	3.16
3-3	Firing Records	3.19
A-1	Computer Program - Interior Ballistic St'd Round	A.03
A-2	Computer Program - Interior Ballistics Modified Rd.	A.05
A-3	Firing Pin Obturator Analysis	A.20
A-4	Obturator Seal Computer Run	A.23
A-5	Firing Pin Time vs Displacement	A.34
A-6	Firing Pin Time vs Displacement	A.40
A-7	Weight Analysis	A.66



Corporation

I. INTRODUCTION

This report has been prepared in accordance with the terms of Contract No. DAAF01-67-C-0724. The objective of the program has been the development of a concept for an individual shoulder fired weapon capable of firing 5.56mm molded caseless propellant cartridges. The weapon concept shall be light weight, gas operated, and possess a selective semi and full automatic fire capability.

The six month program running from 11 June 1967 through 30 November, 1967, consisted of a detailed engineering design and theoretical analysis; and the fabrication and testing of an experimental firing fixture. This program has demonstrated the feasibility of using the firing pin actuated mechanism as a simple and effective means of firing caseless ammunition. Presented herein is a comprehensive summary of all work performed during the course of the above mentioned contract.



II. WEAPON CONCEPT

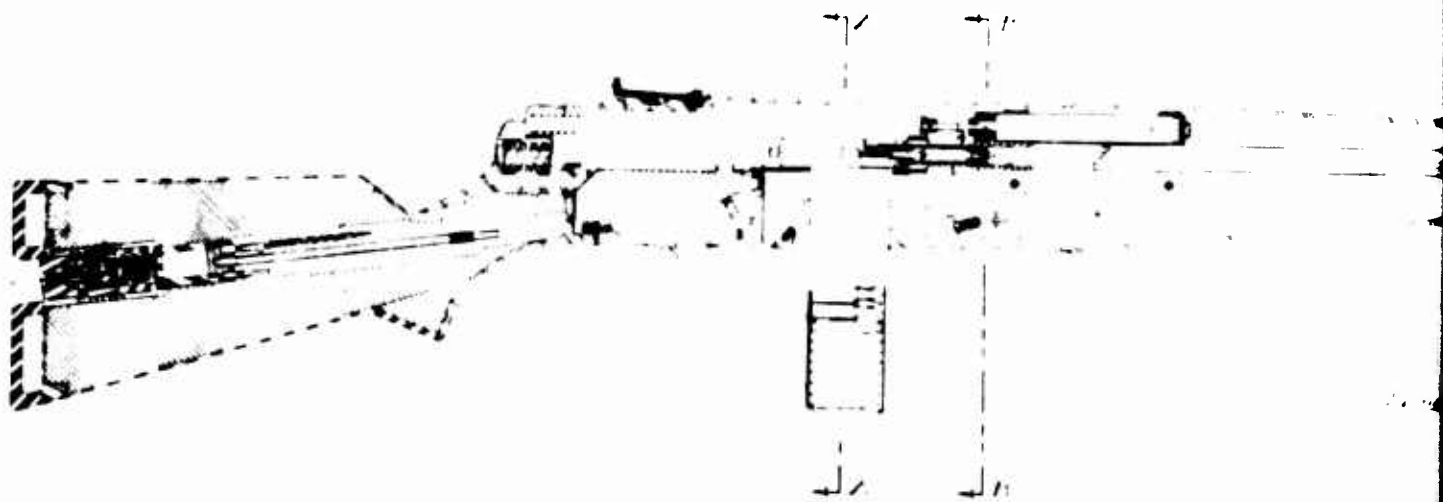
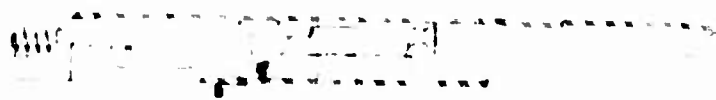
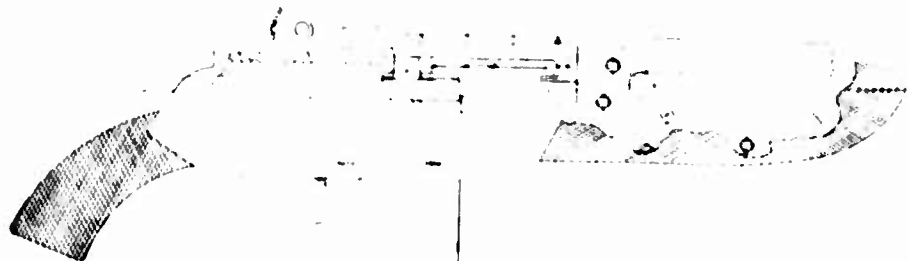
A. General

The final concept for the 5.56mm caseless rifle as developed by AAI under the present contract is shown on the assembly drawing, page 2.02. The firing fixture which was designed, fabricated and tested during the program is exactly as shown in this drawing with the exception of the stock and auxiliary equipment. A photograph of the test fixture is shown on page 2.03. An exterior view of the weapon can be seen in the artist's concept on page 2.04.

A table of specifications is included on page 2.05. This table summarizes the characteristics of the caseless rifle.

B. Action

The basic operating mechanism for this weapon has been designated as firing pin actuated. This means that the firing pin receives its energy directly from the chamber gases and acts as a bolt carrier to cycle the weapon. The weapon fires from the closed bolt position. Figure 2-5 is a schematic representation of the actual firing cycle. A photograph of this cycle is shown in Figure 2-6, page 2.07. The round is fired by the impact of the firing pin on the primer. The gas pressure acts on the face of the firing pin, accelerating it rearward, as the projectile moves down the barrel. The firing pin then cams the bolt to the unlocked position, the chamber pressure having had time to recede, and carries it rearward to the buffer. On the forward stroke, by the action of the drive spring, the next round is fed, the bolt is locked, and the chamber sealed, as the firing pin returns to the seared position.





ASSEMBLY DRAWING
FIGURE 2-1

2.02



ASSEMBLED TEST FIXTURE
FIGURE 2-2



AAI 5.56 MM CASELESS RIFLE

AAI 5.56 MM CASELESS RIFLE



SPECIFICATIONS FOR AAI CASELESS RIFLE

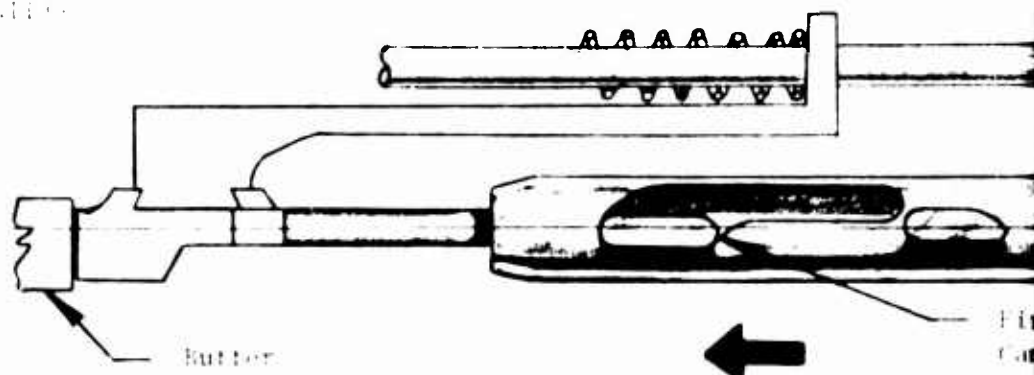
Weight Unloaded with Sling	5.72 lbs.
Weight Loaded with 20 Rounds	5.96 lbs.
Overall Length	40 in.
Barrel Length	20 in.
Rate of Fire	750 rds/min
Modes of Operation	Semiautomatic Full Automatic optional: 3-Round Burst
Caliber	5.56mm
Muzzle Velocity	3250 ft/sec
Method of Operation	Firing Pin Actuation
Firing Method	Closed Bolt
Chamber Cooling	.6 lb. Alum. Heat Sink
Extraction	Compressed Air
Rounds to "Cook-Off" Level (at 750 rds/min)	530

Figure 2-4

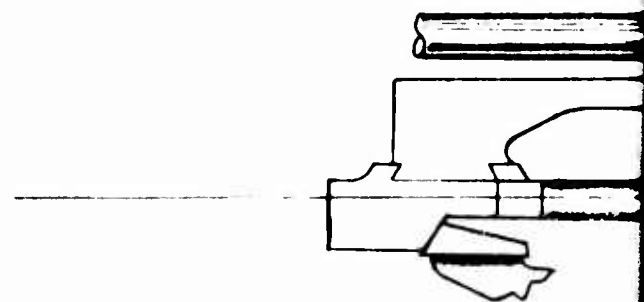
1. Bolt locked, firing pin hits primer, ignites round, and is accelerated rearward by gas pressure as projectile moves down barrel.

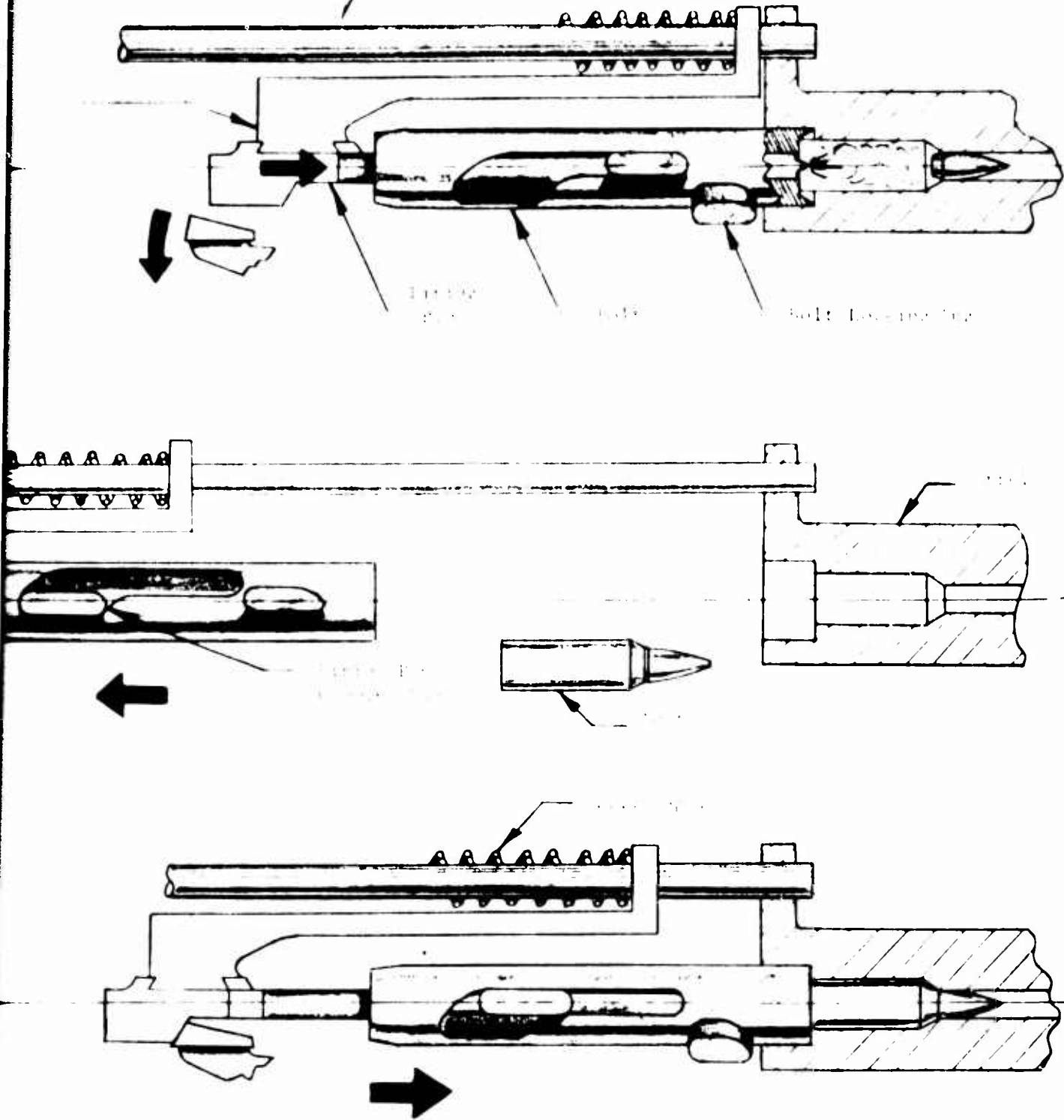
Slide

2. Bolt moves to unlocked position by firing pin, bolt recoils rearward to buffer with firing pin and slide.



3. Drive spring returns firing pin to seared position chambering next round and relocking bolt.





FIRING SEQUENCE
FIGURE 2-5



Corporation



1. FIRING PIN IN SEARED POSITION



2. FIRING PIN IN BATTERY POSITION



3. FIRING PIN UNLOCKING BOLT



4. FIRING PIN AND BOLT AT BUFFER POSITION

SEQUENCE OF OPERATION
FIGURE 2-6

C. Breech Seal

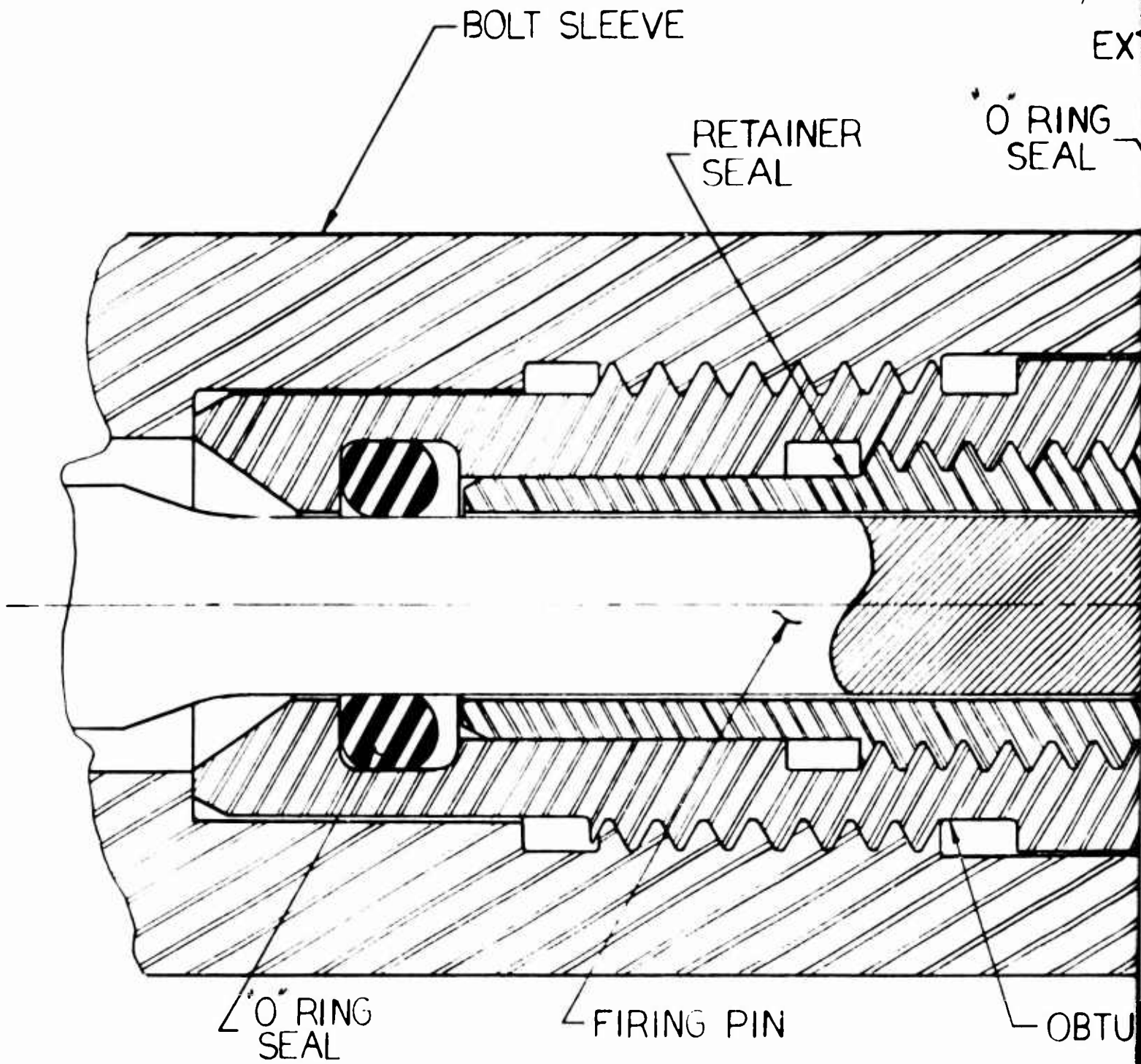
The bolt and firing pin seals developed by AAI have been completely successful in sealing off the chamber during the firing cycle. The drawing on page 2.09, Figure 2-7, shows an enlarged view of the breech sealing mechanism used on the test fixture. A complete theoretical analysis of the mechanics of obturation of these seals is presented in Appendix "A". The basic principle used here is to have a metal obturating surface act as the high pressure seal, followed by a backup "O" ring type seal to block lower pressure gases that may escape the initial seal prior to complete obturation. The actual bolt, firing pin, and seals in use on the test fixture are shown in Figures 2-8 and 2-9 on page 2.10 and 2.11.

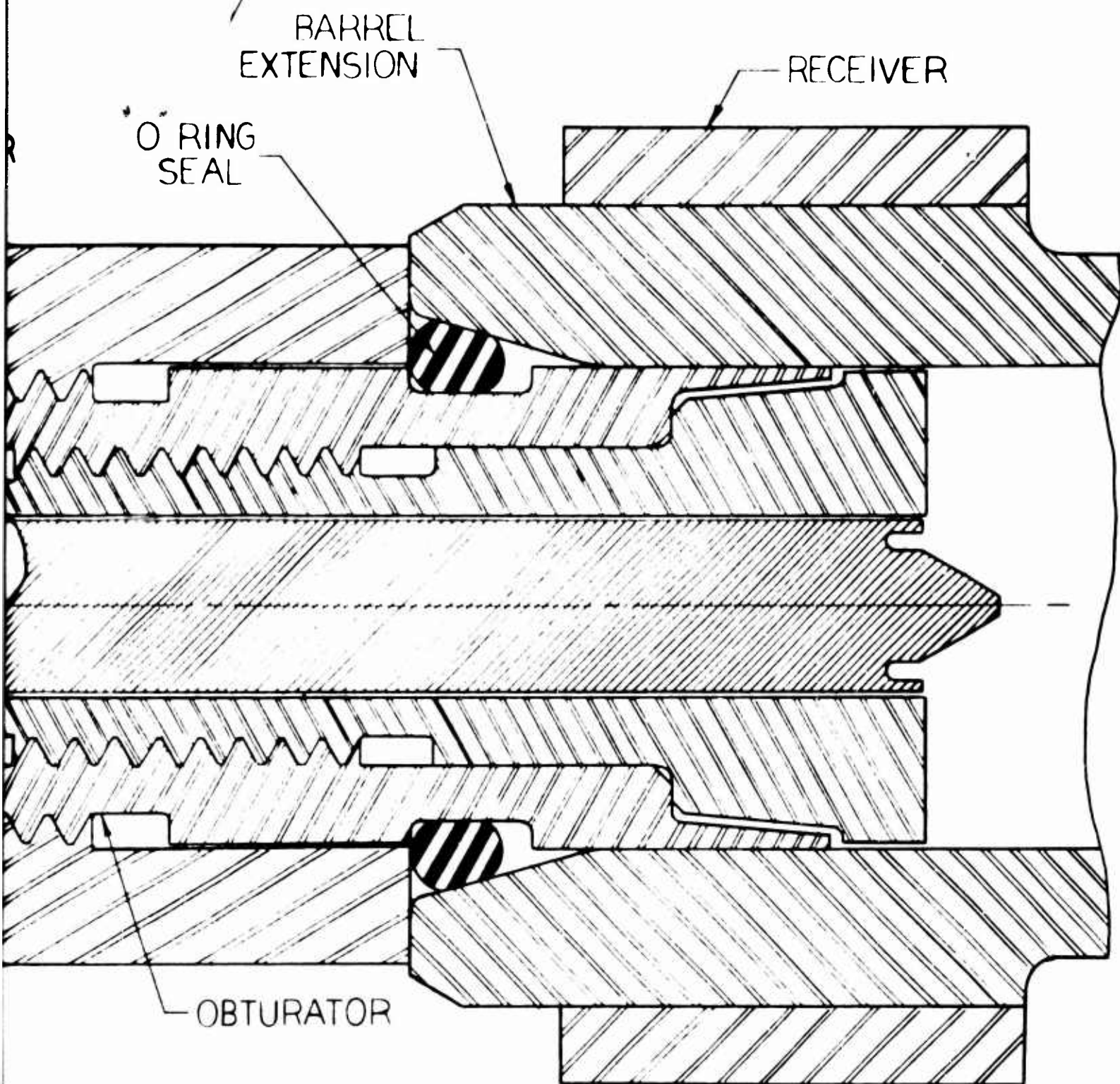
D. Extraction and Ejection

The extractor concept investigated during the recently completed program is shown in Figure 2-10. This device uses pressurized air to force the chambered round out of the barrel into the ejector tray. A photograph of the actual components is shown on page 2.13. The mechanism is actuated by pulling the charging handle which is connected to the pump piston. As the charging handle is moved rearward, the bolt and firing pin move back and the ejector tray drops down. When the piston nears the end of its stroke, the valve is opened, allowing the compressed air to enter the chamber and force the cartridge into the ejector tray. When the charging handle is released, the bolt cams the ejector up throwing the cartridge out the ejection port.

E. Magazine

Figure 2-12 shows the design of a 20 round box type double row magazine. This magazine has a two-piece injection molded case and a molded



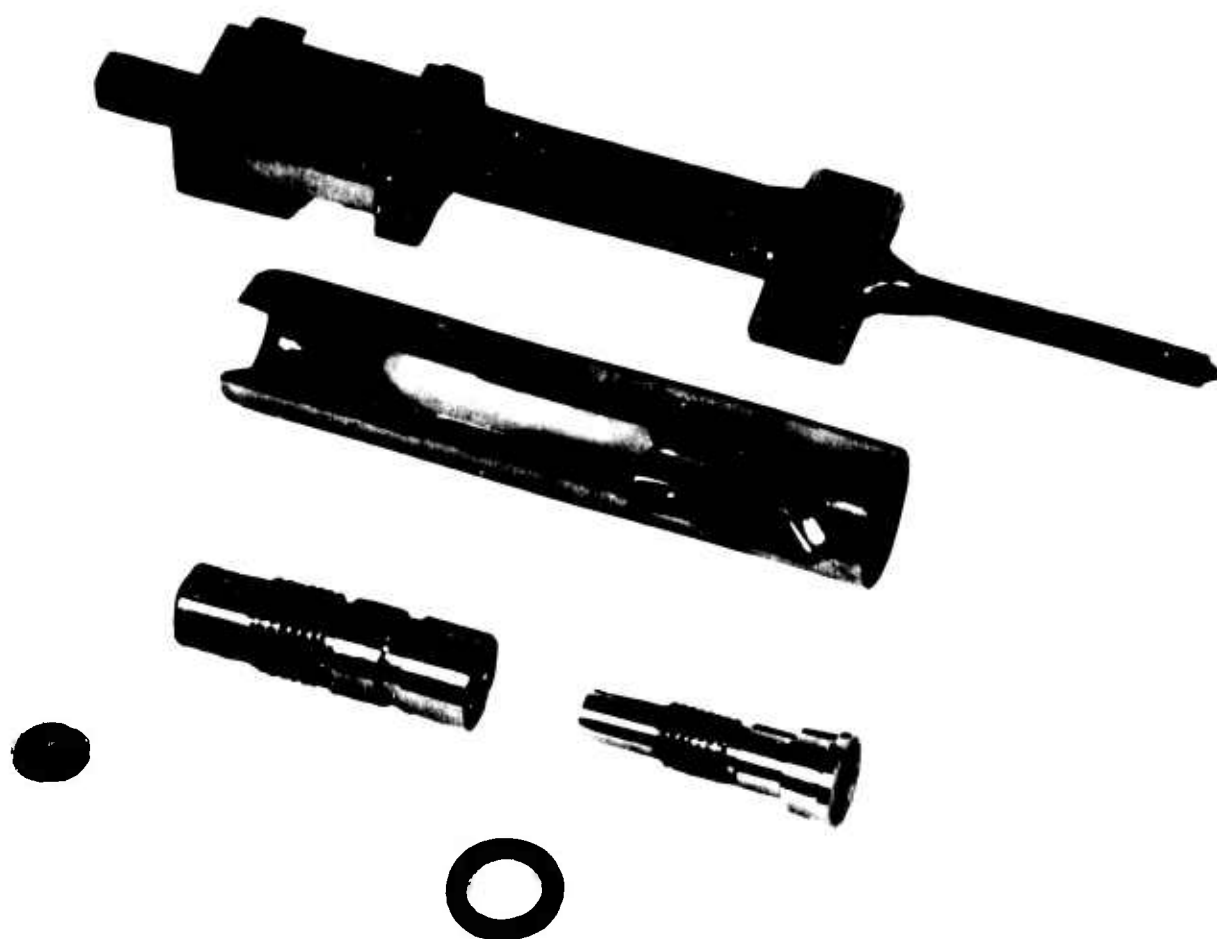


BOLT & FIRING PIN SEAL CONFIGURATION
FIGURE 2-7

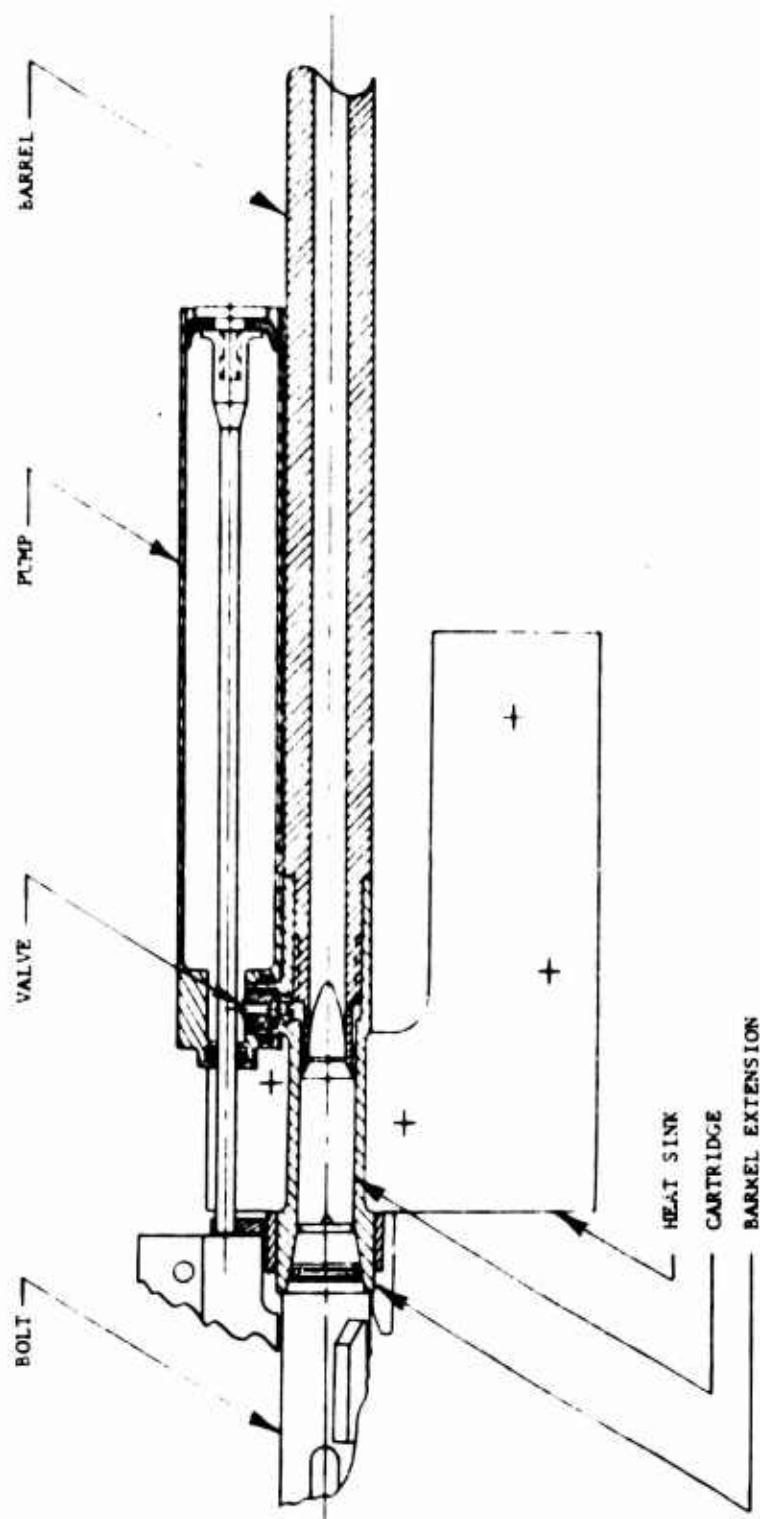
2.09



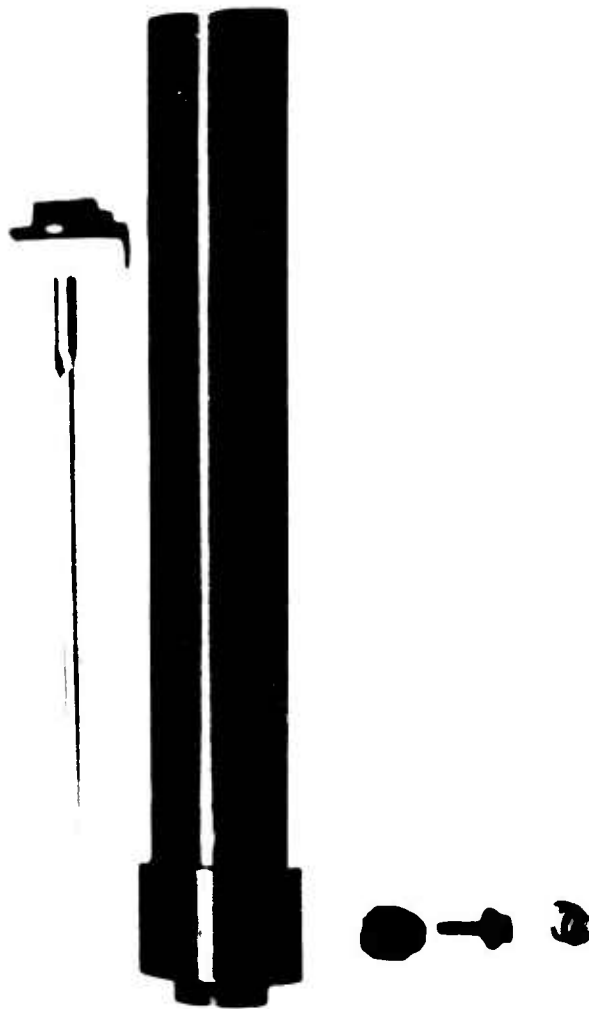
ASSEMBLED BOLT, FIRING PIN, AND SEALS
FIGURE 2-8



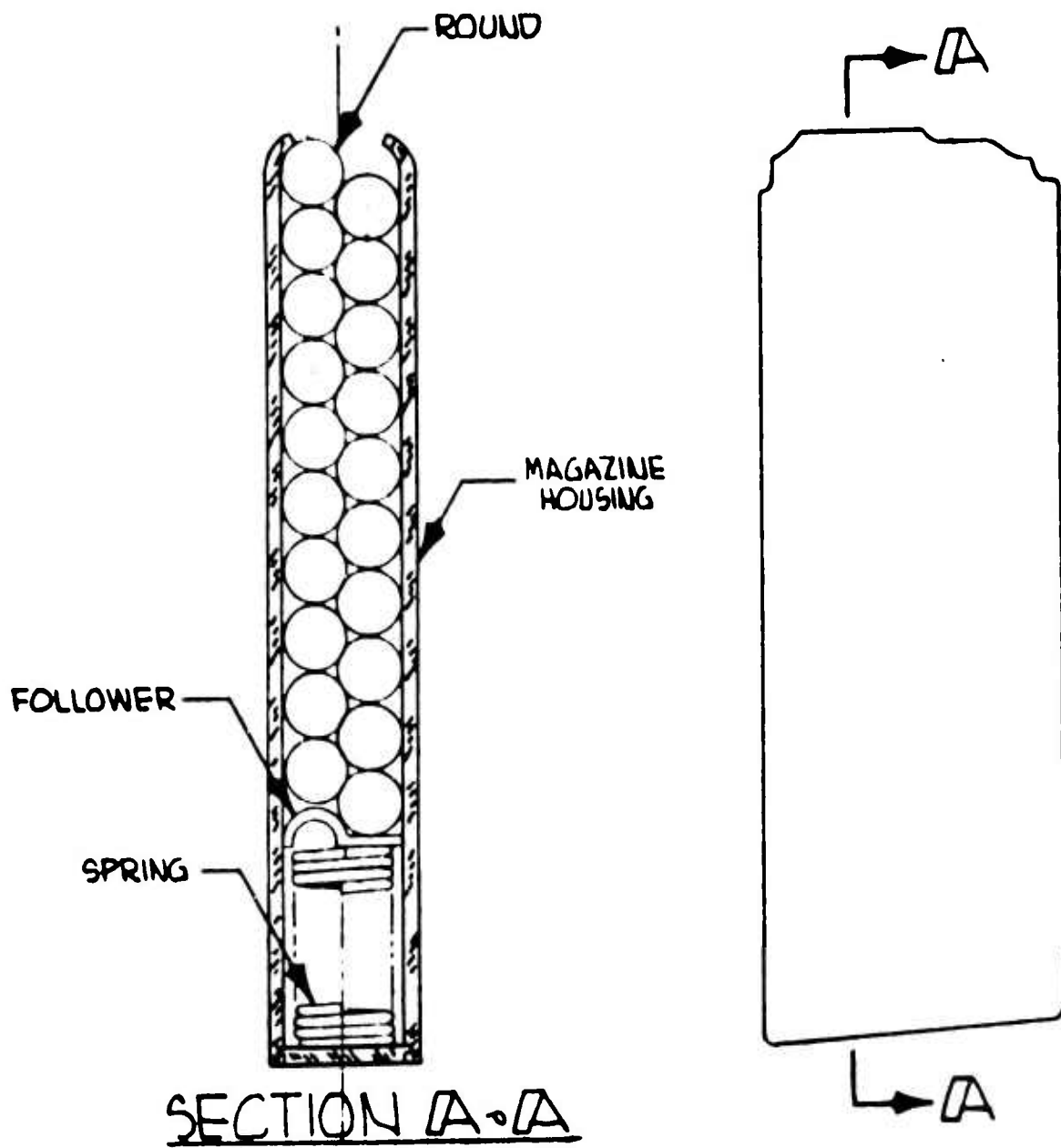
DISASSEMBLED BOLT, FIRING PIN, AND SEALS
FIGURE 2-9



COMPRESSED AIR EXTRACTOR
FIGURE 2-10



COMPRESSED AIR EXTRACTOR
FIGURE 2-11



20 ROUND MAGAZINE DESIGN
FIGURE 2-12

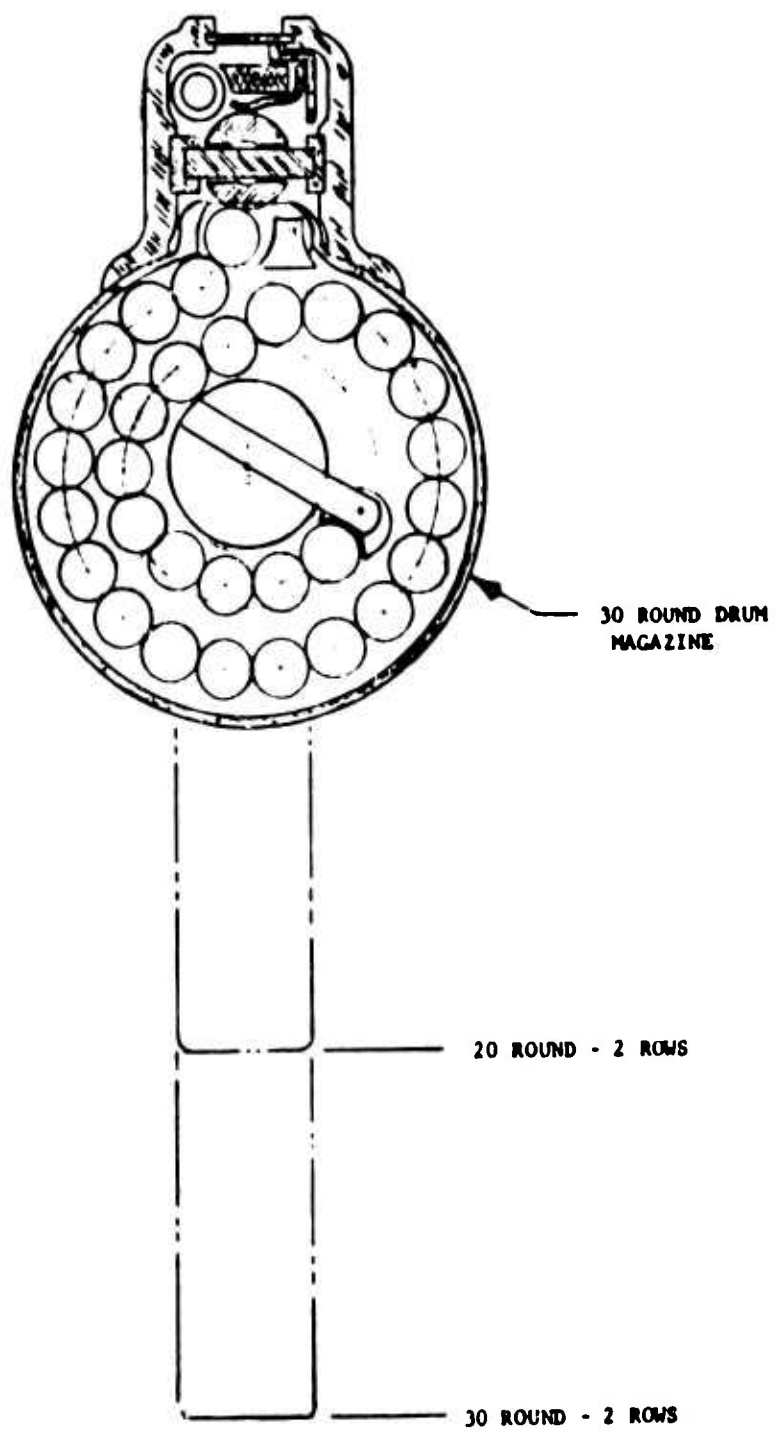
follower all made of glass-filled Nylon. The capacity could, of course, be increased by increasing the length of the magazine. Another way to increase the capacity to thirty or more rounds is by going to a drum type magazine as shown in Figure 2-13.

Actual magazine tests performed during the contract are described in Section III-B-7. These tests indicate the complete feasibility of feeding caseless cartridges at high rates from a conventional magazine of the type described above.

F. Trigger Mechanism

The trigger mechanism design is shown on page 2.17. The mechanism is housed in a molded plastic case which could be fitted with rubber seals to render it air tight. The module design of the trigger mechanism makes replacement of the unit a simple operation. A projecting lug on the stock picks up a groove at the lower left corner of the trigger mechanism about which it is pivoted into place. The sear pin is then inserted through the receiver to lock the unit in place.

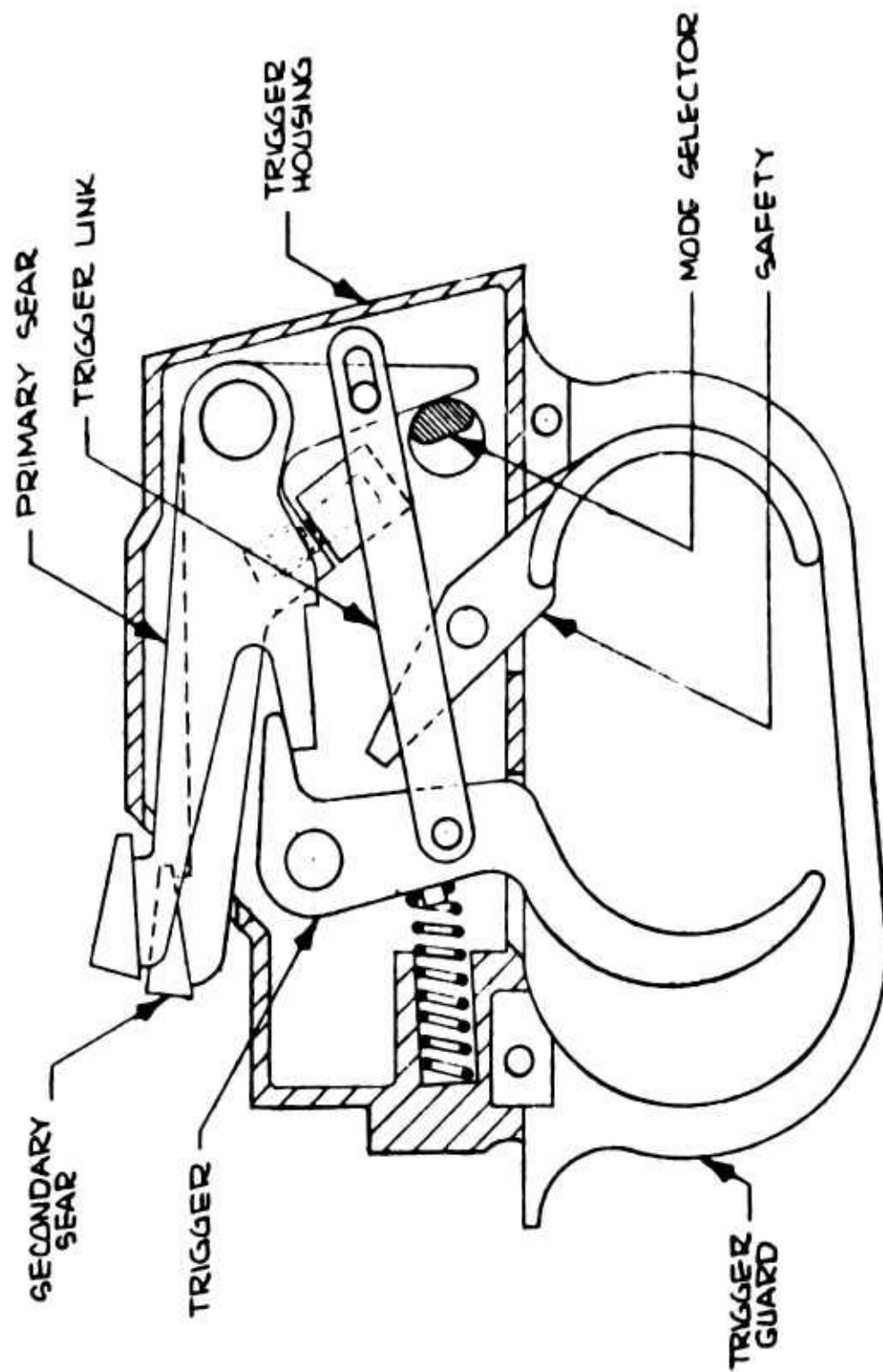
The operation of the trigger mechanism is as follows (Refer to the drawing). With the Mode Selector in the position shown, the mechanism is set for full automatic fire. The Secondary Sear is cammed down so that the Trigger operates the Primary Sear only, and the weapon fires as long as the Trigger is pulled. A ninety degree rotation of the Mode Selector will disengage the Secondary Sear and place the mechanism in the semiautomatic position. Now when the trigger is pulled, the Primary Sear is lowered and the Firing Pin is released to fire the weapon as before; however, at the same time, the



MAGAZINE CONCEPTS
FIGURE 2-13



Corporation



TRIGGER MECHANISM DESIGN
FIGURE 2-14

Secondary Sear is allowed to rotate up, by virtue of the Trigger Link, and retain the Firing Pin after one cycle until the Trigger is released. Releasing the Trigger causes an interchange of sears and resets the mechanism. The Safety is off as shown in the diagram. Clockwise rotation moves the Safety into a position beneath the Primary Sear providing a positive block to prevent inadvertent firing. With the Safety on, the projecting arm blocks the finger area of the trigger providing an easily identifiable means of determining that the gun is in the safe position.

The trigger mechanism on the actual test fixture was made from existing parts and is capable of full automatic operation only.

G. Stock, Sights, and Ancillary Equipment

1. Stock

The weapon concept makes use of the one-piece injection molded stock and foregrip design of the type used on the SPIW Weapon. The stock and foregrip configuration is shown on the assembly drawing on page 2.02. The material is 40% glass-filled Nylon. The stock also serves as a receiver cover, barrel jacket, spare parts kit retainer, and rear sight housing. The photograph on Page 2.19 shows the SPIW stock as it comes from the molder.

2. Sights

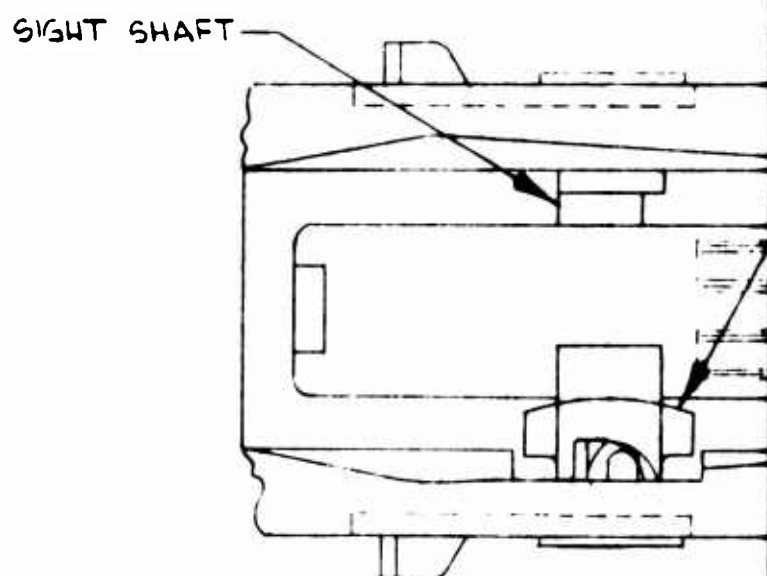
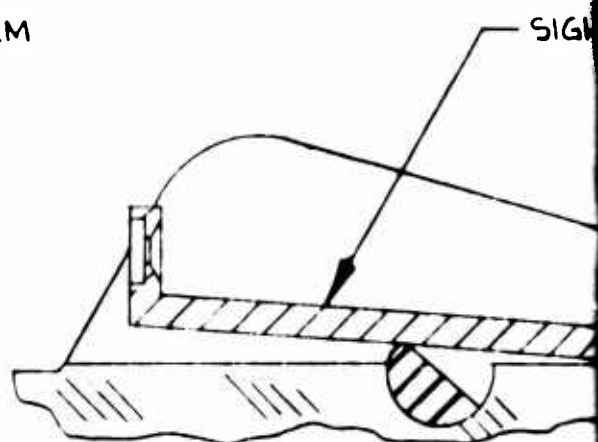
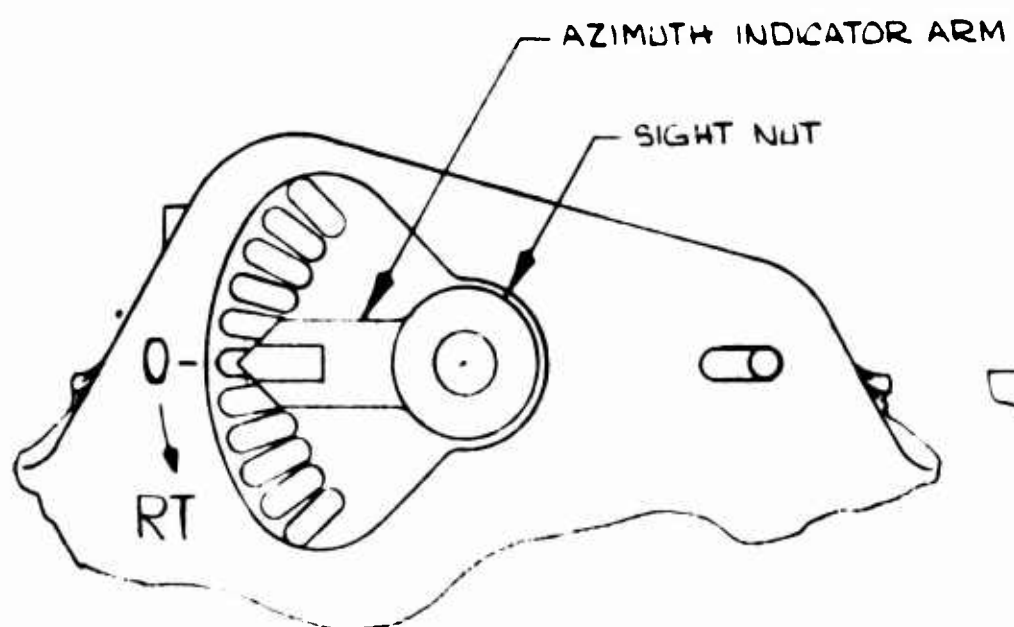
The rear sight design is again, in concept, very similar to the SPIW sight. The adjustment allowed for is a total of $3/8$ inch (15 mils) movement of the aperture for elevation and $1/4$ inch (10 mils) movement azimuth correction. The drawing on page 2.20 shows this concept. The housing is molded as part of the stock, as shown, with detents and graduations included



Corporation

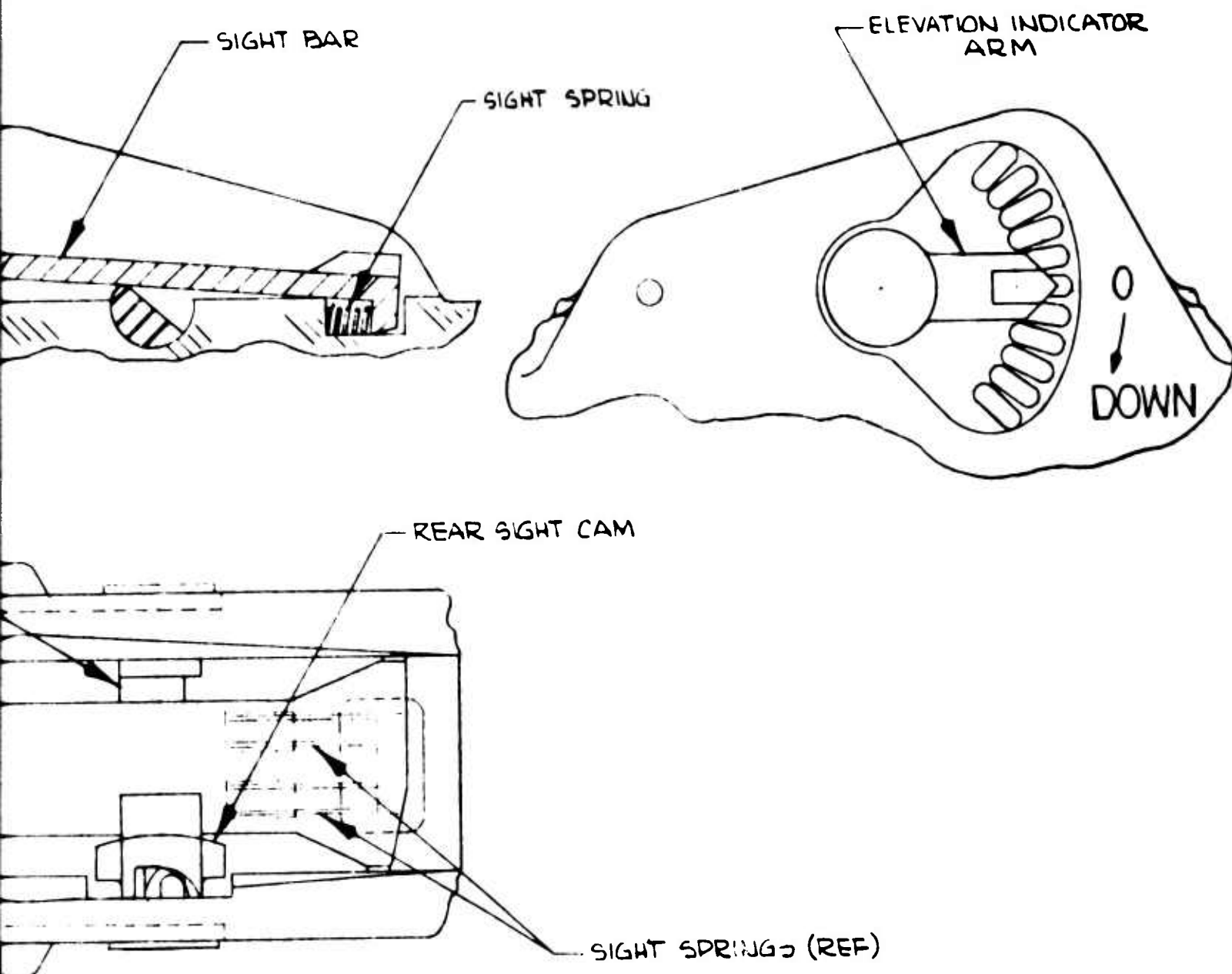


SPIW STOCK
FIGURE 2-15





Corporation



REAR SIGHT DESIGN
FIGURE 2-16

2.20

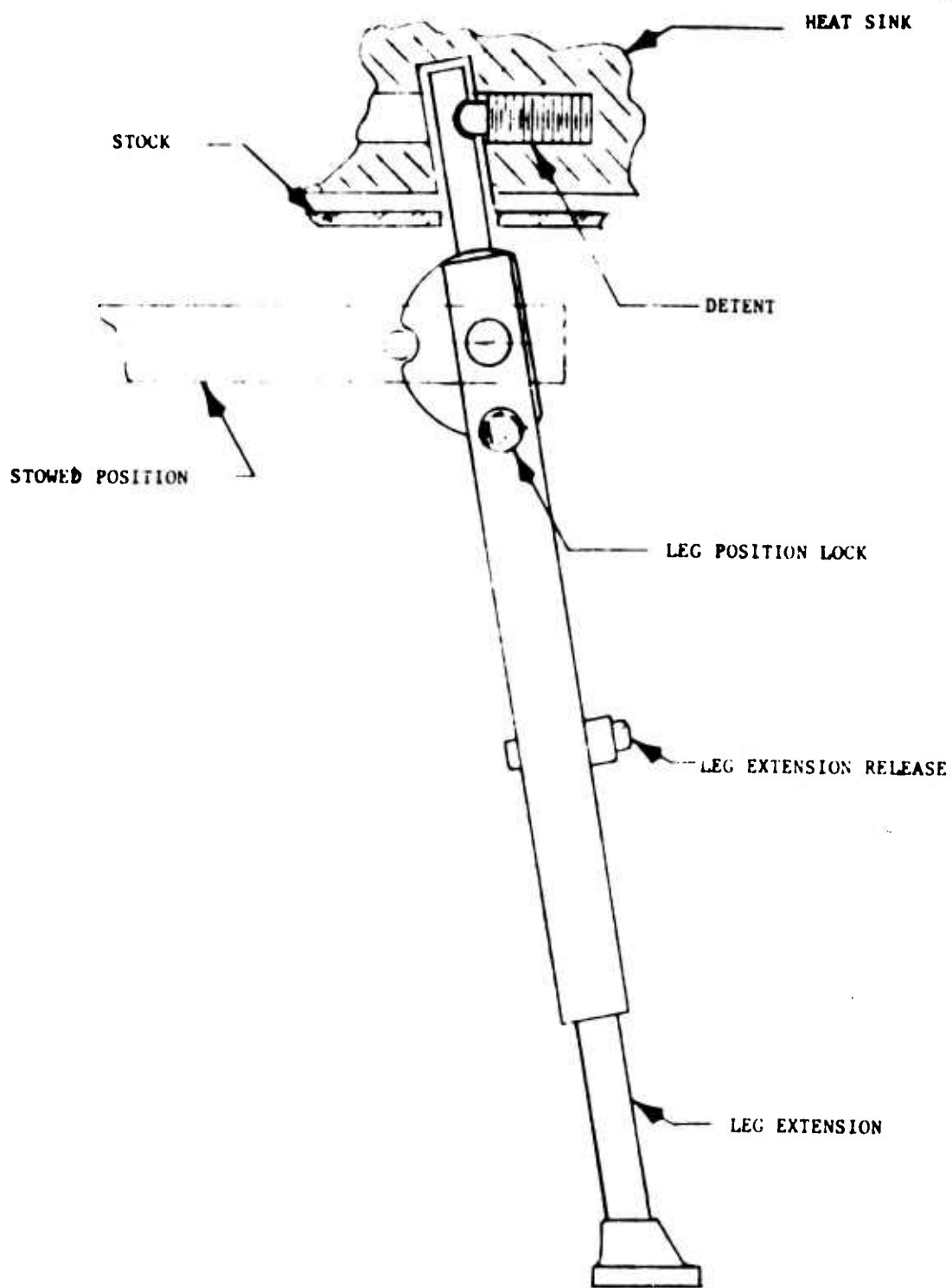


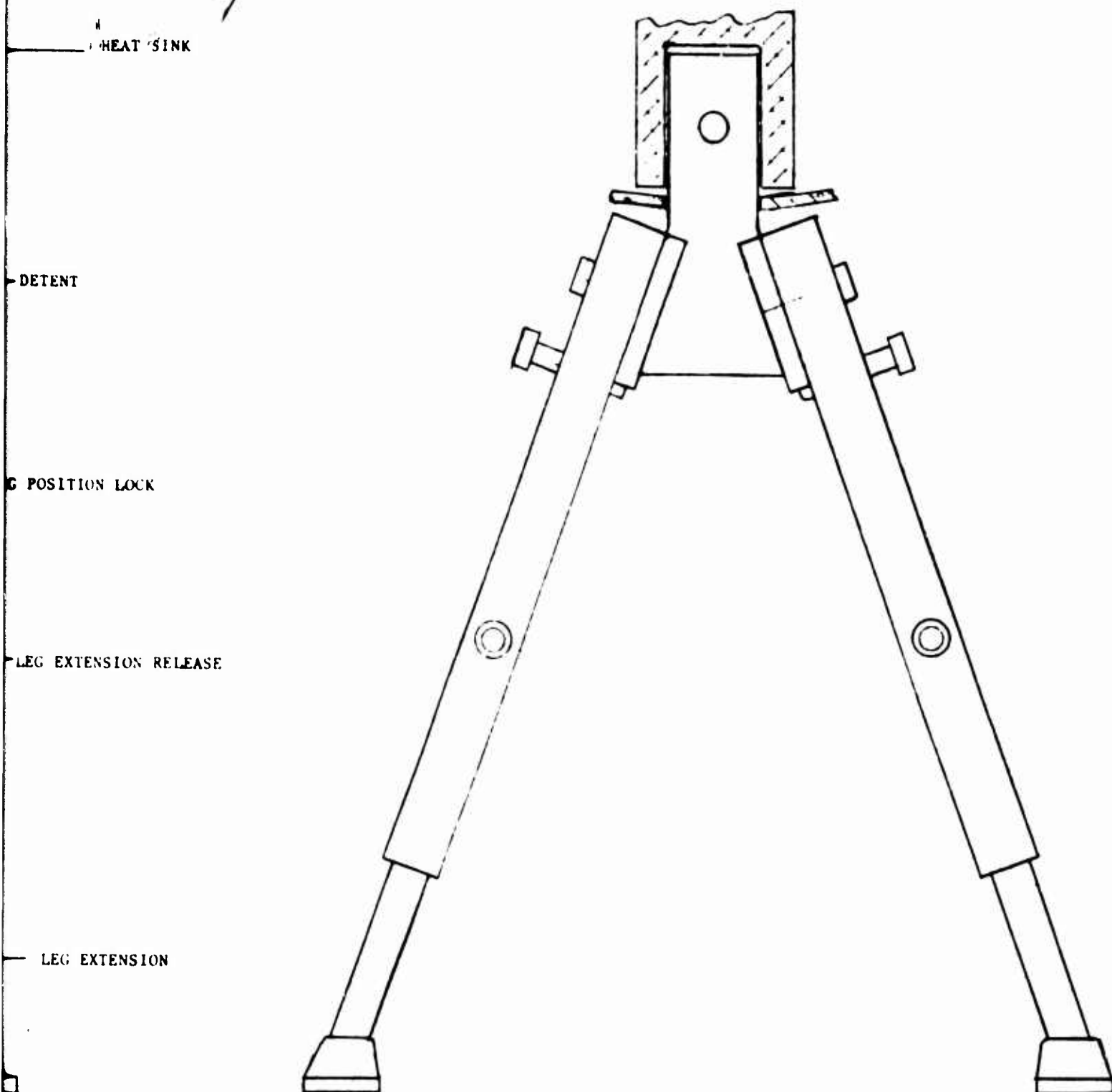
Corporation

in the mold. The low profile of the rear sight allows the front sight post to be kept at a minimum height which is advantageous with regard to handling characteristics and quick fire sighting (pointing). The adjustment is accomplished by the use of two detented levers - one on each side of the sight. They can be moved up or down, by hand, through one mil detented clicks that are easily distinguishable. There is a zero indicator and clearly marked adjustment direction. The operation is as follows. The sight bar is spring loaded against two cams. The Rear Sight Cam moves axially along the Sight Shaft when the Azimuth Indicator Arm is rotated. The cam in turn moves the Sight Bar to provide windage adjustment. The Elevation Indicator Arm is connected directly to the Sight Shaft and, when rotated, cams the Sight Bar in the vertical direction for elevation control. The Sight Nut is staked in place during assembly.

3. Bipod

The bipod mount has been located just forward of the magazine. The heat sink actually serves as the mounting bracket. The rearward location of the bipod has been chosen to eliminate the deterioration in accuracy, caused by the deflection of the barrel, that sometimes occurs when pressure is exerted on the butt stock of a rifle with the bipod mounted near the muzzle end. This location of the mounting bracket provides a solid foundation for the bipod and greatly reduces the magnitude of the bending moment that can be applied to the barrel. The proposed concept is shown in Figure 2-17. Installation is accomplished by simply sliding the projecting tab of the bipod into the detented slot in the heat sink. A means for folding the bipod into





BIPOD
FIGURE 2-17

2.22



a stowed position along the side of the gun as well as adjustment of the leg length is also provided.

4. Bayonet, Sling, and Cleaning Kit

The muzzle device is designed to accept the standard M-7 bayonet now in use by the Government. The sling is a conventional type with the swivel mount locations and method of installation being standard.

The cleaning and spare parts kit is housed in the hollow foam filled butt stock of the rifle. The proposed design is shown on the assembly drawing, page 2.02. The kit contains a cleaning rod, patches, a brush, a small oil container, and a small compartment for spare parts, such as replacement seals for the bolt and firing pin. The cleaning kit is installed by inserting it through a hole in the butt pad, pushing it in against a spring loaded sleeve, rotating it 90 degrees, and allowing it to snap into a recessed lock. To remove it, the process is reversed.

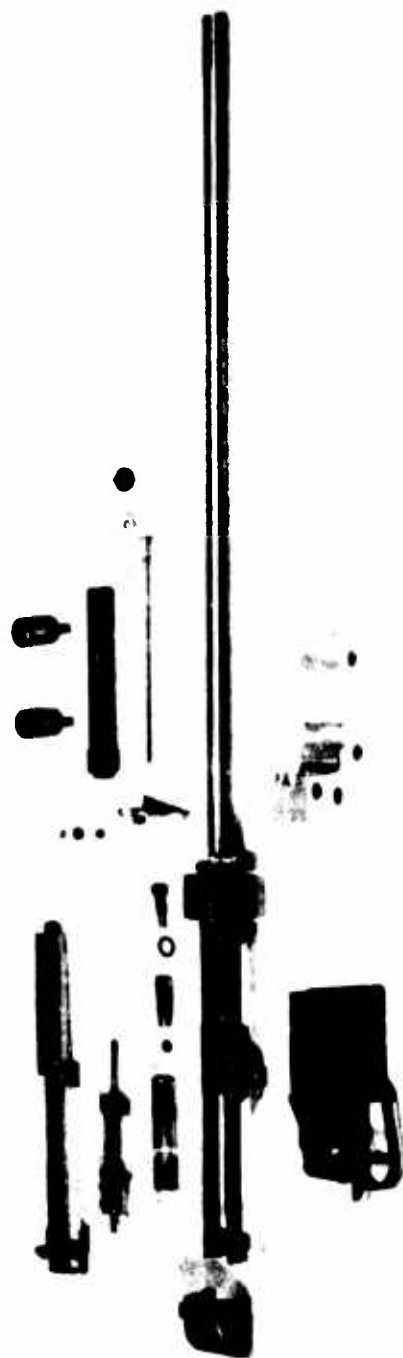


III. TEST RESULTS

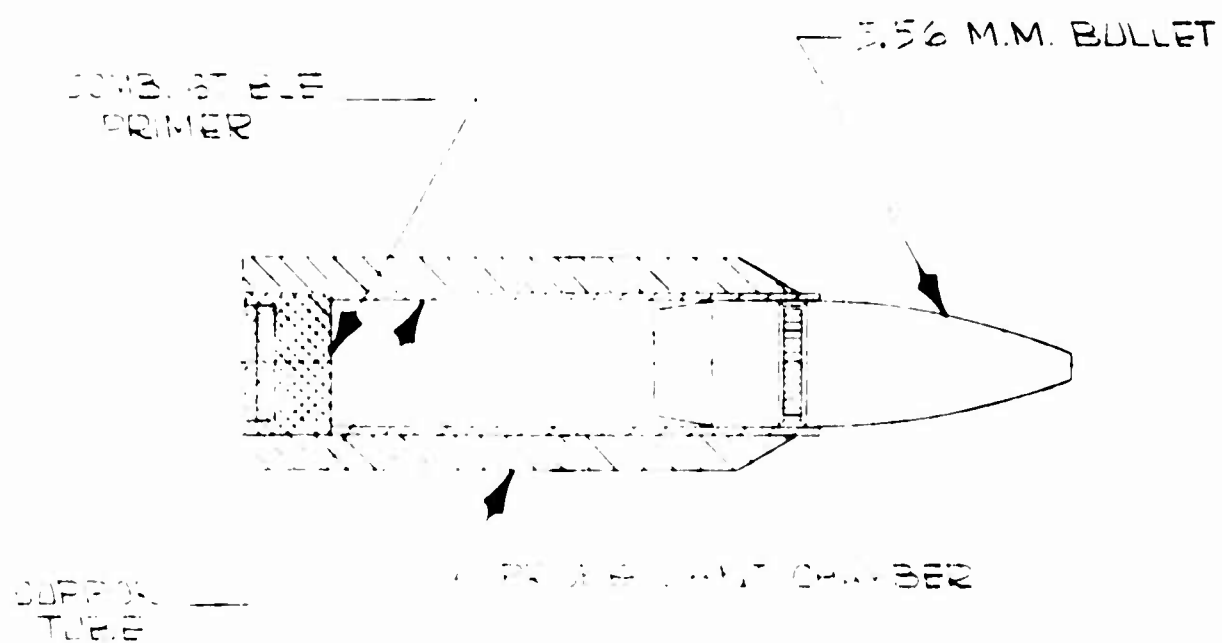
A. Description of Test Program

Early in the contract permission was granted for the fabrication of an experimental test firing fixture. The purpose of this test fixture was to determine the feasibility of the proposed caseless mechanism. It was hoped that information could be obtained on weapon function and performance. Such items as breech sealing, extraction and ejection, barrel heating and cook-off, and automatic feeding and chambering of rounds were to be investigated. A photograph of the assembled test fixture is shown in Figure 2-2 on page 2.03. A disassembled view is shown in Figure 3-1.

During the course of the contract, 103 rounds were expended in firing tests. The rounds tested were furnished as GFE by Frankford Arsenal (Page 3.03). Throughout the test program an unusually long ignition delay was noted on most shots. A great deal of the testing conducted was directed toward the determination of the cause for this delay. Very little testing was done in the areas of heat flow and cook-off level determination of the weapon due to the limited number of rounds available. Determination of the ammunition cook-off point was made. Throughout the tests high speed movies were taken of nearly every round. From the movies information on the breech seal effectiveness, weapon cyclic rate, feed mechanism, and firing pin velocity was obtained. Also recorded for each shot was the muzzle velocity. A "Mann" barrel was fabricated late in the program for the purpose of obtaining pressure-time data. This barrel is shown in Figure 3-3. The following section describes the tests performed and summarizes the results of these tests.



DISASSEMBLED TEST FIXTURE
FIGURE 3-1



CARTRIDGE ASSEMBLY
(TAKEN FROM FRANKFORD ARSENAL DWG FC14444)

FIGURE 3-2



"MANN" BARREL
FIGURE 3-3

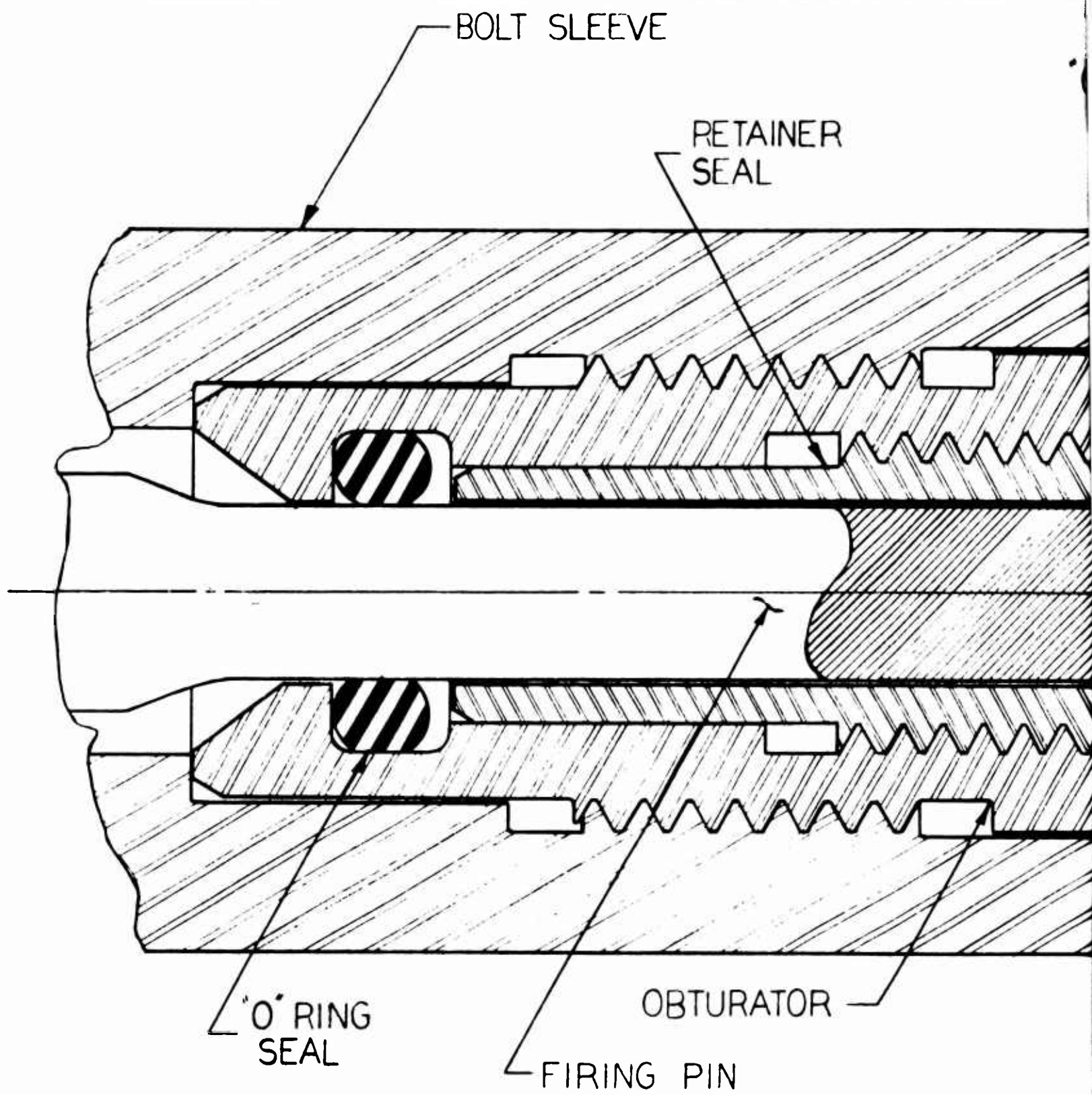
B. Description of Test Results

The test fixture design was based on calculations performed in Appendix "A". The initial shots were successful in that the mechanism cycled, the muzzle velocity was satisfactory, and no part failure occurred. Some of the difficulties encountered in the early testing included the following. The bolt seal allowed some gas leakage to occur, the cyclic rate was approximately 1500 rounds per minute - twice the specified rate, a misfire rate (in the early tests) of approximately 50% was experienced, and the rounds that fired showed an unusually long ignition delay as mentioned in Section A. The results of efforts made to correct these problems and other tests conducted are described below.

1. Breech Sealing

The bolt seal used in the first model consisted of a tapered obturating surface which mated with a similar surface on the barrel. This design is shown in Figure 3-4 , page 3.06. Some leakage occurred with this design, due mostly to the fact that rearward deflection of the bolt causes an increase in the obturator clearance. The tapered bolt seal was replaced with a cylindrical seal as shown in Figure 2-7 , page 2.09 . This new seal was successful in eliminating the gas leakage completely.

Experiments with the breech sealing mechanism showed that the metal obturator on the leading edge of the firing pin was not needed for sealing purposes. The long, thin expansion area between the bolt and firing pin was sufficient to reduce the pressure to a level capable of being sealed by the "O" ring. It was found, however, using this arrangement that noticeable





Corporation

O RING
SEAL

RECEIVER

BARREL
EXTENSION

BOLT & FIRING PIN SEAL CONFIGURATION
FIGURE 3-4

3.06



Corporation

erosion of the firing pin did occur within 30 rounds. It is therefore believed that the obturating surface may be needed for prevention of gas erosion. Evidence of gas erosion, to a much smaller degree, was noted also on the bolt obturator after 50-60 rounds. This is an area that will need further investigation in future tests. In addition, it is believed that subsequent effort needed in the chamber seal area should include optimization of the design to determine the simplest configuration that will do the job, and reliability and durability testing to increase part life.

2. Ignition

The ignition difficulties which were discovered early and continued throughout the testing received greater attention than any of the other problems. These difficulties can be placed in three categories.

- a. No ignition - primer does not fire.
- b. Primer only - primer ignites, primer cup breaks up, but propellant does not burn.
- c. Ignition delay - round ignites satisfactorily after a delay of varying length.

Of the total 103 rounds tested, 41 did not fire. Of the 41 that did not fire, only 9 had no primer ignition; the other 32 were found to have had complete primer burning and primer cup breakup with no propellant igni. Of the 62 rounds that fired, all exhibited an ignition delay ranging from 2.5 millisec to 400 millisec with the average estimated to be around 60 millisec. It should be noted that these values include the results obtained from tests of several firing pin tip configurations, various firing

pin velocities and energies, and varying chamber volumes; some of which displayed very poor ignition characteristics. It is believed that there is a definite relationship between the ignition delay and the rounds that have primer, but no propellant ignition; this relationship being that when the propellant fails to ignite, it is just an extreme case of the same condition that caused the long delay.

In an effort to eliminate the erratic ignition delay and reduce the misfire rate, the following items were tried.

- a. Variation of firing pin mass, velocity, protrusion, and tip configuration.
- b. Reduction of chamber volume.
- c. Addition of a hotter propellant, namely, WC Black, to hollow portion of cartridge ahead of the primer.
- d. Drying of the ammunition.

Table 3-1, page 3.09 shows the effect of firing pin and chamber volume variation on ignition. A review of the data shows that, in general, the misfire rate is improved by reducing the chamber volume. The chamber volume is now at the point, however, where it becomes somewhat impractical to decrease it any further. Increasing the firing pin velocity from 6.8 ft/sec to 10 ft/sec also appears to have reduced the number of misfires. Increasing the velocity any further than this does not seem to affect the ignition, however. The most efficient firing pin tip appears to be one with a .020 inch diameter flat, 60° included angle, and .065 to .070 inch protrusion.

The ignition delay that occurs on all shots that fire is not greatly effected by any of the modifications made. Of the four cartridges that

TABLE 3-1, EFFECT OF FIRING PIN VARIATION ON IGNITION

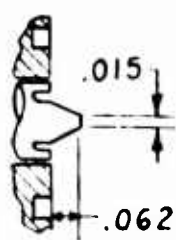
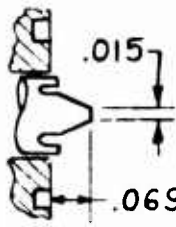
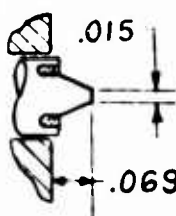


Firing Pin Configuration	Firing Pin Mass lbs.	Firing Pin Vel. fps	Rounds Tested	Ignition
	.42	6.8	8	4 - primer only 4 - OK - avg delay = 80 ms
		8.0	4	1 - no primer fire 2 - primer only 1 - OK delay = 100 ms
	.42	8.0	4	2 - primer only 2 - OK - avg delay = 80 ms
		10.0	3	2 - primer only 1 - OK delay = 100 ms
	.42	10.0	7	7 - OK - avg delay = 80 ms (range 7 ms to 174 ms)
	.42	10.0	5	1 - no primer fire 1 - fired when charged (slip sear) 1 - primer only 2 - OK, delays 108 ms, 271 ms
	.42	6.8	1	1 - no primer fire

TABLE 3-1 (Cont'd)

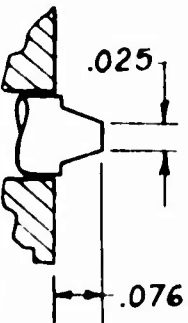
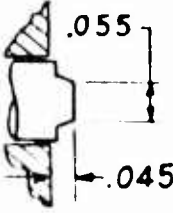
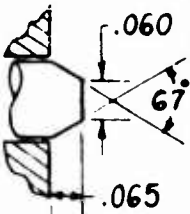
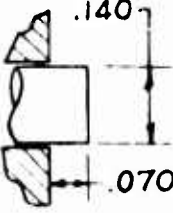
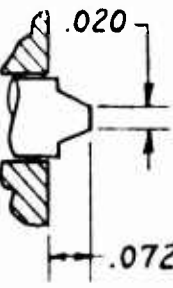
Firing Pin Configuration	Firing Pin Mass lbs.	Firing Pin Vel. fps	Rounds Tested	Ignition
	.42	6.8	1	1 - primer only
		10.0	3	3 - OK - delay = 12 ms, 8 ms, 25 ms
		25	5	1 - primer only 4 - OK - delay = 210 ms, 91 ms, 25 ms, 183 ms
	.33	10	4	1 - primer only 3 - OK - delay 18 ms, 133 ms
		25	6	1 - primer only 5 - OK delay = 15 ms, 18 ms, 11 ms, 8.3 ms
	.23	12	2	2 - OK - delay = 13 ms, 85 ms
		27	4	4 - OK - delay = 14 ms, 7 ms, 6 ms, 26 ms
	.33	7.5	8	2 - primer only 6 - OK - delay = 53 ms, 3 ms, 8 ms

TABLE 3-1 (Cont'd)

Firing Pin Configuration	Firing Pin Mass lbs.	Firing Pin Vel. fps	Rounds Tested	Ignition
	.33	7.5	5	1 - no primer fire 1 - primer only 3 - OK
ALL AMMUNITION DRIED OVER NIGHT AT 122°F				
	.33	8.2	9	2 - no primer fire 1 - primer only 6 - OK - delay = 10 ms, 61 ms, 400 ms, 83 ms
	.33	8.2	3	2 - no primer fire 1 - primer only
	.33	7.5	5	2 - primer only 3 - OK - delay = 86 ms, 20 ms, 6 ms
		.8 gr WC Blank Added	4	1 - no primer fire 1 - primer only 2 - OK - delay = 4 ms, 16 ms

were loaded with an extra charge of WC Blank; one had no primer fire, one had the primer fire only, and the other two fired with an average delay of 10 millisecc. This delay is well below the overall average, however, the small sample makes the results somewhat inconclusive.

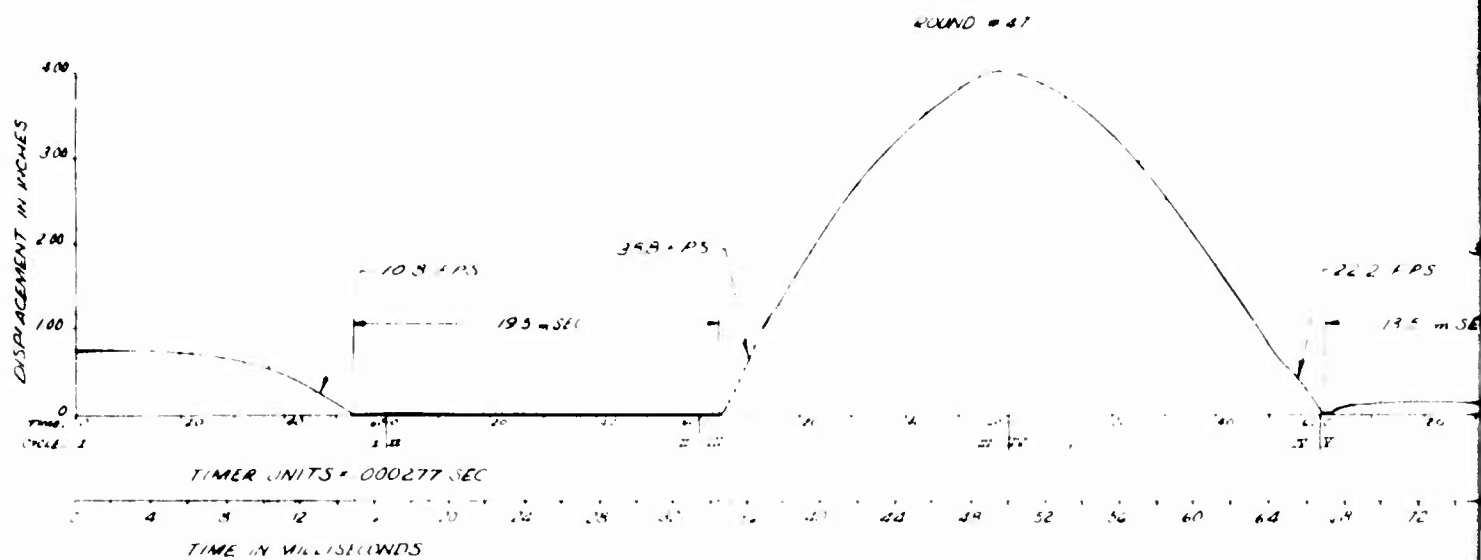
Drying the ammunition in an oven at 122°F for 12 hours produced no noticeable improvement in ignition.

Based on the above test results, it is concluded that the ignition problem lies primarily in the fact that the small size of the primer in the GFE ammunition makes it extremely sensitive to small chamber volume variations; and further, that in order to obtain reliable ignition, the chamber volume must be controlled to a point that is not practical in an automatic weapon of this type.

3. Rate of Fire

An actual time vs. Firing Pin Displacement curve for shots no. 47, 48, and 49 is included on page 3.13. This was a three round burst fired from a magazine. A high speed movie of this burst has been previously supplied to Rock Island and Frankford Arsenal. The cyclic rate of the weapon on this series of shots is approximately 1900 rds/min. This rate does not include the ignition delay. The slide has an added weight of .1 lb. If this weight is increased to .2 lb. the cyclic rate is decreased to less than 1500 rds/min. Removal of the weight altogether will increase the rate to over 2600 rds/min. Further adjustment of the rate can be accomplished by several means. Variation of firing pin mass, tip diameter, and stroke will regulate the recoil velocity of the firing pin and subsequently the cyclic rate.

3. STAND BLD. 1
 3.401 VOS 22.88, 2.19
 TIME DISPLACEMENT CURVE
 3.0 11.1 51 2 OCTOBER 1967



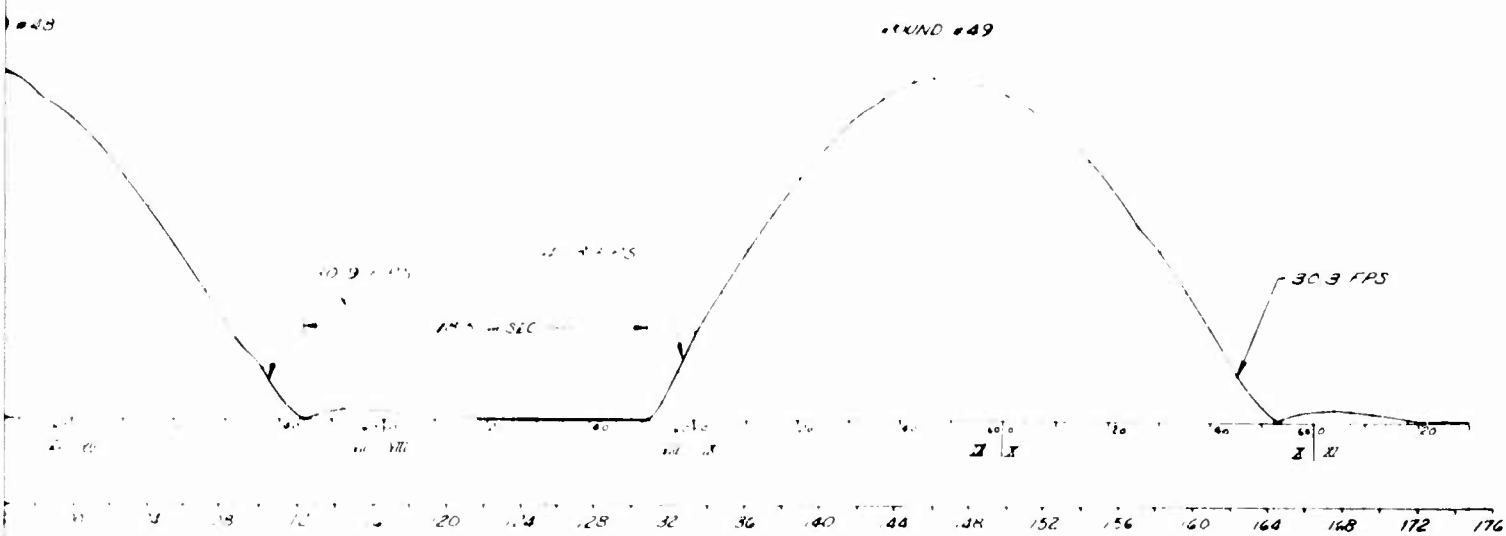


FIGURE 3-5

Other methods include the use of an energy absorbing buffer, or a mechanical low rate mechanism, and the variation of the length of the bolt cam tracks, which affect the bolt dwell time and determine the unlocking pressure. The contract specifies a cyclic rate of 790 rounds per minute. By using one or more of the above-mentioned means, this rate can be attained. If a high rate burst capability should be desired, this can also be accomplished.

4. Extraction and Ejection

The compressed air extractor is shown in Figure 2-10, page 2.12.

A working model was fabricated for use on the test fixture. A bolt operated ejector was also manufactured and installed on the test fixture. Tests conducted with this system have shown that the extractor-ejector combination is capable of clearing loose unfired cartridges from the weapon; however, there is not enough force available to extract a tightly jammed round. In order to improve the effectiveness of this system, a mechanism has been laid out which can be used with the existing design and may provide the force needed to extract tight rounds. This device is a cam for the nose of the round that offers an initial mechanical boost while it also blocks the bore ahead of the air inlet so that less air pressure is lost in the muzzle direction.

5. Erosion

The effects of gas erosion on the test fixture were most noticeable on the firing pin tip. This is discussed in Section 1. above. Since only 62 rounds were actually fired, and none of these were in sustained bursts, it would be expected that not too much erosion would occur. No noticeable barrel or chamber erosion was in evidence. It is believed that



this subject is one that will require extensive investigation on future programs.

6. Cook-Off

A theoretical analysis of the barrel heating and cook-off problems is presented in Appendix "A", Section B. No actual firing tests were conducted to substantiate this data, due mainly to the small number of rounds and the limited time available.

The test fixture was fitted with a .6 lb. aluminum heat sink and a thin walled 18% Nickel Maraging Steel chamber which had been established as the most efficient means of deterring cook-off according to the theoretical analysis. Firing tests showed that this arrangement was structurally sound.

The cook-off temperature of the 5.56mm Frankford Arsenal caseless ammunition was found to be between 300°F and 325°F. It was determined also that the primer cooks off at a temperature equal to or above that of the propellant. To determine the cook-off temperature, several rounds were separated into two pieces - one containing the primer and the other with no primer material. The test rounds were placed in a preheated oven and left there for 30 minutes or until they ignited. The chart on page 3.16 shows the ammunition cook-off test results.

7. Automatic Feed

A ten round single row box type magazine was fabricated in order that the feed system could be tested. The photograph on page 3.17 shows this magazine. A total of 22 rounds in three-round bursts were fed

Table 3-2 Cook-Off Temperature Determination

Test No.	Portion of Round Tested	Oven Temp. °F	Results
1	Propellant only	250	Did not ignite in 30 min.
2	Propellant only	300	Did not ignite in 30 min.
3	Propellant only	350	Ignited after 5 min. 11 sec.
4	Propellant only	350	Ignited after 3 min. 44 sec.
5	Propellant only	325	Ignited in < 30 min - time not recorded
6	Propellant only	325	Ignited after 9 min. 15 sec.
7	Propellant only	300	Did not ignite in 30 min.
8	Propellant & primer	300	Did not ignite in 30 min.
9	Propellant & primer	325	Ignited after 6 min. 56 sec.



Corporation



MAGAZINE
FIGURE 3-6

from the magazine in actual tests and at weapon cyclic rates varying from 1500 to 2600 rounds per minute. One damaged round occurred on a short cycle that caused a partial feed. These tests have indicated that the ammunition is sufficiently rugged to withstand the loads encountered in stripping and chambering at high rates of fire, and that the mechanism is capable of delivering the round from the magazine to the chamber.

C. Firing Records

This section presents a complete list of all shots fired from the AAI Caseless Test Fixture. All recorded data from each shot as well as observed results and modifications performed are included.



Corporation

TABLE 3-3
FIRING RECORDS

Shot No.	Date	Modification Made	Results			
			Firing Pin Vel. & Primer Impact Ft/Sec	Ignition	Muzzle Velocity Ft/Sec	Comments
1	9/7		6.4	71ms delay	3049	Weapon cycled, some bolt seal leakage
2	9/8	headspace decreased .010 in.		** primer only		
3	9/8			primer only		
4	9/8			70ms delay	2959	Cycle OK, some leakage
5	9/8	30% stiffer drive spg. installed to increase firing pin velocity		primer only		
6	9/8			70ms delay	2966	Cycle OK, some leakage
7	9/11			primer only		
8	9/11		7.3	130ms delay	2929	Cycle OK, some leakage
9	9/14			primer only		
10	9/14	Firing pin protrusion increased from .062 to .069		none		
11	9/14			primer only		
12	9/14			100ms delay	2907	Cycle OK. some leakage
13	9/14		8.6	83ms delay	2890	Some leakage
14	9/14	Heavier drive spring installed		81ms delay	2959	Some leakage
15	9/15		8.0	primer only		
16	9/15			primer only		
17	9/20		11.4	100ms delay	2793	Some leakage

TABLE 3-3 (Continued)

Shot No.	Date	Modification Made	Results			
			Firing Pin Vel. @ Primer Impact Ft/Sec	Ignition	Muzzle Velocity Ft/Sec	Comments
18	9/20		10.4	primer only		
19	9/20		10.0	primer only		
20	9/21		11.7	166ms delay	2976	No leakage
21	9/21	Tapered seal replaced with straight seal on bolt; Firing pin obturator filled in and chamber volume decreased		83ms delay	2941	No leakage
22	9/21			7ms delay	2857	No leakage
23	9/22			125ms delay	2857	
24	9/22			25ms delay	2924	
25	9/22			174ms delay	2890	
26	9/22			12ms delay	2907	
27	9/26	New Firing Pin tip - Short point, less volume		primer only		
28	9/26			none		
29	9/26			108ms delay	3012	
30	9/26			271ms delay	2976	
31	9/26			OK *		Round fired when charging (slipped sear?)
32	9/28	Firing pin tip squared off- less protrusion- light drive spring installed		none		
33	9/28			primer only		



Corporation

TABLE 3-3 (Continued)

Shot No.	Date	Modification Made	Results		
			Firing Pin Vel. Primer Impact Ft/Sec	Initiation	Muzzle Velocity Ft/Sec Comments
34	9/28	Heavy drive spring installed 2 rds in magazine - 1 round in chamber			
35	9/28				
36	9/28	1 rd. in chamber - 2 rds. in magazine			
37	9/28				
38	9/28	1 round in chamber - 2 rds. in magazine			
39	9/28				
40	9/28	1 of slide weight removed to increase firing pin velocity 3 rounds in magazine			
41	9/28				
42	9/28				
43	9/28				
44	9/28				
45	9/28				
46	9/28				

TABLE 3-3 (Cont'd)

Shot No.	Date	Modification Made	Results			
			Firing P.M. Tel. Primer Impact Pt. Sec.	Ignition	Muzzle Velocity Pt. Sec.	Comments
47	10/2	3 of slide weight removed, three rounds in Magazine	9.4	14 ms delay	2941	All Fed's Fired OK
48	10/2		10.0	14 ms delay		
49	10/2		10.0	14 ms delay		
50	10/2	3 rounds in Magazine	7.0	13.7 ms delay	2941	All Fed's Fired OK
51	10/2		10.0	14.0 ms delay		
52	10/2		10.0	14.1 ms delay		
53	10/4	All added weight removed from slide three rounds in Magazine	12.0	13.1 ms delay	2907	All Fed's Fired OK
54	10/4		10.0	26 ms delay		
55	10/4		10.0	5.6 ms delay		
56	10/4	three rounds in Magazine	4.0	85 ms delay	2907	All Fed's Fired OK
57	10/4		13.0	6.6 ms delay		
58	10/4		29.4	14 ms delay		
59	10/5	light drive spg. installed, 1 slide wt. installed		primer only		
60	10/5			OK*	2959	
61	10/5		7.0	4.3 ms delay	2994	
62	10/5		7.7	2.5 ms delay	-	
63	10/5		8.0	53 ms delay	2907	
64	10/5				2959	

TABLE 3-3 (Cont'd)

Shot No.	Date	Modification Made	Results			
			Priming Pin Set	Primer Ignition Pt. Set	Ignition Delay	Results
65	10/5	F.P. filed to a .055 flat			Primer only	
66	10/5				OK	29.1
67	10/5				OK	29.7
68	10/5				Primer only	
69	10/5				OK	29.1
70	10/5	New F.P. tip installed .006 flat by .065 protrusion. All ammunition dried from this point on.			none	
71	10/5				OK	29.1
72	10/20		5.1		9.1 ms delay	29.1
73	10/20		5.1		9.1 ms delay	29.1
74	10/20		5.1		9.1 ms delay	29.1
75	10/20	New F.P. tip installed blunt .140 dia., .070 protrusion "Q" ring replaced			OK	29.1
76	10/20				Primer only	
77	10/20				OK	29.1
78	10/20				none	
79	10/20				none	
80	10/20				5.1 ms delay	29.1
81	10/25				none	
82	10/25				none	

TABLE 3-3 (Cont'd)

Shot No.	Date	Modification Made	Results			
			Firing Pin Vel. Primer Impact Ft/Sec	Ignition	Muzzle Velocity Ft/Sec	Comments
83	10/25	New F.P. tip installed .020 flat, .072 protrusion		primer only		
84	10/25			primer only		
85	10/25		2.3	20 ms delay	1044	slight leak
86	10/25		2.3	20 ms delay	1044	
87	10/25			primer only		
88	10/25		2.2	4.8 ms delay	1044	slight leak
89	10/25		2.2	3.7 ms delay	1044	leakage
90	10/25			primer only		
91	10/25		4.2	16.0 ms delay	1044	leakage
92	10/25			none		
93	10/26		4.3	232 ms delay	2725	mult leakage - sparks visible from breech - "O" ring blown off.
94		solid plug used to replace obturator and retainer - "O" ring on bolt only		primer only		primer cup remained intact
95				primer only		
96				primer only		
97				primer only		

* OK - denotes only that round fired & delay was not measured.

** - primer cup broke up on all shots marked "primer only" unless noted in comments.



Corporation

Table 3-4 Mann Barrel Test Results

Shot No.	Ignition	Peak Chamber Pressure psi	Muzzle Velocity ft/sec	Comments
98	Primer only			
99	OK - 21.6 ms delay	53,535	2959	Some leakage - "O" Ring blown off
100	OK - 119 ms delay	43,860	2907	Some leakage - "O" Ring blown off
101	Primer only			
102	Primer only			
103	Primer only			



Corporation

IV. HUMAN FACTORS ENGINEERING

Human Engineering analyses were performed upon the test fixture design to insure that appropriate human engineering features will be incorporated in the developed weapon configuration. The weapon is capable of being fired comfortably from either shoulder. As shown in the photographs on pages 4.02 and 4.03, and based on tests performed with the mock-up, no problems are encountered when firing from the prone or standing positions.

Anticipated impulse noise and peak sound pressure level measurements were not taken due to the devotion of time and funds to some of the more immediate problems associated with caseless ammunition.



FIELD MODEL, 1904-1905
11.11.11



Corporation



FIGURE 1-2



V. CONCLUSIONS

The recently completed program as described in the body of this report, as the first step in the development of an automatic rifle capable of firing 5.56mm caseless cartridges, has produced the following accomplishments.

1. A detailed design has been prepared for a complete caseless weapon based on engineering analysis and actual test data.
2. Firing tests have proven the firing pin actuated mechanism to be a simple and effective means of firing caseless ammunition.
3. Effective breech seals have been fabricated and tested under automatic fire conditions.
4. Complete weapon cycles and good projectile muzzle velocity have been consistently achieved with the test fixture.
5. Feeding and chambering of caseless cartridges from a magazine under high rate automatic fire condition has been accomplished with no problems encountered in gun functioning or cartridge strength.

The feasibility of the caseless rifle concept has definitely been proven. Many problems still remain; some of these have shown up as a result of testing done on the present program. A partial list of items that should be included in future follow-on programs is presented below.

1. Establishment and improvement of barrel and bolt face heat transfer characteristics in relation to the associated cook-off problems.
2. Development and testing of a reliable extraction and ejection mechanism for removal of unfired cartridges.

3. Investigation of erosion problems that may arise in the chamber and breech sealing areas, especially when subjected to rapid fire tests.

4. Establishment and improvement of the reliability and durability level of all components with special emphasis on the breech seals, bolt face, firing pin, and chamber since these are the areas most likely to be affected by elevated temperatures and gas erosion.

5. Reduction of the cyclic rate of fire of the mechanism either by alteration of firing pin mass, stroke, and diameter; or by use of a low rate wheel. The latter is more desirable if a controlled burst mode of fire is to be considered.

One other area that is possibly in need of additional investigation is that of the cartridge ignition system. It is believed that the addition of an ignition booster or an increase in the size of the primer of the present 5.56mm Frankford Arsenal caseless cartridge would improve the reliability of ignition of the system.



Corporation

APPENDIX "A"

A.01

A. Interior Ballistics

Results from the Multiple Charge Interior Ballistic Computer Program developed at AAI showed that a 28 grain charge of IMR4895 was necessary to obtain a velocity of 3322 ft/sec in a 20 inch barrel.

A copy of the computer input data and results are included in this section. See Table A-1.

Also included are the results of the computer run for a standard round modified by adding .8 grains of WC Blank propellant. See Table A-2.

Figure A-1 is a theoretical comparison of the standard and modified round. Figure A-2 shows the experimental results of the two configurations fired at Frankford Arsenal. The actual and theoretical pressures differed by no more than 6%. The velocities for the standard round differed by 5%. Velocities for the modified round were not measured.



TABLE A-1

RUN556 MM NUMBER OF CHARGES 1 CONTRACT CASELESS AMMO

TABLE OF F VERSIIS Z

IMR 4895

0.000000000	1.000000000
0.100000000	0.923000000
0.200000000	0.835000000
0.300000000	0.740000000
0.400000000	0.654000000
0.500000000	0.556000000
0.600000000	0.454000000
0.700000000	0.347000000
0.800000000	0.236000000
0.900000000	0.120000000
1.000000000	0.000000000

CHAMBER VOLUME	VO =	0.097700000	(CU.IN.)
PROJECTILE BASE AREA	A =	0.039300000	(SQ.IN.)
PROJECTILE VELOCITY	VE =	0.000000000	(FT./SEC)
RESISTANCE FUNCTION ... $R = K1 + K2 \cdot X$			
	K1 =	0.000000000	
	K2 =	0.000000000	
RATIO OF SPECIFIC HEATS	GAMMA =	1.240000000	
PROJECTILE MASS	M =	0.000244000	(SLUGS)
STOP AT PROJECTILE TRAVEL	XEND =	29.999999999	(IN)
INITIAL CHAMBER PRESSURE	P =	1000.000000000	(PSI)
EXPONENT OF INIT CHMR PRESS	KP =	1.000000000	

C H A R G E N O. 1

IMR 4895

PROPELLANT IMPETUS	CF =	379999.999960000	(FT)
INITIAL CHARGE WEIGHT	C =	0.004000000	(LBS)
INITIAL TEMPERATURE	T =	5103.999999900	(DEG R)
PROPELLANT DENSITY	DELTA =	0.060000000	(LBS/CU.IN.)
BURNING RATE COEFF/WEB SIZE ..	BETA/U =	0.037000000	(IN/SEC/PSI/IN)
PHASE 1 TIME INCREMENT	DT1 =	0.000020000	(SEC)
PHASE 2 TIME INCREMENT	DT2 =	0.000020000	(SEC)

TABLE A-1 (Cont'd)

TIME (SEC)	PRESSURE (PSI)	VELOCITY (FT/SEC)	TRAVEL (IN)	TEMPERATURE (DEG F)	FORM FUNCTIONS
0.000000000	1000.1000	1.1700	0.1000	5100.0000	0.0000
0.000000000	4456.4866	2.7435	0.1010	5104.0000	0.0000
0.000000000	6944.7077	5.9761	0.1020	5108.0000	0.0000
0.000000000	10363.2725	14.4444	0.1030	5092.3236	0.0000
0.000000000	15012.4474	43.3442	0.1040	5076.3274	0.0000
0.000000000	21067.7444	104.7211	0.1050	5052.1444	0.0000
0.000000000	28416.7654	142.7434	0.1117	5010.2311	0.0000
0.000000000	36488.4402	241.7419	0.1190	4973.7121	0.0000
0.000000000	44338.4715	341.5415	0.1270	4919.1072	0.0000
0.000000000	50441.4813	443.5533	0.1344	4855.6362	0.0000
0.000000000	54994.4942	542.5684	0.1413	4786.5677	0.0000
0.000000000	57278.7913	744.4273	0.1486	4719.0387	0.0000
0.000000000	57464.4344	742.1419	0.1554	4641.9610	0.0000
0.000000000	56137.7444	1073.3492	1.2713	4570.4421	0.0000
0.000000000	54279.7444	1225.4205	1.2800	4501.8352	0.0000
0.000000000	51555.4010	1374.7532	1.2919	4435.9220	0.0000
0.000000000	48661.7654	1516.7087	2.3149	4373.4732	0.0000
0.000000000	45429.4777	1642.4977	2.7272	4313.1862	0.0000
0.000000000	42700.4474	1776.1354	3.1444	4256.1537	0.0000
0.000000000	39958.7044	1873.9101	3.5372	4203.4545	0.0000
0.000000000	37260.7644	2113.7074	4.1313	4152.4106	0.0000
0.000000000	34618.4240	2116.3924	4.5492	4104.5562	0.0000
0.000000000	32579.4054	2212.2431	5.1042	4059.6110	0.0000
0.000000000	30454.4427	2291.4771	5.7517	4016.4269	0.0000
0.000000000	28449.4107	2315.2424	6.3313	3975.3117	0.0000
0.000000000	26442.2544	2444.7592	6.7249	3936.5112	0.0000
0.000000000	25277.9710	2516.6731	7.1447	3899.8541	0.0000
0.000000000	23431.7023	2594.2751	8.1746	3865.1291	0.0000
0.000000000	22475.7546	2643.8911	8.4218	3832.4483	0.0000
0.000000000	21232.7444	2715.7777	9.4844	3797.4351	0.0000
0.000000000	20194.7012	2744.2411	10.1517	3766.0141	0.0000
0.000000000	19155.7077	2814.5484	10.8448	3736.0957	0.0000
0.000000000	18190.7044	2892.1221	11.5492	3707.5636	0.0000
0.000000000	17205.4174	2941.8325	12.2612	3680.3132	0.0000
0.000000000	16189.9075	2942.2774	12.9843	3654.3744	0.0000
0.000000000	15137.7577	3114.1361	13.7140	3629.5414	0.0000
0.000000000	14139.4473	3177.1925	14.4617	3605.7214	0.0000
0.000000000	14291.5476	31.0527	15.2111	3542.9842	0.0000
0.000000000	13688.7891	3117.8784	15.7717	3541.0619	0.0000
0.000000000	13127.7054	3115.5701	16.7492	3539.9619	0.0000
0.000000000	12402.4674	3211.7151	17.5291	3519.6340	0.0000
0.000000000	12112.7246	3216.4161	18.1172	3500.0315	0.0000
0.000000000	11453.7057	3249.7667	19.1112	3481.1077	0.0000
0.000000000	11222.7647	3311.4531	19.2147	3462.8255	0.0000
0.000000000	10412.7145	3342.7534	20.7274	3444.4334	0.0000
0.000000000	10420.4116	3372.9247	21.5452	3429.8038	0.0000
0.000000000	10152.4877	3411.7179	22.1697	3407.7748	0.0000
0.000000000	9705.5349	3448.8971	23.7014	3390.3240	0.0000
0.000000000	9178.2741	3475.6238	24.7341	3373.4174	0.0000
0.000000000	9449.7173	3511.4435	24.4815	3357.0195	0.0000
0.000000000	8776.9898	3516.4152	25.7309	3341.1777	0.0000
0.000000000	8500.7547	3540.5422	26.3840	3325.6571	0.0000
0.000000000	8238.7150	3573.9474	27.4445	3310.6450	0.0000
0.000000000	7989.4571	3595.6711	28.3125	3296.0498	0.0000
0.000000000	7757.2329	3618.6697	29.1876	3281.8517	0.0000
0.000000000	7524.6540	3610.0179	30.7597	3268.0319	0.0000
0.001094634	7443.9714	3618.5422	30.1000	3248.9742	0.0000

END OF RUNS.55 MM



TABLE A-2

RUN NUMBER OF CHARGES 2 CONTRACT CASELESS AMMO

TABLE OF F VERSUS Z

	IMR 4895	
	MC BLANK	
0.000000000	1.000000000	1.000000000
0.100000000	0.923000000	0.995000000
0.200000000	0.835000000	0.990000000
0.300000000	0.748000000	0.983000000
0.400000000	0.654000000	0.979000000
0.500000000	0.556000000	0.973000000
0.600000000	0.454000000	0.968000000
0.700000000	0.347000000	0.963000000
0.800000000	0.236000000	0.943000000
0.900000000	0.120000000	0.760000000
1.000000000	0.000000000	0.000000000

CHAMBER VOLUME	VO =	0.097700000 (CU. IN.)
PROJECTILE BASE AREA	A =	0.039300000 (SQ. IN.)
PROJECTILE VELOCITY	VE =	0.000000000 (FT./SEC)
RESISTANCE FUNCTION ... R=K1+K2*x		
	K1 =	0.100000000
	K2 =	0.000000000
RATIO OF SPECIFIC HEATS	GAMMA =	1.240000000
PROJECTILE MASS	M =	0.000244000 (SLUGS)
STOP AT PROJECTILE TRAVEL	YEND =	29.999999999 (IN)
INITIAL CHAMBER PRESSURE	P =	1000.000000000 (PSI)
EXPONENT OF INIT CHMBR PRESS	XP =	1.000000000

CHARGE NO. 1

	IMR 4895	
	MC BLANK	
PROPELLANT IMPETUS	CF =	379999.999990000 (FT)
INITIAL CHARGE WEIGHT	C =	0.004000000 (LBS)
INITIAL TEMPERATURE	T =	5103.999999900 (DEG R)
PROPELLANT DENSITY	DELTA =	0.060000000 (LBS/CU. IN.)
BURNING RATE COEFF/WER SIZE ..	HETA/D =	0.037000000 (IN/SEC/PSI/IN)

CHARGE NO. 2

PROPELLANT IMPETUS	CF =	314999.999990000 (FT)
INITIAL CHARGE WEIGHT	C =	0.000115000 (LBS)
INITIAL TEMPERATURE	T =	5099.999999900 (DEG R)
PROPELLANT DENSITY	DELTA =	0.060000000 (LBS/CU. IN.)
BURNING RATE COEFF/WER SIZE ..	HETA/D =	0.096400000 (IN/SEC/PSI/IN)
PHASE 1 TIME INCREMENT	DT1 =	0.000020000 (SEC)
PHASE 2 TIME INCREMENT	DT2 =	0.000020000 (SEC)

TABLE A-2 (Cont'd)

TIME (SEC)	W-35000 (PSI)	VELOCITY (FT/SEC)	TRAVEL (IN)	TEMPERATURE (°F)	FORM FUNCTIONS
0.00000000	1710.1000	0.000	0.1000	9104 0130	0.0000 0.0000
0.00000000	9747.0400	2.742	0.0010	9104 7.30	0.0000 0.0147
0.00000000	9115.2001	7.117	0.0020	9099 4.32	0.0000 0.0015
0.00000000	15417.6500	42.112	0.0100	9084 5.11	0.0114 0.2250
0.00000000	24934.7070	44.360	0.0002	9058 1.12	0.0273 0.4500
0.00010000	37242.7760	142.641	0.0001	9010 5.12	0.0404 0.7734
0.00012000	48931.7017	244.781	0.1035	8970 4.02	0.0425 0.9040
0.00014000	57147.7011	347.782	0.2725	8887 0.10	0.1254 0.9575
0.00016000	63413.9609	546.243	0.4226	8806 7.90	0.1744 0.9672
0.00018000	68741.1042	711.214	0.6147	8723 3.71	0.2200 0.9734
0.00020000	68739.1542	814.218	0.4547	8639 2.50	0.2844 0.9804
0.00022000	64422.4269	1047.136	1.1346	8540 1.70	0.3197 0.9875
0.00024000	61445.9190	1244.881	1.4615	8483 1.50	0.3913 0.9945
0.00026000	57982.1431	1413.969	1.6270	8407 0.20	0.4441 1.0000

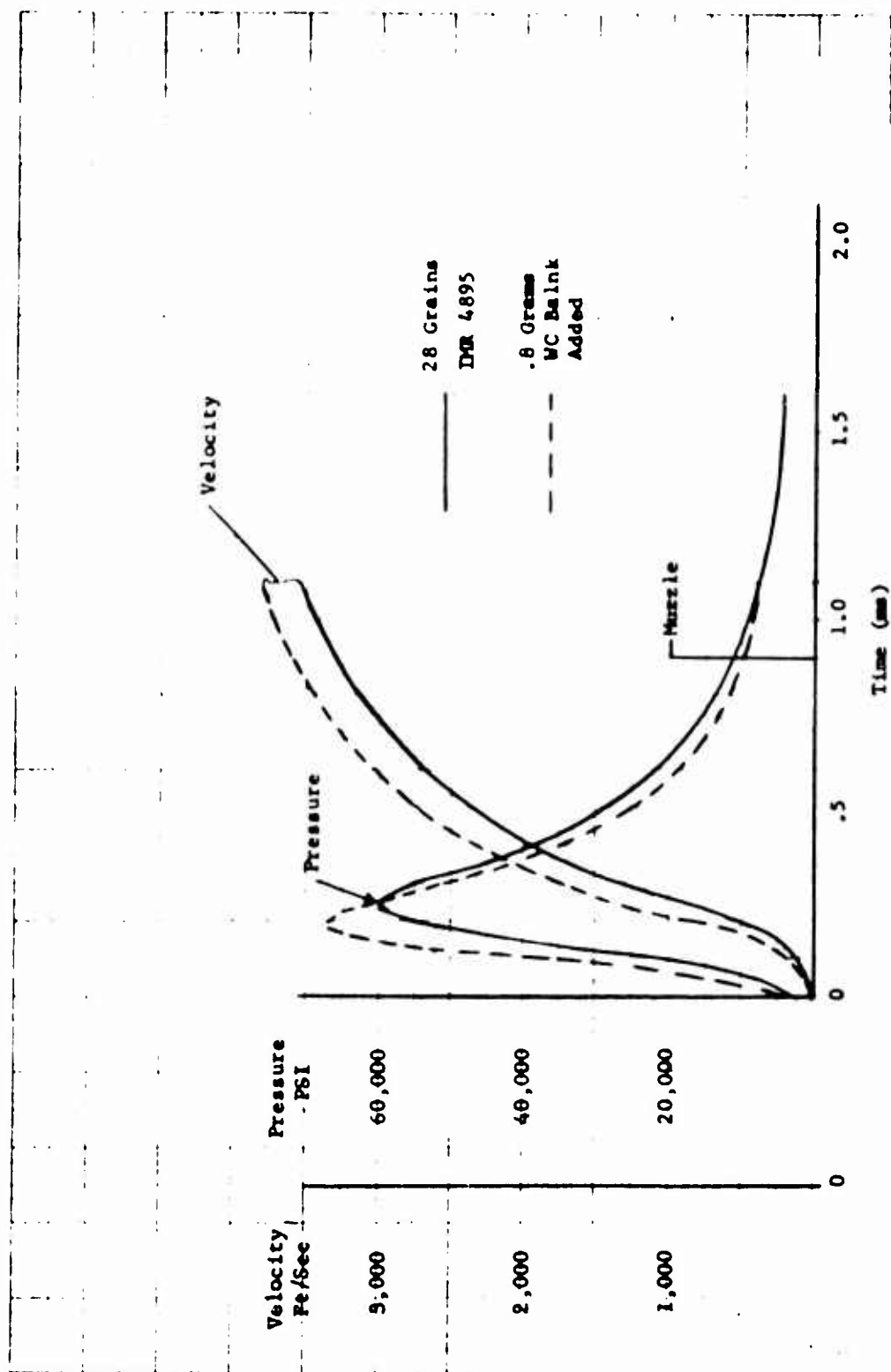
ALL PROPELLANT BURN - CHARGE NO. 2

0.00028000	54427.0862	1532.994	2.2293	8337 2.93	0.4845 1.0000
0.00030000	51316.4779	1741.141	2.6849	8271 0.54	0.5253 1.0000
0.00032000	48454.4511	1874.974	3.1113	8211 0.14	0.5620 1.0000
0.00034000	42941.9750	2275.942	3.5230	8153 1.47	0.5945 1.0000
0.00036000	35414.1256	2131.946	4.1579	8099 2.57	0.6277 1.0000
0.00038000	36967.1103	2213.072	4.7549	8048 9.45	0.6545 1.0000
0.00040000	34512.9643	2314.456	5.2743	8000 6.32	0.6822 1.0000
0.00042000	31459.4301	2470.578	5.8689	7955 4.94	0.7041 1.0000
0.00044000	29421.4851	2544.214	6.4829	7913 0.97	0.7243 1.0000
0.00046000	27497.4261	2597.979	7.1142	7873 0.31	0.7400 1.0000
0.00048000	26054.1414	2674.447	7.7611	7833 4.44	0.7644 1.0000
0.00050000	24477.2192	2746.743	8.4344	7790 1.42	0.7817 1.0000
0.00052000	23710.4871	2813.120	9.1141	7740 0.34	0.7995 1.0000
0.00054000	21478.0626	2876.214	9.8140	7727 4.30	0.8143 1.0000
0.00056000	20445.2899	2935.650	10.5277	7695 7.36	0.8283 1.0000
0.00058000	19141.1804	2991.774	11.2574	7665 7.23	0.8415 1.0000
0.00060000	18751.4108	3044.044	11.9896	7637 2.59	0.8541 1.0000
0.00062000	17449.9251	3095.184	12.7344	7610 1.07	0.8641 1.0000
0.00064000	16521.4314	3142.944	13.4895	7584 1.72	0.8774 1.0000
0.00066000	15767.1523	3148.482	14.2692	7559 3.11	0.8842 1.0000
0.00068000	15761.4703	3211.697	15.1500	7535 5.29	0.8945 1.0000
0.00070000	14369.0702	3277.906	15.8454	7512 7.42	0.9043 1.0000
0.00072000	13706.4722	3312.451	16.5442	7490 8.63	0.9177 1.0000
0.00074000	13147.1144	3357.252	17.4440	7449 7.99	0.9242 1.0000
0.00076000	12425.1332	3344.741	18.2650	7447 0.76	0.9337 1.0000
0.00078000	12118.4405	3437.049	19.0077	7425 1.01	0.9409 1.0000
0.00080000	11425.4085	3444.195	19.9240	7405 4.58	0.9476 1.0000
0.00082000	11174.1763	3446.364	20.7644	7385 7.42	0.9544 1.0000
0.00084000	10751.0411	3515.671	21.6121	7368 7.82	0.9608 1.0000
0.00086000	10155.7451	3546.190	22.4647	7348 3.40	0.9649 1.0000
0.00088000	9743.484	3574.444	23.3240	7330 6.210	0.9728 1.0000
0.00090000	9411.4234	3611.924	24.1940	7313 4.29	0.9785 1.0000
0.00092000	9111.7614	3679.344	25.0600	7296 7.62	0.9840 1.0000
0.00094000	8922.7146	3693.457	25.9407	7280 6.79	0.9893 1.0000
0.00096000	8424.9422	3676.513	26.8345	7244 4.16	0.9944 1.0000
0.00098000	8111.414	3712.364	27.7270	7249 1.43	0.9994 1.0000
0.00100000	7413	3725.457	28.6270	7227 6.17	1.0000 1.0000

ALL PROPELLANT BURN - CHARGE NO. 1

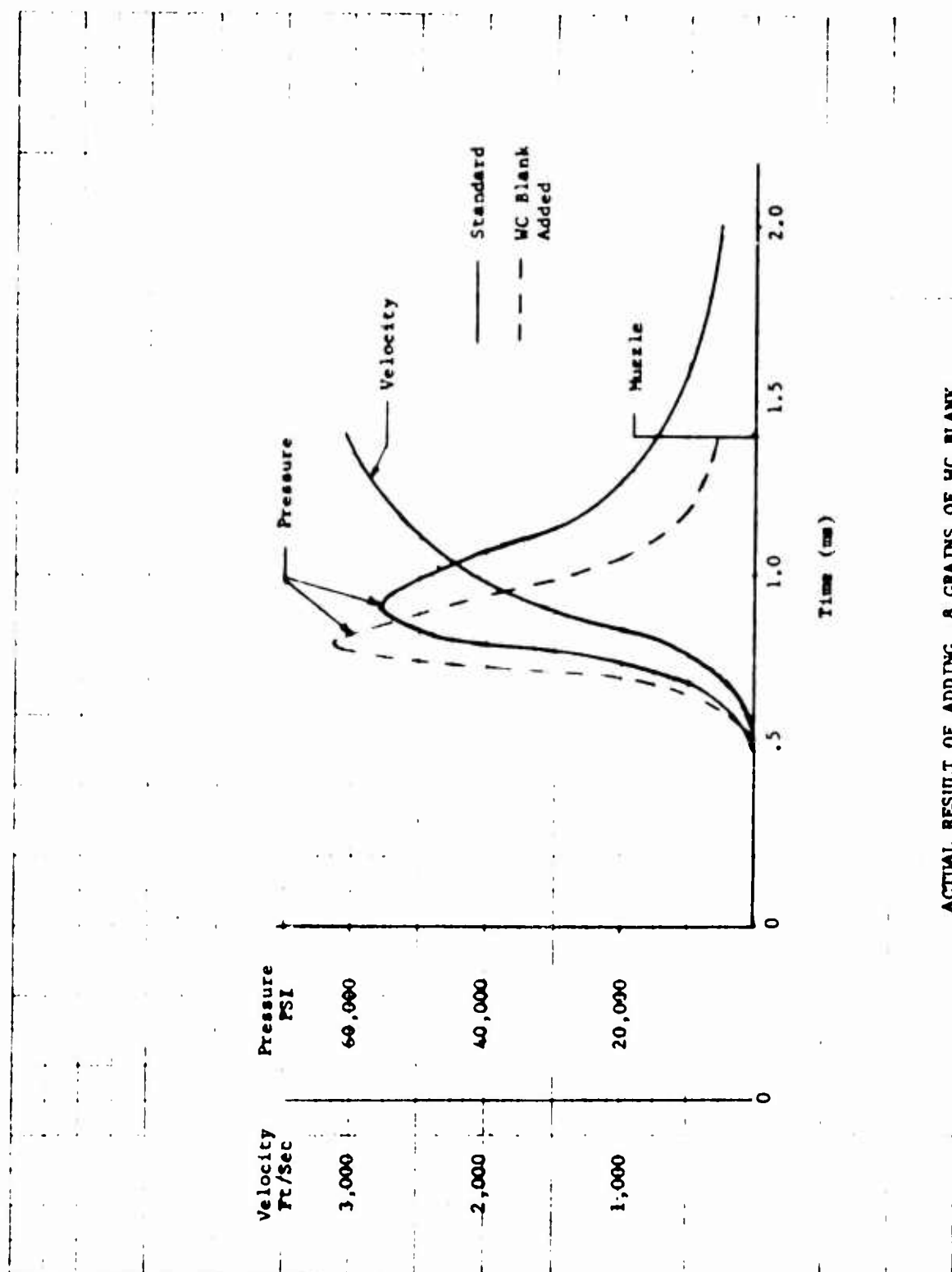
0.00102000	7830.4643	3747.721	29.5240	7205 0.54	1.0000 1.0000
0.00104000	7557.9815	3749.193	30.4332	7183 1.47	1.0000 1.0000
0.00106000	7488.1724	3748.941	30.0000	7193 4.64	1.0000 1.0000

END OF RUN



THEORETICAL EFFECT OF ADDING WC BLANK PROPELLANT

Figure A-1



ACTUAL RESULT OF ADDING .8 GRAINS OF WC BLANK

Figure A-2



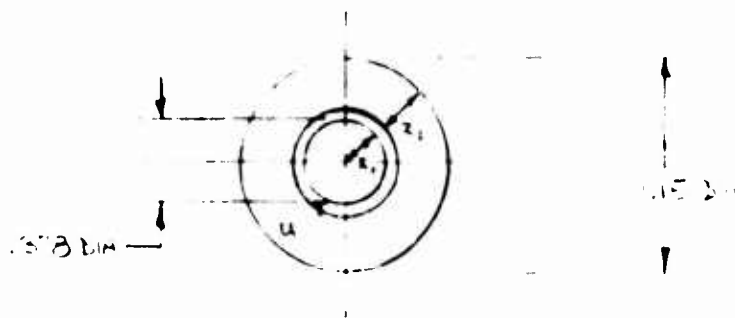
Corporation

B. Chamber Heating

1. Heat Transfer

The following analysis will demonstrate how the heat transfer to the chamber during firing can be computed.

Consider a chamber whose outside diameter is 1.15 inches.



The cyclic rate at 750 rounds per minute is one round every 80 milliseconds. The barrel time for the projectile is approximately one millisecond.

A small surface element stores heat during the barrel time. Conduction from this element to the outer surface without external surface convection is assumed during the rest of the cycle.

The heat input into the thin annular element during the barrel time, t , is

$$\Delta Q_{n1} = hA_1 (T_g - T_{(n-1)2}) t_1 \quad (1)$$

The increase in the element's temperature during this time,

$$t_1, \text{ is } \Delta T_{n1} = \frac{\Delta Q_{n1}}{m_1 C_p} \quad (2)$$

and
$$T_{n1} = T_{(n-1)2} + \Delta T_n \quad (3)$$

During the remainder of the cycle time, the heat is transferred from the thin element to the outer element according to

$$\Delta Q_{n2} = \frac{-KA_2}{\frac{X_2}{(-\frac{r}{2})}} (T_{n1} - U_{n-1}) t_2 \quad (4)$$

Then the final temperature of each section at the end of the cycle is

$$T_{n2} = T_{(n-1)} + \frac{\Delta Q_{n1} + \Delta Q_{n2}}{m_1 C_p} \quad (5)$$

$$U_n = U_{n-1} - \frac{\Delta Q_{n2}}{m_2 C_p} \quad (6)$$

Consider a chamber length of 1 inch, an inner diameter of .378 inch, an average convection coefficient of $1.0 \text{ cal/sec-cm}^2\text{-}^\circ\text{C}$ ($7373 \text{ BTU/hr-ft}^2\text{-}^\circ\text{F}$), gas temperature of 4000°F , an average barrel temperature of 150°F and a heating time of 1 millisecond. Substituting into equation (1),

$$\Delta Q_{n1} = 7,373 \frac{(\pi)(.378)(1)}{144} (4000-150) \frac{1 \times 10^{-3}}{3600}$$

$$\Delta Q_{n1} = .0646 \text{ BTU/shot}$$



Corporation

Equation (4) will give the conduction rate per shot assuming a surface temperature drop. Thus,

$$\Delta Q_{n2} = \frac{-KA_2}{\frac{x_2}{2}} (\Delta T) t_2$$

$$= \frac{-16.6 \times \frac{(\frac{.378 + .550}{2}) \times 1}{144} \times \Delta T \times 80 \times 10^{-3}}{(\frac{.378}{12 \times 2}) \times 3.6 \times 10^3}$$

$$\Delta Q_{n2} = .240 \times 10^{-3} \Delta T \text{ BTU/Shot}$$

When the temperature drop across the wall of the chamber approaches 269°F , the heat conducted per shot approaches the heat input per shot. Assuming an equilibrium with a temperature differential of 269°F , the total number of rounds fired to reach a surface temperature of 325°F is

$$N = \frac{m C_p [T_{co} - \frac{\Delta T}{2} - T_o]}{\Delta Q_{n1}} \quad (7)$$

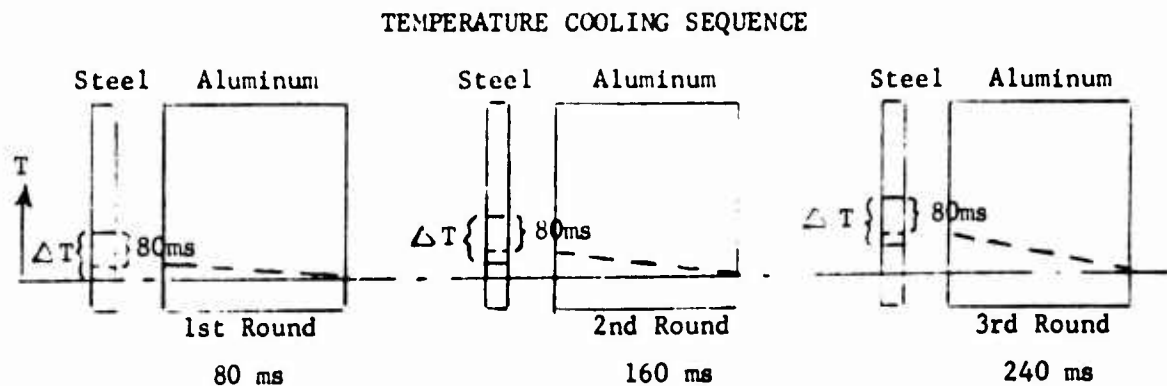
The weight of a 1 inch length of barrel of 1.15 inch outer diameter is .26 lb.

$$N = \frac{(.26) (.11) \left[325 - \frac{269}{2} - 70 \right]}{.0646}$$

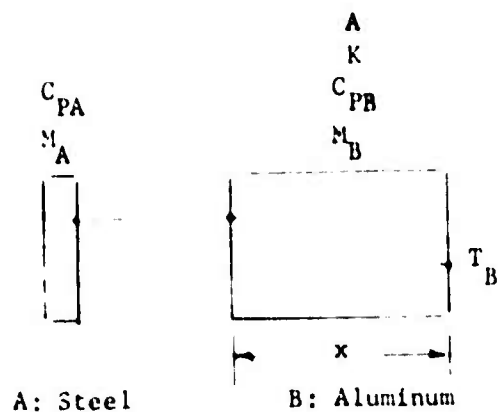
= 54 rounds

2. Operation of Heat Sink

For convenience, the temperature drop across the steel is assumed negligible and to vary linearly across the wall of the aluminum sleeve. It is also assumed that a constant amount of heat input occurs for each shot and is uniformly stored in the steel chamber. Then, heat flows from the steel into the aluminum for 80 milliseconds. The following sketches depict the assumed conditions:



Only radial flow is assumed and a one dimensional analysis is presented for simplicity.



After heat is put into the chamber wall, the temperature is T_{AO} and the rate of heat flow from the chamber is,

$$\frac{dQ}{dt} = \frac{-kA}{x} (T_A - T_B) \quad (8)$$

The amount of heat contained in A is,

$$Q_A = M_A C_{PA} T_A \quad (9)$$

The amount of heat contained in B is,

$$Q_B = M_B C_{PB} \left(\frac{T_B + T_A}{2} \right) \quad (10)$$

For any time during cooling, the total heat is constant.

Therefore,

$$M_A C_{PA} T_{AO} + M_B C_{PB} T_{BO} = M_A C_{PA} T_A + M_B C_{PB} \left(\frac{T_A + T_B}{2} \right) \quad (11)$$

Solving for the temperature T_B for any time during cooling,

$$T_B = \frac{(T_{AO} + K_1 T_{BO}) - (1 + \frac{K_1}{2}) T_A}{(\frac{K_1}{2})} \quad (12)$$

Where:

$$K_1 = \frac{M_B C_{PB}}{M_B C_{PA}} \quad (13)$$

Differentiate equation (9) and equate it to (8).

$$\frac{dT_a}{dt} = \frac{-KA}{M_A C_{PA} X} (T_A - T_B) \quad (14)$$

Substituting equation (12) into equation (14) and integrating results in,

$$T_A = T_{AO} \left\{ e^{-\left[\frac{2KA}{M_A C_{PA} X} \left(1 + \frac{M_A C_{PA}}{M_B C_{PB}} \right) t \right]} \left[1 - \frac{1 + \left(\frac{M_B C_{PB}}{M_A C_{PA}} \right) \frac{T_{BO}}{T_{AO}}}{1 + \frac{M_B C_{PB}}{M_A C_{PA}}} \right] + \frac{1 + \left(\frac{M_B C_{PB}}{M_S C_{PS}} \right) \frac{T_{BO}}{T_{AO}}}{1 + \left(\frac{M_B C_{PB}}{M_S C_{PB}} \right)} \right\} \quad (8)$$

Equation (15) gives the steel chamber temperature T_A after the cooling time t when the initial temperature from the heat input was T_{AO} and the temperature of the aluminum was T_{BO} . If the expression in the braces $\{\}$ is a constant, the ratio of $\frac{T_{BO}}{T_{AO}}$ is a constant or an expression whose variance has a small effect and equation (15) can be written

$$T_A + RT_{AO} \quad (16)$$

Examine equation (16) for a series of rounds fired

$$\begin{aligned} T_1 &= R[T_0 + \Delta T] \\ T_2 &= R[T_1 + \Delta T] = R^2 T_0 + R^2 \Delta T + R \Delta T \\ T_3 &= R[T_2 + \Delta T] = R^3 T_0 + R^3 \Delta T + R^2 \Delta T + R \Delta T \\ &\vdots \\ T_n &= R^n T_0 + (R^n + R^{n-1} + \dots + R) \Delta T \end{aligned} \quad (17)$$

Simplifying and recognizing the sum of a convergent geometric series, equation (17) becomes,

$$T_n = R [R^{n-1} T_0 + \left(\frac{1-R^{n-1}}{1-R} \right) \Delta T] \quad (18)$$

Based on the dimensions now in use, the following values are used to calculate the chamber temperature versus the number of rounds fired for a one-inch chamber length. For consistency, it is assumed that the aluminum sleeve around the chamber is cylindrical.

A (equivalent aluminum flow area)	=	2.68 in^2
C_{PA} (Specific heat of steel)	=	$.11 \text{ BTU/lb-}^\circ\text{F}$
C_{PB} (Specific heat of aluminum)	=	$.22 \text{ BTU/lb-}^\circ\text{F}$
K (conductivity of aluminum)	=	$177 \text{ BTU-ft/hr-ft}^2\text{-}^\circ\text{F}$
M_A (weight of Steel Chamber)	=	$.0352 \text{ lb.}$
M_B (weight of aluminum sleeve)	=	$.060 \text{ lb.}$
T_{BO} (reservoir temperature)	=	70°F
X (radial aluminum conductor)	=	$.303 \text{ in.}$



Calculating the temperature rise in the steel chamber per shot for a heat input of .0646 BTU as found earlier.

$$\Delta T = \frac{Q}{M_A C_{PA}} = \frac{.0646}{.0352 \times .11}$$

$$= 16.6^{\circ} \text{F}$$

Then the initial temperature for a 16.6 F rise after the first shot is,

$$T_0 = (460 + 70) + 16.6$$

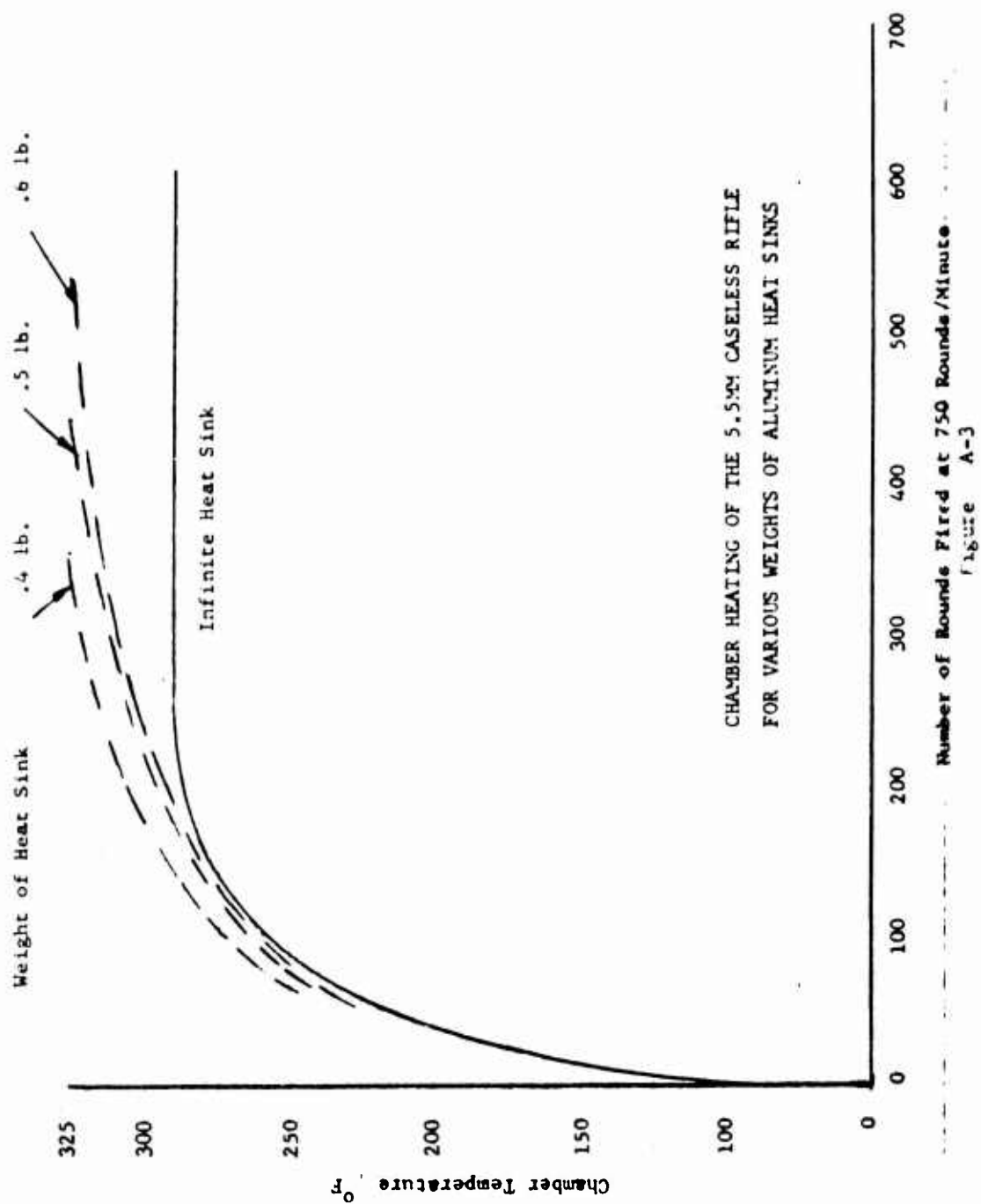
$$= 546.6^{\circ} \text{Rankine}$$

Using the previous values for the remaining constants, the ratio factor R is .928 and equation (18) becomes

$$T_n = .978 \quad (.978)^{n-1} \quad (546.6) + \left(\frac{1 - (.978)^{n-1}}{1 - .978} \right) (16.6)$$

This equation is plotted in Figure A-3, showing temperature ($^{\circ}\text{F}$) in the steel chamber as a function of the number of rounds fired.

The above deviation assumes an infinite heat sink capable of returning the outside of the aluminum sleeve to the ambient temperature of 70° after 80 milliseconds of the thermal lag can be neglected, an estimate of the number of rounds to reach the cook-off temperature of 325°F can be made for various weight of aluminum. For a constant heat input per round,





Corporation

$$\begin{aligned} N &= \frac{Q_T}{Q} = \frac{MC_P \Delta T}{Q} \\ &= \frac{.22 \times (325 - 70)}{.0646} \text{ M} \\ &= 880 \text{ M} \end{aligned}$$

Figure A-3 illustrates the number of rounds that can be fired until cook-off temperature is reached.

As previously mentioned a .60 pound heat sink is being used. This enables approximately 530 rounds to be fired until a chamber temperature of 350°F is reached.

C. Ammunition/Weapon Interface

1. Firing Pin and Bolt Sealing

A computer program analysis was applied to determine the effectiveness of the bolt and firing pin obturating seals. The results of the analysis for the firing pin are compiled in Table A-3. Figure A-4 is a schematic of the obturator showing the variables under consideration.

TABLE A-3

FIRING PIN OBTURATOR ANALYSIS

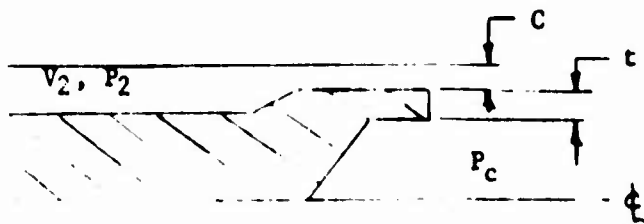
$$V_2 = .0036 \text{ in}^2$$

$$V_2 = .0028 \text{ in}^2$$

t in.	c in.	P _c psi	P ₂ psi	t in.	c in.	P _c psi	P ₂ psi
.0025	.002	11397	1395				
.0050	.002	13078	1798	.0050	.002	13078	2312
.0100	.002	12798	1800	.0100	.002	12798	2315
.0025	.001	8887	427				
.0050	.001	10556	633	.0050	.001	10556	813
.0100	.001	10883	696	.0100	.001	10883	894



Corporation



Nomenclature

P_c	= chamber pressure when obturator is closed	- psi
P_2	= downstream pressure when obturator seals	- psi
V_2	= downstream volume	- in ³
c	= obturator deflection	- in
t	= obturator thickness	- in

FIRING PIN OBTURATOR

Figure A-4

The purpose of this analysis was to determine whether or not the firing pin obturator would seal when there was clearance between it and the bolt. If a seal could be accomplished, it would be necessary to know the allowable clearance, the obturator wall thickness, and the maximum downstream pressure felt by the "O" ring seal prior to completion obturation. It can be seen from the table that the values calculated for the larger downstream

volume ($V_2 = .0036 \text{ in}^3$, obtained by undercutting the firing pin) produce lower downstream pressures. The smaller volume was used in the actual design, however, in order to make the "O" ring seal practical. In order to maintain the maximum strength and resistance to erosion for the obturating surface, a wall thickness of .010 in. was chosen as most desirable. A radial clearance of .001 in. (.002 in. diametral) or less can be maintained fairly easily. From Table A-3 it can be seen that these values will produce downstream pressure of 894 psi, well within the realm of a standard "O" ring.

The bolt obturator operates with a diametral clearance of .001 inch. An analysis similar to that for the firing pin was undertaken in order to find the effectiveness of the bolt seal. The first and last page of this computer analysis are given in Table A-4 showing that the downstream pressure reaches 820 psi before complete sealing takes place. This value presents no problems for standard "O" rings.



Corporation

TABLE A-4

OBTURATOR SEAL STUDY

INSIDE RADIUS OF OBTURATOR A= 0.173000000(IN)
OUTSIDE RADIUS OF OBTURATOR R= 0.180000000(IN)
MAXIMUM RADIUS R= 0.188500000(IN)
DOWNSTREAM VOLUME V2= 0.002060000(CU IN)
PROPELLANT IMPETUS F= 379999.999990000(FT-LB/LB)
RATIO OF SPECIFIC HEATS GAMMA= 1.240000000
MATERIAL MODULUS OF ELASTICITY E= 26499999.999900000(Psi)
MATERIAL DENSITY RHO= 0.290000000(LB/CU IN)
MAXIMUM DEFLECTION XMAX= 0.000500000(IN)
TIME AT PEAK PRESSURE TMAX= 0.000250000(SEC)
TIME INCREMENT DT= 0.000000200(SEC)

TIME (SEC)	CHAMBER PRESSURE (PSI)	DOWNSTREAM PRESSURE (PSI)	OBTURATOR RADIAL DEFLECTION (INCHES)
0.00000000	0.0000	0.0000	0.000000
0.00000020	40.0000	0.0569	0.000000
0.00000040	80.0000	0.1510	0.000000
0.00000060	120.0000	0.2846	0.000001
0.00000080	160.0000	0.4552	0.000001
0.00000100	200.0000	0.6634	0.000002
0.00000120	240.0000	0.9091	0.000003
0.00000140	280.0000	1.1970	0.000004
0.00000160	320.0000	1.5110	0.000006
0.00000180	360.0000	1.8675	0.000008
0.00000200	400.0000	2.2594	0.000010
0.00000220	440.0000	2.6865	0.000012
0.00000240	480.0000	3.1485	0.000015
0.00000260	520.0000	3.6448	0.000017
0.00000280	560.0000	4.1747	0.000020
0.00000300	600.0000	4.7379	0.000023
0.00000320	640.0000	5.3339	0.000026
0.00000340	680.0000	5.9623	0.000028
0.00000360	720.0000	6.6229	0.000031
0.00000380	760.0000	7.3155	0.000033
0.00000400	800.0000	8.0401	0.000035
0.00000420	840.0000	8.7967	0.000037
0.00000440	880.0000	9.5855	0.000039
0.00000460	920.0000	10.4067	0.000040
0.00000480	960.0000	11.2607	0.000041
0.00000500	1000.0000	12.1477	0.000042
0.00000520	1040.0000	13.0683	0.000043
0.00000540	1080.0000	14.0227	0.000043
0.00000560	1120.0000	15.0114	0.000043
0.00000580	1160.0000	16.0346	0.000043
0.00000600	1200.0000	17.0925	0.000043
0.00000620	1240.0000	18.1852	0.000043
0.00000640	1280.0000	19.3127	0.000043
0.00000660	1320.0000	20.4748	0.000043
0.00000680	1360.0000	21.6709	0.000044
0.00000700	1400.0000	22.9007	0.000044
0.00000720	1440.0000	24.1635	0.000045
0.00000740	1480.0000	25.4583	0.000046
0.00000760	1520.0000	26.7842	0.000047

TABLE A-4 (Cont'd)

0.00004030	12120.0000	765.7239	0.000430
0.00004080	12160.0000	767.3435	0.000430
0.00004100	12200.0000	768.9557	0.000431
0.00004120	12240.0000	770.5658	0.000431
0.00004140	12280.0000	772.1784	0.000431
0.00004160	12320.0000	773.7969	0.000431
0.00004180	12360.0000	775.4233	0.000431
0.00004200	12400.0000	777.0583	0.000431
0.00004220	12440.0000	778.7009	0.000431
0.00004240	12480.0000	780.3488	0.000431
0.00004260	12520.0000	781.9982	0.000431
0.00004280	12560.0000	783.6443	0.000431
0.00004300	12600.0000	785.2809	0.000432
0.00004320	12640.0000	786.9012	0.000433
0.00004340	12680.0000	788.4979	0.000435
0.00004360	12720.0000	790.0631	0.000436
0.00004380	12760.0000	791.5894	0.000438
0.00004400	12800.0000	793.0693	0.000440
0.00004420	12840.0000	794.4963	0.000443
0.00004440	12880.0000	795.8645	0.000446
0.00004460	12920.0000	797.1694	0.000448
0.00004480	12960.0000	798.4078	0.000451
0.00004500	13000.0000	799.5777	0.000454
0.00004520	13040.0000	800.6790	0.000457
0.00004540	13080.0000	801.7129	0.000460
0.00004560	13120.0000	802.6822	0.000462
0.00004580	13160.0000	803.5911	0.000465
0.00004600	13200.0000	804.4451	0.000467
0.00004620	13240.0000	805.2504	0.000469
0.00004640	13280.0000	806.0143	0.000470
0.00004660	13320.0000	806.7442	0.000472
0.00004680	13360.0000	807.4478	0.000473
0.00004700	13400.0000	808.1327	0.000473
0.00004720	13440.0000	808.8057	0.000474
0.00004740	13480.0000	809.4729	0.000474
0.00004760	13520.0000	810.1394	0.000474
0.00004780	13560.0000	810.8088	0.000474
0.00004800	13600.0000	811.4834	0.000474
0.00004820	13640.0000	812.1639	0.000474
0.00004840	13680.0000	812.8491	0.000474
0.00004860	13720.0000	813.5366	0.000474
0.00004880	13760.0000	814.2222	0.000474
0.00004900	13800.0000	814.9003	0.000475
0.00004920	13840.0000	815.5643	0.000475
0.00004940	13880.0000	816.2066	0.000476
0.00004960	13920.0000	816.8190	0.000478
0.00004980	13960.0000	817.3931	0.000479
0.00007000	14000.0000	817.9205	0.000481
0.00007020	14040.0000	818.3930	0.000484
0.00007040	14080.0000	818.8035	0.000486
0.00007060	14120.0000	819.1457	0.000489
0.00007080	14160.0000	819.4144	0.000492
0.00007100	14200.0000	819.6063	0.000494
0.00007120	14240.0000	819.7193	0.000497
0.00007140	14280.0000	819.7532	0.000500
MAX DEFLECTION REACHED			



Corporation

2. Erosion of Firing Pin Face

Redesigning the firing pin by removing the obturator lip has been considered. This presents the problem of erosion due to chamber gases. However, this problem can be overcome.

The mechanics of high velocity, high temperature gas erosion involves such theoretical complexity that only generalizations can be offered concerning the selection of materials to resist erosion. A preliminary dimensional analysis concerning several erosion parameters indicates increased resistance to erosion at mach 1 flow by

<u>Decreasing</u>	<u>Increasing Material</u>
Gas Pressure	Shear Strength
Gas Temperature	Melting Temperature
Surface Roughness	
Material Specific Heat	
Material Density	Thermal Conductivity

It follows that decreasing the gas pressure will decrease the density and dynamic drag forces against the minute surface projections tending to dislodge them. Likewise lowering this gas temperature will reduce the mach 1 flow velocity lessening the erosive force. Minimizing the surface projections will offer the least area for frictional heat transfer and dynamic impact resisting the flow of the hot gases.

High thermal conductivity transfers the heat away from the surface increasing the time to either melt or weaken the surface projections

impacted by the high velocity gases. Increasing the specific heat and density of the material will provide a lower temperature for the heat that is not conducted away, again decaying material shear or melting. Finally, increasing the melting point and material shear strength will add to the erosion resistance whether failure is through shear of heated weakened particles or through dynamic drag and removal of melted, fluid surfaces.

Following is a dimensionless analysis derivation and an attempt to evaluate several candidate materials to resist erosion. Removal of this obturator lip permits mach 1 flow along this firing pin until the gas pressure reaches the downstream low pressure O-ring seals. An assumption would be negligible at lower velocities.

Expressing the surface erosive rate at \dot{e}_r ,

$$\dot{e}_r = G [P_g, T_g, e, S_s, T_m, \rho_m, C_p, K_p] \quad (1)$$

And using four basic units of M:mass, T:time, L:length and θ :temperature, the dimensional equivalents of each parameter are,

$$\begin{array}{lll} \dot{e}_r = \frac{L}{T} & P_g: \frac{F}{L^2} = \frac{M}{T^2 L} & T_m: \theta \\ & T_g: \theta & \rho_m: \frac{M}{L^3} \\ & e: L & C_p: \frac{L^2}{T^2 \theta} \\ & S_s: \frac{F}{L^2} = \frac{M}{T^2 L} & K_p: \frac{ML}{T^3 \theta} \end{array}$$



In dimensional form,

$$\frac{L}{T} = \left(\frac{M}{T^2 L}\right)^a (\theta)^b (L)^c \left(\frac{M}{T^2 L}\right)^d (\theta)^e \left(\frac{M}{L^3}\right)^f \left(\frac{L^2}{T^2 \theta}\right)^g \left(\frac{ML}{T^3 \theta}\right)^h \quad (2)$$

Equating the exponents of the basic units,

$$M: \quad 0 = a + d + f + h \quad (3)$$

$$T: \quad -1 = -2a - 2d - 2g - 3h \quad (4)$$

$$L: \quad 1 = -a + c - d - 3f + 2g + h \quad (5)$$

$$\theta: \quad 0 = b + e - g - h \quad (6)$$

Adding equations (3) and (5),

$$1 = c - 2f + 2g + 2h \quad (7)$$

Multiplying equation (3) by 2,

$$0 = 2a + 2d + 2f + 2h \quad (8)$$

Adding equations (4) and (8)

$$-1 = 2f - 2g - h \quad (9)$$

substituting equation (9) into equation (5)

$$1 = -a + c - d - f + 1$$

$$f = -a + c - d \quad (10)$$

Substituting equation (10) into equation (3)

$$0 = a + d + h - a + c - d$$

$$h = -c \quad (11)$$

Substituting equations (11) and (10) into (9),

$$\begin{aligned} -1 &= -2a + 2c - 2d + c - 2g \\ g &= \frac{1}{2} - a + \frac{3c}{2} - d \end{aligned} \quad (12)$$

Finally, substituting equations (10), (11) and (12) into equation (6)

$$\begin{aligned} 0 &= b + c - \frac{1}{2} + a - \frac{3}{2}c + d + c \\ e &= \frac{1}{2} - a - b + \frac{1}{2}c - d \end{aligned} \quad (13)$$

Returning to equations (2) and (1)

$$\dot{e}_r = C_o [P_g]^a [T_g]^b [\epsilon]^c [S_s]^d [T_n]^{\frac{1}{2} - a - b + \frac{c}{2} - d} [\rho_m]^{-a + c - d} [C_p]^{\frac{1}{2} - a + \frac{3c}{2} - d} [K_p]^{-c} \quad (14)$$

combining

$$\dot{e}_r = C_o \left[\frac{P_g}{T_m \rho_m C_p} \right]^a \left[\frac{T_g}{T_m} \right]^b \left[\frac{\epsilon \sqrt{T_m} \rho_m C_p}{S_s} \right]^{\frac{3}{2}c} \left[\frac{S_s}{T_m \rho_m C_p} \right]^d \sqrt{\frac{T_m C_p}{T_m C_p}} \quad (15)$$

Of course, considerable experimental data is required to evaluate the scaling factor C_o and the exponents a , b , c and d , but some speculation might be made concerning the sign and relative magnitude. "a" can be assumed positive since the higher the gas pressure, the more dense will be the gas; and, hence, higher erosive forces. "b" is likewise positive, since the higher the gas temperature, the more the erosion. "c" must be positive since erosion is known to increase with increased surface roughness. "d" must be negative to offer

resistance to shear forces and probably equal in magnitude to "a" since it reacts similarly to forces imposed as a result of P_g .

If $a = -d = \frac{1}{2}$, $c = 1$, the erosive rate would become,

$$\dot{e}_r = C_o \left(\frac{P}{S_s} \right)^{\frac{1}{2}} \left(\frac{\epsilon T_m \rho_m C^2}{K_p} \right) \left(\frac{T_g}{T_m} \right)^b \quad (16)$$

In order for the erosive rate to decrease with increasing melting temperatures, "b" must be greater than 1 and perhaps as large as 4 to account for radiant heating. For purposes of making academic comparisons consider $b = 2$, then

$$\dot{e}_r = C_o \left(\frac{P}{S_s} \right)^{\frac{1}{2}} \left(\frac{\epsilon P_m C^2}{K_p} \right) \left(\frac{T_g}{T_m} \right)^2 \quad (17)$$

If this formula is representative, a comparison of materials with equal surface finish can be made by the ratio

$$R_y = \frac{\rho_m C^2}{\sqrt{S_s} K_p T_m} \quad (18)$$

Comparing the following,

	<u>Tantalum T-222</u>	<u>Recrystallized Carbon Graphite</u>	<u>4340 Steel</u>	<u>7075-T6 Aluminum</u>
ρ_m (lb/in ³)	.604	.07	.283	.101
C_p (BTU/lb-°F)	.036	.18	.11	.23
S_s (lb/in ²)	70,000	20,000	150,000	48,000
K_p (BTU/ft-hr-°F)	32	100	16.6	70
T_m (°K)	5,800	6,400	3,200	1600
R_y	1.6×10^{-11}	7.9×10^{-11}	17.3×10^{-11}	21.7×10^{-11}
Comparison	1.0	4.9	10.8	13.6

From this comparison, tantalum T-222 will provide approximately 11 times the number of rounds that 4340 steel could withstand for an equivalent amount of erosion.

Roughly approximating the erosion rate on the firing pin design without the obturator seal, a maximum of 42 rounds are expected before the erosion reaches the small tip to affect performance. On this basis, replacing this tip with tantalum T-222 would raise the number of erosive shots to approximately 460 firings.



D. Cycle Analysis

Upon ignition, the propellant gases impart a recoil velocity to the firing pin. The gas pressure acts on the firing pin for the duration of the dwell travel and the residual pressure continues to act on the recoiling firing pin after the bolt unlocks.

A typical Pressure-Time curve is plotted in Figure A-5 and shows a peak pressure of approximately 60,000 psi. Calculations show that the projectile exits the barrel before bolt begins unlocking.

During the time the projectile is in the barrel, the following condition applies.

$$\frac{M_{FP}}{A_{FP}} v_{FP} = \int P dt = \frac{M_P}{A_P} v_P$$
$$\therefore v_{FP} = \frac{M_P}{M_{FP}} \frac{A_{FP}}{A_P} v_P$$

Throughout the analysis, the subscript FP designates the firing pin and slide weight assembly and the subscript P designates the projectile.

$$\text{let } K = \frac{M_P}{M_{FP}} \frac{A_{FP}}{A_P}$$

$$M_P = \text{mass of projectile} = .00786 \text{ lb.} = 2.45 \times 10^{-4} \text{ slugs}$$

$$M_{FP} = \text{mass of firing pin} = .39 \text{ lb.} = .0122 \text{ slugs}$$

$$A_{FP} = \text{area of firing pin} = .0177 \text{ in}^2$$

$$A_P = \text{area of projectile} = .0393 \text{ in}^2$$

TYPICAL PRESSURE-TIME CURVE
28 GRAIN CHARGE - CASELESS ROUND

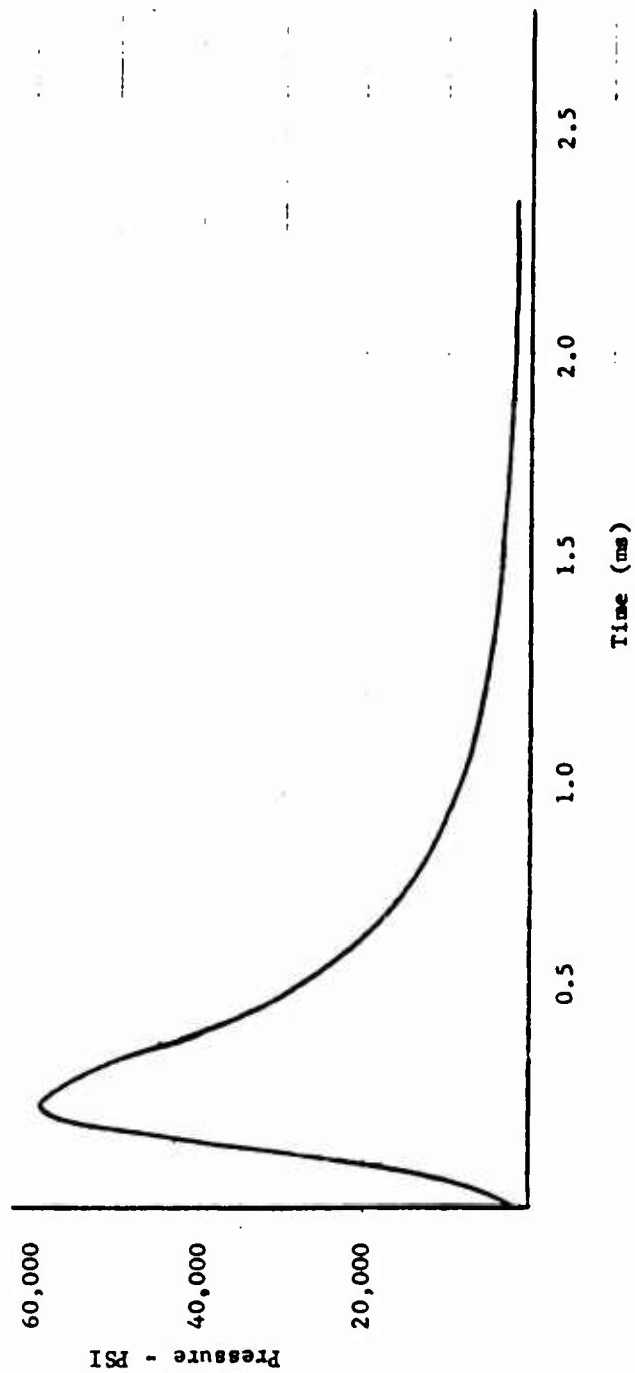


Figure A-5



Corporation

$$K = \left(\frac{.00786}{.39}\right) \left(\frac{.0177}{.0393}\right) = .00907$$

$$X_{FP} = KX_P$$

$$v_{FP} = Kv_P$$

The position and velocity of the firing pin when the projectile is at the muzzle are:

$$X_{FP} = .00907 \times 20" = .181"$$

$$v_{FP} = .00907 \times 3300 = 30 \text{ ft/sec}$$

After the projectile leaves the barrel, the gases expand and the above equation no longer applies. However, knowing the firing pin position and velocity, and the gas pressure at this time, the recoil of the firing pin is determined by writing the equation of motion of firing pin motion.

$$M_{FP} \frac{dv}{dt} = PA_P - F$$

$$\Delta v = \frac{\overline{PA_P} - \overline{F}}{M_{FP}} \Delta t$$

$$\Delta X = \overline{V} \Delta t$$

where:

\bar{P} = average pressure over time increment Δt

F = average resistance force

Δv = change in velocity from t_1 to t_2

Δx = change in distance from t_1 to t_2

Δt = change in time from t_1 to t_2

$\bar{v} = v + \frac{\Delta v}{2}$

The resistance force F is again neglected in this analysis, since it does not effect the final solution. Table A-5 shows the velocity of the firing pin to the point of bolt unlocking.

TABLE A-5

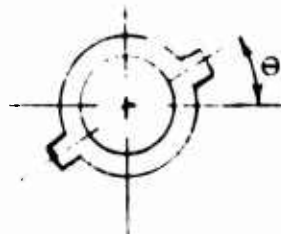
t ms	Δt ms	P psi	\bar{P} psi	Δv fps	v fps	\bar{v} fps	Δx in	x in
.86		11800			30			.181
	.14		10400	2.1		31.05	.052	
1.00		9000			31.1			.233
	.20		7850	2.3		33.7	.081	
1.20		6700			35.4			.314
	.20		6050	1.7		36.3	.087	
1.40		5400			37.1			.401
	.40		4300	2.5		38.8	.186	
1.80		3200			39.6			.587
	.35		2600	1.3		40.3	.16	
2.15		2000			40.9			.755



Corporation

Bolt Unlocking

$$\begin{aligned} &= \dot{\theta} \\ \theta &= kx \\ \dot{\theta} &= k\dot{x} = kv_{FP2} \end{aligned}$$



Bolt Camming Operation

M_B = mass of bolt sleeve



Assuming conservation of momentum:

$$M_{FP} v_{FP} = (M_{FP} + M_B) v_{FP2} + I_{BS} \bar{r}$$

Consider the unlocking cam surface of the bolt sleeve to a helix and for any angular rotation θ the linear displacement x is determined by the constant K . Equating the momentum:

$$v_{FP2} = \frac{M_{FP} v_{FP}}{M_{FP} + M_B + \frac{KI_{BS}}{r}}$$

$$M_B = \text{mass of the bolt} = .148 \text{ lb.}$$

$$r = \text{mean radius of the bolt sleeve}$$

$$I_{BS} = \text{Moment of inertia of bolt sleeve}$$

$$= (m)r^2$$

$$= (.148)(.203)^2$$

$$= 6.10 \times 10^{-3} \text{ lb-in}^2$$

$$K = \frac{\theta}{x} = \frac{26 \times \pi / 180}{.25} = 1.81 \text{ rad/in}$$

substituting,

$$v_{FP2} = \frac{.40 \times 40.9}{.40 + .148 \frac{1.81 \times 6.10 \times 10^{-3}}{.203}}$$

$$= 27 \text{ ft/sec}$$

Energy stored in the drive spring during recoil results in the following velocity just before contact with the buffer.

$$\frac{1}{2} (M_{FP} + M_B) v_{FP2}^2 = E_s + \frac{1}{2} (M_{FP} + M_B) v_{FP3}^2$$

where: E_s = spring energy at 3.4 inch stroke

$$= \frac{1}{2} (.88)(9.75)^2$$

$$= 38 \text{ in-lb} = 3.16 \text{ ft-lb}$$

$$v_{FP3} = \sqrt{v_{FP2}^2 - \frac{2E_s}{M_{FP} + M_B}}$$



Corporation

Substituting;

$$v_{FP_3} = \sqrt{(27.0)^2 - \left(\frac{2 \times 3.16}{.40 + 0.148} \right) 32.2}$$
$$= 18.7 \text{ ft/sec}$$

Counterrecoil

If there is no energy returned by the buffer, the increase in velocity of the firing pin and bolt is caused by the drive spring. The velocity prior to stripping a round is determined as follows:

$$\frac{1}{2} (M_{FP} + M_B) v_{FP_4}^2 + \Delta E_S = \frac{1}{2} (M_{FP} + M_B) v_{FP_5}^2$$

$$v_{FP_5}^2 = v_{FP_4}^2 + \frac{2E_S}{M_{FP} + M_B}$$

$$= 0 + \left(\frac{2 \times 1.97}{.40 + 0.148} \right) 32.2$$

$$= 15.2 \text{ ft/sec}$$

In stripping a round, the added mass results in the following velocity reduction.

$$(M_{FP} + M_B) v_{FP_5} = (M_{FP} + M_B + M_R) v_{FP_6}$$

$$v_{FP_6} = \left(\frac{.40 + 0.148}{.40 + 0.148 - 0.012} \right) 15.2$$

$$14.8 \text{ ft/sec}$$

During chambering, the counterrecoiling velocity is increased by the drive spring and reduced by the friction force between the rounds.

$$\frac{1}{2} (M_{FP} + M_B + M_R) v_{FP_6}^2 + \Delta E_S = \frac{1}{2} (M_{FP} + M_B + M_R) v_{FP_7}^2 + \mu NL$$

N = normal force of rounds during feeding

μ = coefficient of friction

L = stripping distance

$$v_{FP_7} = \sqrt{v_{FP_6}^2 + 2 \left(\frac{\Delta E_S - \mu NL}{M_{FP} + M_B + M_R} \right)}$$

$$= \sqrt{(14.8)^2 + 2 \left(\frac{.77 - 0.2 \times .119 \times 1.0}{0.39 + .148 + .012} \right)} \quad 32.2$$

$$= 17.5 \text{ ft/sec}$$

The velocity change caused by locking the bolt is determined from:

$$(M_{FP} + M_B) v_{FP_7} = M_{FP} v_{FP_8} + I_{B5} \frac{K}{r} v_{FP_8}$$



$$v_{FP8} = \left(\frac{.40 + 0.148}{.40 + \frac{1.81 \times 6.10 \times 10^{-3}}{.203}} \right) 17.5$$

$$= 21.3 \text{ ft/sec}$$

The drive spring accelerates the firing pin through the one-inch dwell stroke, and the velocity at contact is,

$$\frac{1}{2} M_{FP} v_{FP8}^2 + \Delta E_S = \frac{1}{2} M_{FP} v_{FP9}^2$$

$$v_{FP9} = \sqrt{(21.3)^2 + \left(\frac{2 \times .53}{.39} \right)} 32.2$$

$$= 23.1 \text{ ft/sec}$$

The theoretical displacement-time curve which results from the preceeding firing pin velocity compilations after each event is determined by summing the time increments between events.

$$\Delta t = \frac{\Delta X}{\bar{v}_{FP}}$$

$$\bar{v}_{FP} = \frac{v_{FP1} + v_{FP1+1}}{2}$$

$$T = \sum \Delta t$$

where: Δt = time between cyclic events

\bar{v}_{FP} = average velocity between cyclic event

T = total cycle time

These equations were used to compute Table A-6 from which the T-D Curve of Figure A-6 was plotted. The resulting cycle was computed to be approximately 1,000 rounds per minute. This analysis did not include friction or any secondary velocity loss caused by the buffer.

TABLE A-6

Firing Pin Station (Inches)	Δx (Inches)	Firing Pin Velocity (FPS)	\bar{v}_{FP} (FPS)	Δt (MS)
0		0		3.12
	.75		20.4	
.75		40.9		.62
	.25		33.8	
1.00		27.0		8.72
	2.40		22.9	
3.40		18.7		12.30
	1.40		9.4	
4.80		0		25.30
	2.30		7.6	
2.50		15.2		6.90
	1.50		18.2	
1.00		21.3		3.70
	1.00		22.2	
0		23.1		

59.66 ms = 1000 rds/min

where: Δt = time between cyclic events

\bar{v}_{FP} = average velocity between cyclic event

T = total cycle time

These equations were used to compute Table A-6 from which the T-D Curve of Figure A-6 was plotted. The resulting cycle was computed to be approximately 1,000 rounds per minute. This analysis did not include friction or any secondary velocity loss caused by the buffer.

TABLE A-6

Firing Pin Station (Inches)	Δx (Inches)	Firing Pin Velocity (FPS)	\bar{v}_{FP} (FPS)	Δt (MS)
0		0		3.12
	.75		20.4	
.75		40.9		.62
	.25		33.8	
1.00		27.0		8.72
	2.40		22.9	
3.40		18.7		12.30
	1.40		9.4	
4.80		0		25.30
	2.30		7.6	
2.50		15.2		6.90
	1.50		18.2	
1.00		21.3		3.70
	1.00		22.2	
0		23.1		

59.66 ms = 1000 rds/min



Corporation

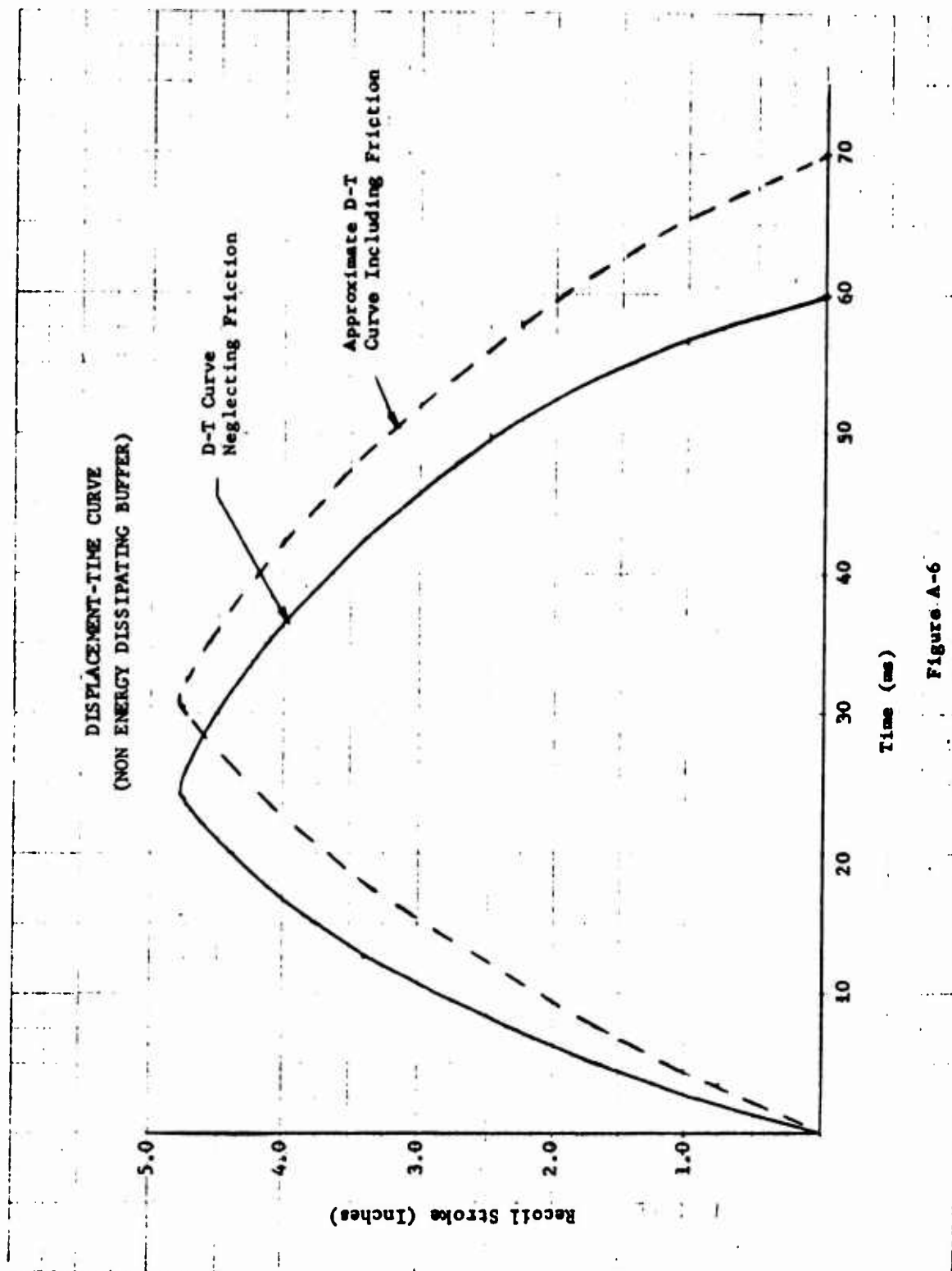


Figure A-6

In addition to an energy-absorbing buffer, the cycle time could be increased by slightly increasing the weight of the firing pin. Figure A-7 plotted from actual data taken with a non-energy dissipating buffer, shows how increasing the firing pin weight decreases the firing rate.

Firing Pin Weight (Lb.)	Maximum Recoil Velocity (FPS)	Cycle Time (NS)	Cycle Rate (Rds/Min)
.416	30.3	35.8	1675
.327	38.8	32.6	1840
.327	37.0	32.0	1875
.327	41.3	33.8	1775
.234	59.5	23.1	2600
.234	52.1	24.2	2480
.234	66.7	22.1	2720



Corporation

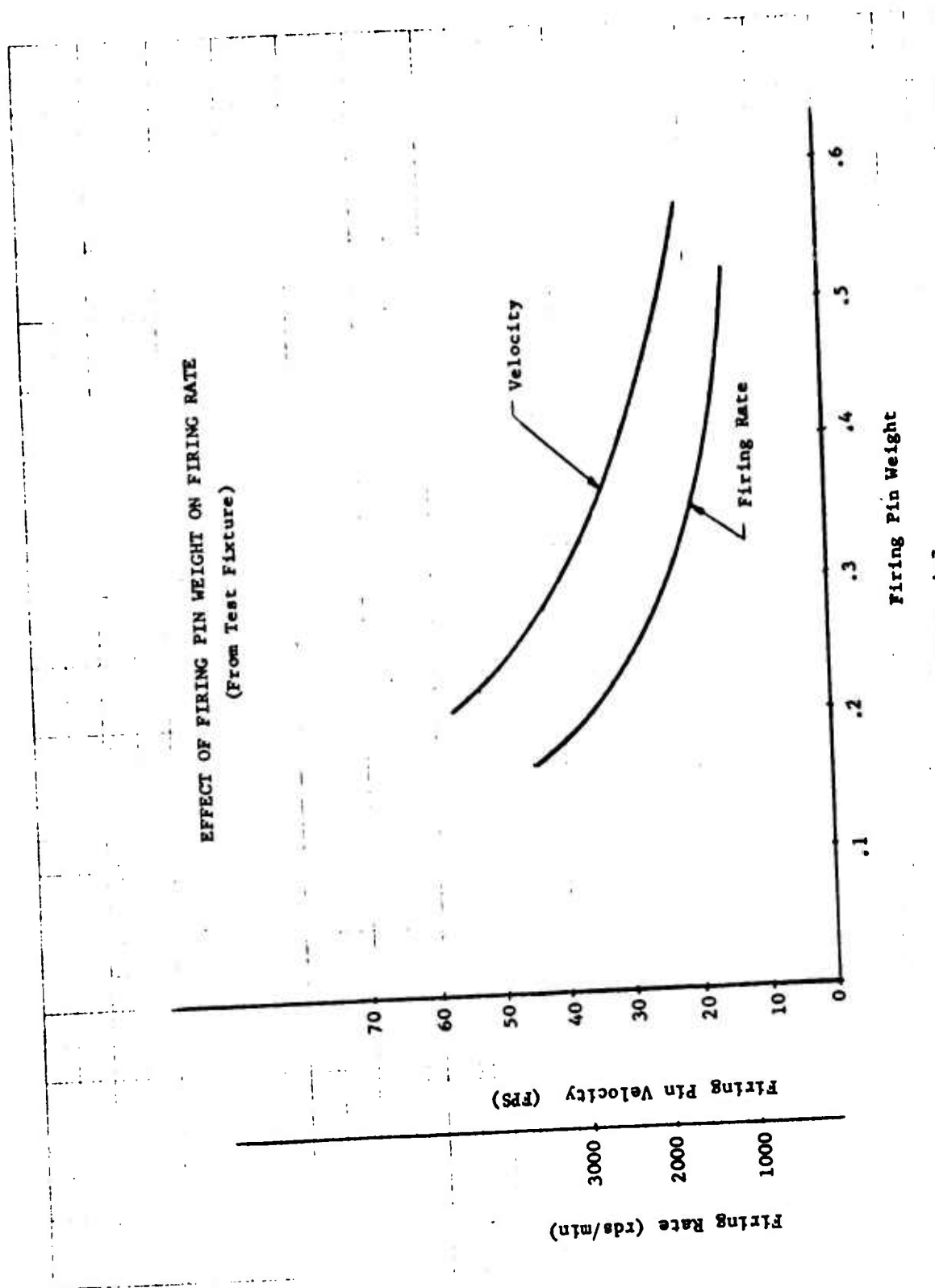


Figure A-7

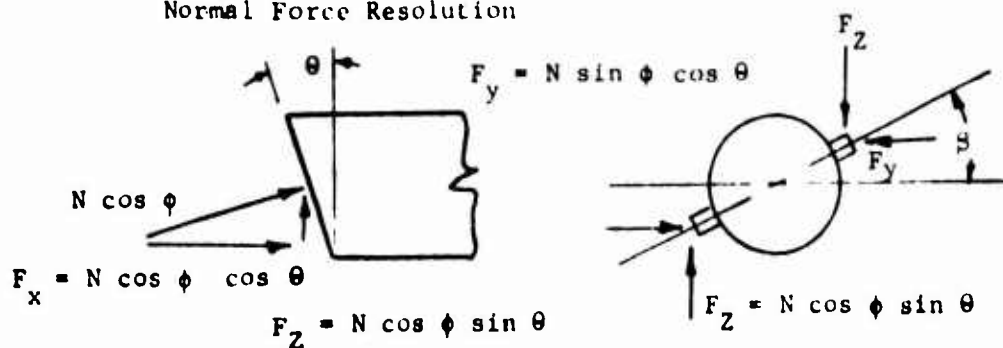
E. Stress Analysis

1. Load Reactions

The gas pressure acting on the bolt face area A results in a force F_p . This force is supplied at the face of the bolt sleeve and motion is restrained by the barrel extension engaging the bolt sleeve lugs. The torque transmitted through the angled bolt sleeve lugs is taken by the lugs of the firing pin.

Since the bolt sleeve lugs are canted at several angles, the normal and friction forces acting on the lug face were resolved in their various components and used as such.

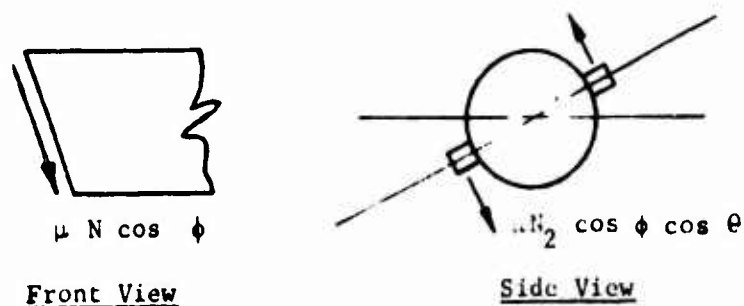
Normal Force Resolution



Front View

Side View

Friction Force Resolution:



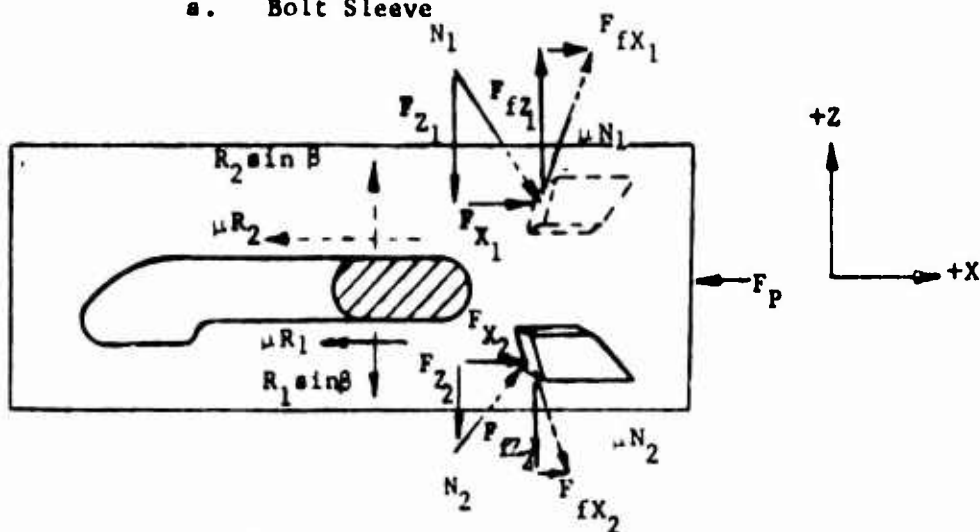
Front View

Side View



Corporation

a. Bolt Sleeve



Summing forces in the recoil, x, direction:

$$\Sigma F_X = 0 = F_{X1} + F_{fX1} + F_{X2} + F_{fX2} - \mu(R_1 + R_2) - F_p \quad (1)$$

$$\text{where: } F_{X1} = N_1 \cos \phi \cos \theta \quad (2)$$

$$F_{X2} = N_2 \cos \phi \cos \theta \quad (3)$$

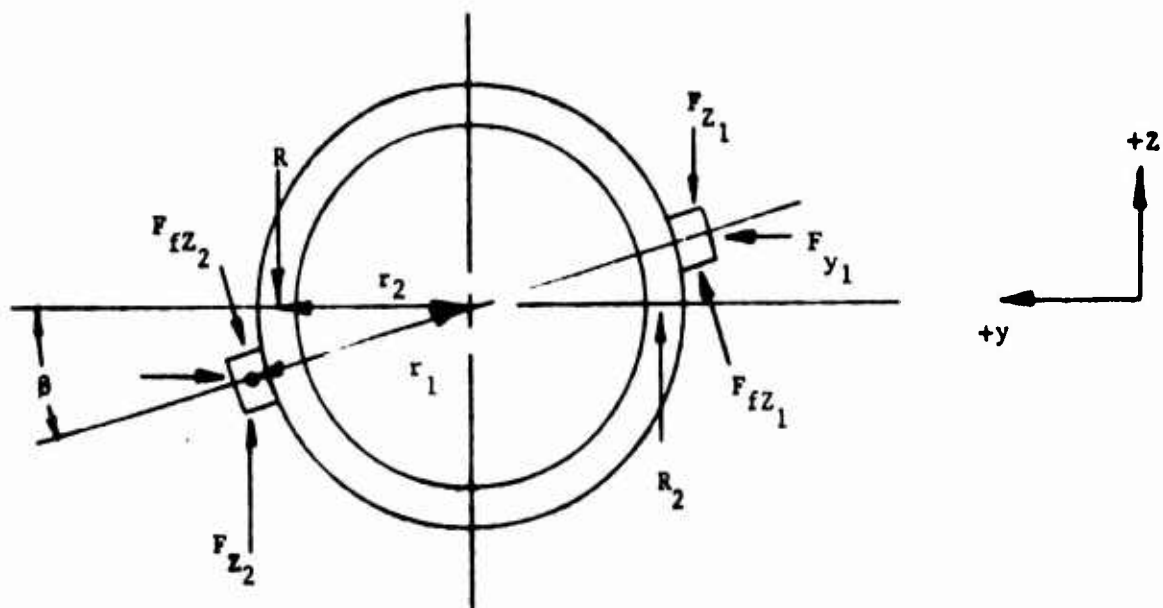
$$F_{fX1} = \mu N_1 \cos \phi \sin \theta \quad (4)$$

$$F_{fX2} = \mu N_2 \cos \phi \sin \theta \quad (5)$$

$$F_p = PA \quad (6)$$

and using equations (2) through (6), equation (1) becomes:

$$(N_1 + N_2) (\cos \phi \cos \theta + \mu \cos \phi \sin \theta) - \mu (R_1 + R_2) = PA \quad (7)$$



Summing forces in the Z direction:

$$\Sigma F_Z = 0 = R_3 - R_1 + F_{fz1} \cos \theta - F_{fz2} \cos \theta - F_{Z1} + F_{Z2} \quad (8)$$

where: $F_{Z1} = N_1 \cos \phi \sin \theta \quad (9)$

$$F_{Z2} = N_2 \cos \phi \sin \theta \quad (10)$$

$$F_{fz1} = \mu N_1 \cos \phi \cos \theta \quad (11)$$

$$F_{fz2} = \mu N_2 \cos \phi \cos \theta \quad (12)$$

$$(R_2 - R_1) + (N_1 - N_2)(\mu \cos \theta \cos \theta - \cos \phi \sin \theta \cos \phi) = 0 \quad (13)$$



Corporation

Summing forces in the y direction:

$$\Sigma F_y = 0 = F_{y1} - F_{y2} + F_{fz1} \sin \beta - F_{fz2} \sin \beta \quad (14)$$

where: $F_{y1} = N_1 \cos \theta \sin \phi \quad (15)$

$$F_{y2} = N_2 \cos \theta \sin \phi \quad (16)$$

$$\therefore N_1 = N_2 \quad (17)$$

$$\therefore R_1 = R_2 \quad (18)$$

Summing the torques about the bolt sleeve center O

$$\Sigma T_O = 0 = (R_1 + R_2)r_2 + (F_{fz2} + F_{y2} \sin \beta - F_{z2} \cos \beta + F_{fz1} + F_{y1} \sin \beta - F_{z1} \cos \beta)r_1 \quad (19)$$

and using equations (17) and (18):

$$R_1 \frac{r_2}{r_1} + N_1 (\mu \cos \theta \cos \beta \cos \phi \cos \theta \sin \phi \sin \beta - \cos \phi \sin \theta \cos \beta) = 0 \quad (20)$$

Again using equations (17) and (18) equation (7) becomes:

$$\mu R_1 + N_1 (\cos \phi \cos \theta + \mu \cos \beta \sin \theta) = PA/2 \quad (21)$$

Solving equations (20) and (21) simultaneously

$$R_1 = \frac{\begin{vmatrix} 0 & K_1 \\ PA/2 & K_2 \end{vmatrix}}{\Delta} = -\frac{PAK_1}{2\Delta} \quad (22)$$

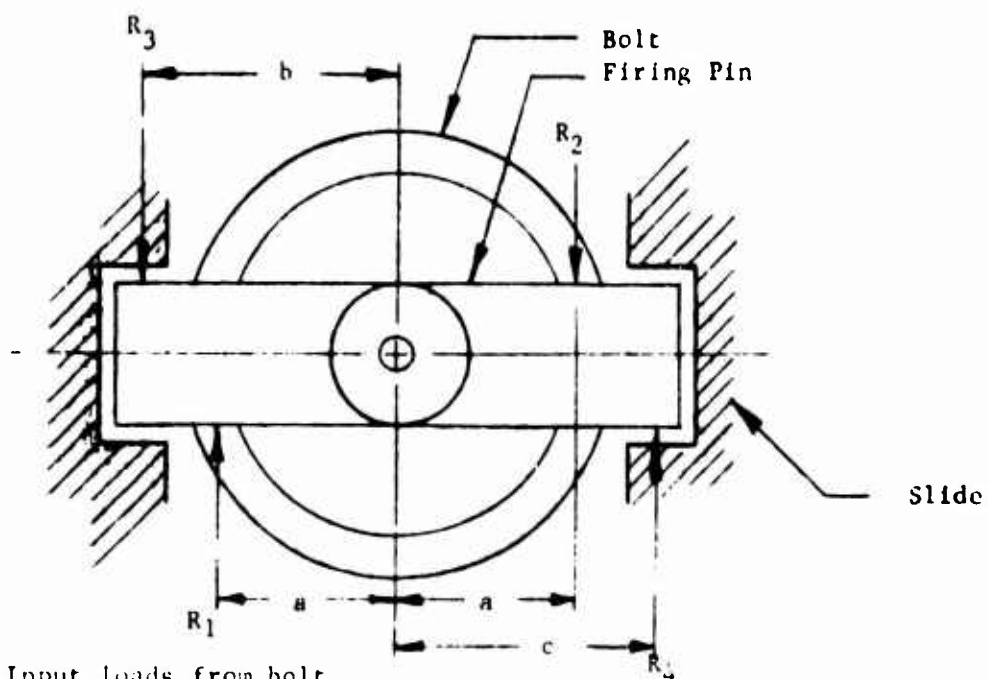
where:

$$\Delta = \begin{vmatrix} \frac{r_2}{r_1} & K_1 \\ \mu & K_2 \end{vmatrix} = \frac{r_2}{r_1} K_2 - \mu K_1 \quad (23)$$

$$K_1 = \cos \theta \cos \beta \cos \phi + \cos \theta \sin \phi \sin \beta - \cos \theta \cos \beta \sin \theta \quad (24)$$

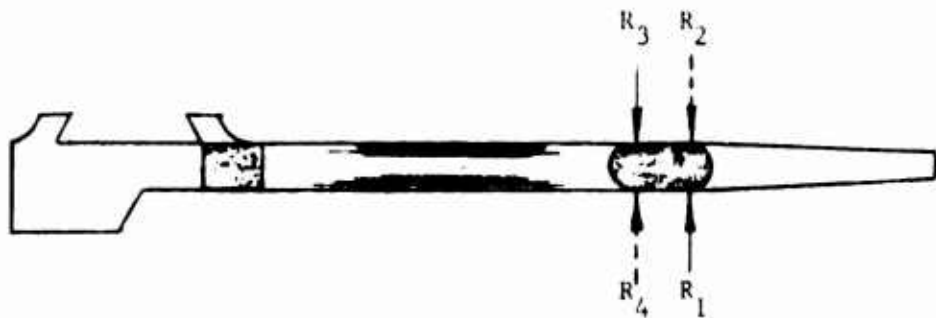
$$K_2 = \cos \phi \cos \theta + \mu \cos \beta \sin \theta \quad (25)$$

b. Firing Pin



$R_1 = R_2$ = Input loads from bolt

$R_3 = R_4$ = Reaction loads on firing pin lugs



$$\sum M_O = 0 = 2R_1 a - R_3 b - R_4 c$$

$$\sum F_z = 0 = R_1 - R_2 + R_3 - R_4$$

$$\therefore R_3 = R_4 \quad (26)$$

$$R_3(b+c) = 2aR_1$$

$$R_3 = R_4 = \left(\frac{2a}{b+c}\right) R_1 \quad (27)$$



c. Load Reaction Calculations

Using the following list of parametric values, the reaction R_1 is computed.

$$A = \frac{\pi}{4} (\overline{.370}^2 - \overline{.150}^2) = .0894 \text{ in}^2$$

$$\phi = 5^\circ \quad a = r_1 = .25''$$

$$\theta = 18.5^\circ \quad b = c = r_2 = .327''$$

$$\beta = 26^\circ$$

$$\alpha = 0.2$$

$$K_1 = -.076 \quad \text{Equation (24)}$$

$$K_2 = 1.002 \quad \text{Equation (25)}$$

$$\Delta = \frac{.25}{.327} (1.002) + 0.2(-.076) = 0.75 \quad \text{Equation (23)}$$

$$R_1 = \frac{-PAK_1}{2} = \frac{-(.0894)(-.076)}{2(0.75)} P = .00451P$$

$$R_3 = \left(\frac{2a}{b+c} \right) R_1 = \left(\frac{2 \times .25}{2 \times .327} \right) .00451P = .00344P$$

Using the overpressure of 80,000 psi, the resulting reaction forces are:

$$R_1 = R_2 = 360 \text{ lbs.}$$

$$R_3 = R_4 = 275 \text{ lbs.}$$

2. Bolt and Firing Pin Stress Analysis.

The stresses developed in the bolt and firing as a result of the input loads computed in Part 1. of this Section are investigated to determine the structural integrity of bolt and firing pin. The material used in both parts is Maraging Steel, 18% Nickel Series 300 and the allowable stress levels are:

Ultimate	$S_u = 286,000 \text{ psi}$
Yield Tension	$S_y = 280,000 \text{ psi}$
Shear	$S_s = 170,000 \text{ psi}$
Bearing Yield	$S_{br} = 400,000 \text{ psi}$

a. Firing Pin

The firing pin first feels the pressure force acting on the recoiling thrust area A_{FP} . The force developed is

$$F_{FP} = PA_{FP}$$

and the bearing stress is

$$S_{br} = \frac{F_{FP}}{A_{FP}} = 80,000 \text{ psi}$$

Therefore, the margin of safety is

$$MS = \frac{400,000}{80,000} - 1 = 4.0$$

A torsion load is applied to the firing pin through the firing pin lugs. The resulting shear stress is determined from

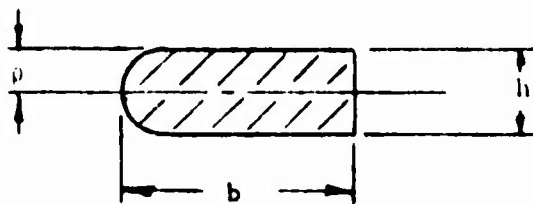
$$S_s = \frac{T \rho}{J}$$



Corporation

where: T = torque load in-lb
 ρ = half width of lug in
 J = polar moment of inertia in⁴

The firing pin lug cross-section is



$$J = 1/12 (bh^3 + hb^3)$$

$$J = 9.6 \times 10^{-4} \text{ in}^4$$

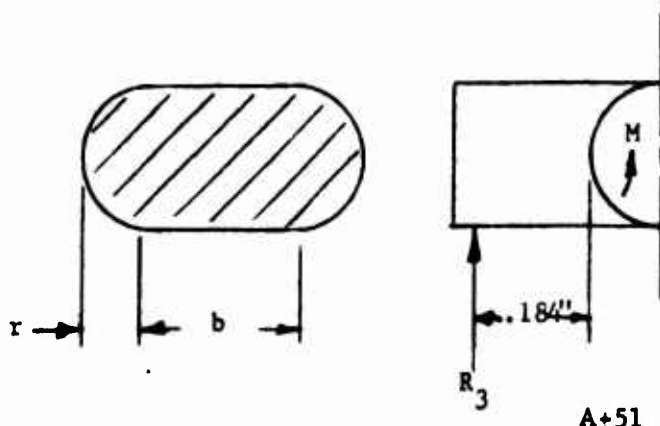
$$T = 2r_1 R_3 = 2(.359)(275) = 198 \text{ in-lb.}$$

$$S_s = \frac{198 \times .125}{9.6 \times 10^{-4}} = 24,800 \text{ psi}$$

and the margin of safety is

$$MS = \frac{170,000}{24,800} - 1 = 5.85$$

The shear and bending stresses in the firing pin lugs caused by the reaction force R_3 and R_4 are computed below.



$$A = bh + \pi r^2 = .0625 \text{ in}^2$$

$$I = \frac{bh^3}{12} + \frac{\pi r^4}{4} = .000167 \text{ in}^4$$

$$S_s = \frac{R_3}{A} = \frac{275}{.0625} = 4400 \text{ psi}$$

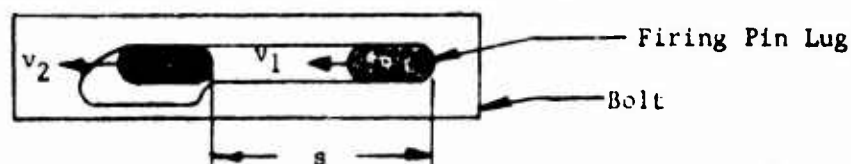
$$S_B = \frac{Mc}{I} = \frac{(275 \times .184)(.095)}{.000167} = 28,800 \text{ psi}$$

The margins of safety are computed to be

$$MS = \frac{170,000}{4,400} - 1 = 37.6 \quad (\text{Shear})$$

$$MS = \frac{280,000}{28,000} - 1 = 8.72 \quad (\text{Be})$$

The load developed in the firing pin coming lug impacting the bolt cam surface during unlock is determined below.



$$v_2^2 - v_1^2 = 2as \quad (\text{neglecting friction})$$

$$a = \frac{(37.7)^2}{2 \times .75/12} = 11300 \text{ ft/sec/sec}$$

Therefore, the inertial load developed is

$$F = ma = .0084 \times 11300 = 95 \text{ lbs.}$$

and the resulting stresses are:

$$S_s = \frac{P}{A} = \frac{95}{.190 \times .30} = 1670 \text{ psi}$$

$$S_B = \frac{(95 \times .184)(.150)}{1/12 (.190)(.30)^3} = 6180 \text{ psi}$$

Neither of these stresses are critical.



Corporation

b. Bolt Sleeve

Due to the high recoil velocity of the firing pin, the bolt experiences a large angular acceleration when unlocking occurs. The angular acceleration is determined from:

$$\alpha = \frac{dw}{dt} = \frac{d^2\theta}{dt^2}$$

and assuming the angular rotation of the bolt is defined as

$$\theta = Kx^2$$

then

$$\alpha = 2Kx\dot{x} + 2K(\dot{x})^2$$

The angular acceleration α is computed by approximating the translational velocity and acceleration of the firing pin.

$$\dot{x} = \frac{v_{FP1} + v_{FP2}}{2} = \frac{37.7 + 29.8}{2} = 33.7 \text{ fps}$$

$$\ddot{x} = a_{FP} = \frac{v_{FP1}^2 - v_{FP2}^2}{2S} = \frac{37.7^2 - 29.8^2}{2 \times .75/12} = 4270 \text{ ft/sec}^2$$

$$K = \frac{\theta}{x^2} = \frac{26 \times \frac{\pi}{180}}{(.25)^2} = 7.24 \text{ rad/in}^2$$

$$\therefore \alpha = 2 \times 7.24 [4270 + (33.7)^2] = 7.82 \times 10^4 \text{ rad/sec}^2$$

The inertial force of bolt during unlocking is

$$\begin{aligned} F_B &= m_B \alpha r_l \\ &= .00311 (7.82 \times 10^4) \left(\frac{.359}{12} \right) = 7.46 \text{ lb.} \end{aligned}$$

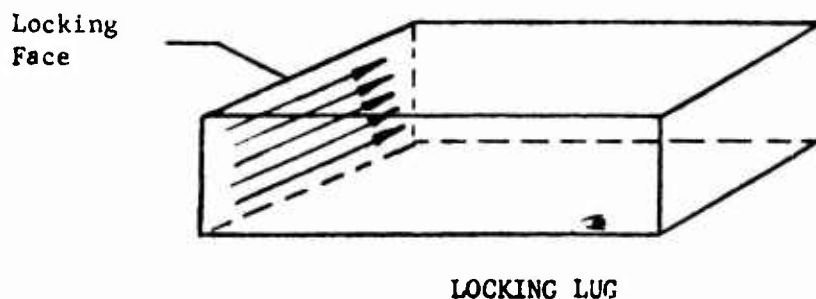
The small magnitude of this force reveals that no critical stresses are developed in the bolt as a result of the rotational inertial force. The locking lugs on the bolt experience the most severe loads. The loads and stresses developed in the bolt locking lugs are analyzed as follows:

Bearing Stress

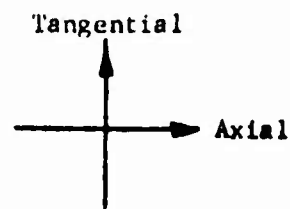
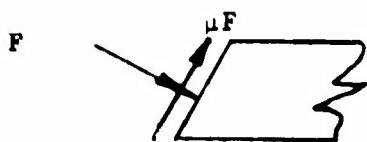
$$\begin{aligned} S_{br} &= \frac{F_p}{A_{LUGS}} = \frac{80,000 \times \frac{1}{4} (.370^2 - .150^2)}{2 \cos 18.5^\circ (.190 \times .156)} \\ &= 127,000 \text{ psi} \end{aligned}$$

$$MS = \frac{400,000}{127,000} - 1 = 2.15$$

Shear Stress



The locking lug experiences shearing force in two directions, axial and tangential.



$$F_p = PA = 7150 \text{ lbs.}$$

$$F = \frac{F_p}{\cos 18.5} = 7550 \text{ lbs.}$$

$$\begin{aligned} F_{\text{AXIAL}} &= 1/2 \left[F_p \tan 18.5 + \mu F_p \right] \\ &= 1/2 \left[7150 \times .355 + 0.2 \times 7150 \right] = 1910 \text{ lbs} \end{aligned}$$

$$\begin{aligned} F_{\text{TANG.}} &= 1/2 \left[F \cos 18.5 - \mu F \sin 18.5 \right] \\ &= 1/2 \cdot 7550 \left[.948 - 0.2 \times .317 \right] = 3340 \text{ lbs.} \end{aligned}$$

Since the tangential force is the most critical, the shear stress developed in the tangential direction is

$$S_{S_{TANG.}} = \frac{F_{TANG.}}{A}$$

$$= \frac{3340}{(.190 \times .769)(.900)} = 25,500 \text{ psi}$$

$$MS = \frac{170,000}{25,500} - 1 = 5.67$$

The load caused by the firing fin lug impacting the bolt during unlocking is determined by equating the strain energy of the bolt to the rotational energy of the bolt being unlocked.

$$E_R = 1/2 I_B \omega^2$$

$$U = \int_0^L \frac{T^2 dx}{2GJ} = \frac{T^2 L}{2GJ}$$

$$E_K = U$$

$$T = \sqrt{\frac{2 E_K GJ}{L}}$$

where: I_B = mass moment of inertia of bolt
 ω = rotational velocity of bolt
 T = torque
 L = length of bolt

Units
 slugs-ft²
 rad/sec
 in-lbs
 ft



Corporation

	<u>Units</u>
G = modulus of rigidity	psi
J = polar moment of inertia of bolt	in ⁴
E _K = rotational energy of bolt	ft-lbs
U = strain energy of bolt	ft-lbs

$$I_B = M_B r^2 = .0031 \times \left(\frac{.203}{12}\right)^2 = 8.9 \times 10^{-7} \text{ slugs-ft}^2$$

$$\omega = 2K\dot{x} = 2(7.24)(.208)(33.7 \times 12) = 1220 \frac{\text{rad}}{\text{sec}}$$

$$E_K = 1/2 (8.9 \times 10^{-7})(1220)^2 = .658 \text{ ft-lb}$$

$$J = 1/2 \pi (r^4 - r_i^4) = \frac{\pi}{2 \times 16} \left[(.562)^2 - (.250)^2 \right] 0.7$$
$$= .0065 \text{ in}^4$$

$$G = 11.5 \times 10^6 \text{ (Steel)}$$

$$\therefore T = \sqrt{\frac{2(.658)(11.5 \times 10^6)(.0065)}{1.87/12}}$$

$$= 795 \text{ in-lb}$$

The shear stress which results from the torque load
calculated above is,

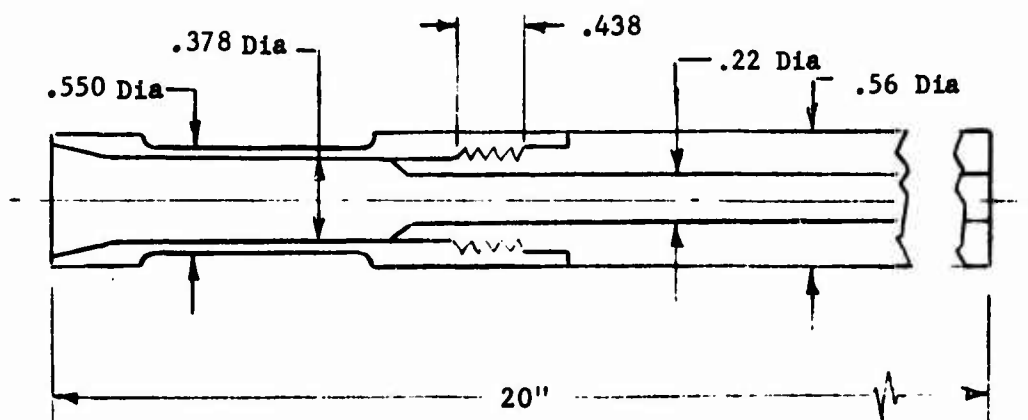
$$S_s = \frac{T \rho}{J}$$
$$= \frac{795 \times .203}{.0065} = 24,800 \text{ psi}$$

$$MS = \frac{170,000}{24,800} - 1 = 5.85$$

Therefore, it can be seen that the critical components of the
weapon have stress levels low enough to ensure a life of 10,000 cycles.

3. Barrel Analysis

The gun barrel is analyzed for an assumed proof pressure curve which exhibits a peak pressure of 80,000 psi. Using a peak average service pressure of 60,000 psi, the high pressure proof round with heating effects and overpressure factors becomes 80,000 psi. The present configuration is shown below.



The maximum stress developed in any section of the gun barrel due to the gas pressure is determined from the following equation.

$$S = P_1 \left[\frac{\left(\frac{b}{a}\right)^2 + 1}{\left(\frac{b}{a}\right)^2 - 1} \right]$$

where:

- a = inside radius of barrel section
- b = outside radius of barrel section
- P_1 = internal gas pressure
- S = hoop stress

The stress level as a function of travel along the barrel is plotted in Figure A-8.

The maximum stress occurs in the chamber section and is,

$$S_{\max} = 80,000 \frac{\left(\frac{.275}{.189}\right)^2 + 1}{\left(\frac{.275}{.189}\right)^2 - 1}$$

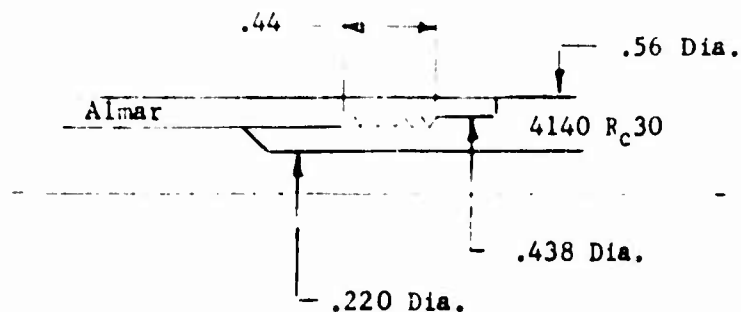
$$= 225,000 \text{ psi}$$

The material is Maraging Steel, 18% Nickel with a yield stress of 280,000 psi. Therefore, the margin of safety is,

$$M.S. = \frac{280,000}{225,000} - 1 = .25$$

The thin steel chamber is necessary to allow heat to flow rapidly into the 6101-T6 aluminum heat sink.

In addition to the circumferential stresses, the gas pressure tends to shear the threads connecting the barrel extension and barrel. The shear stress for the proof pressure is found as follows:





Corporation

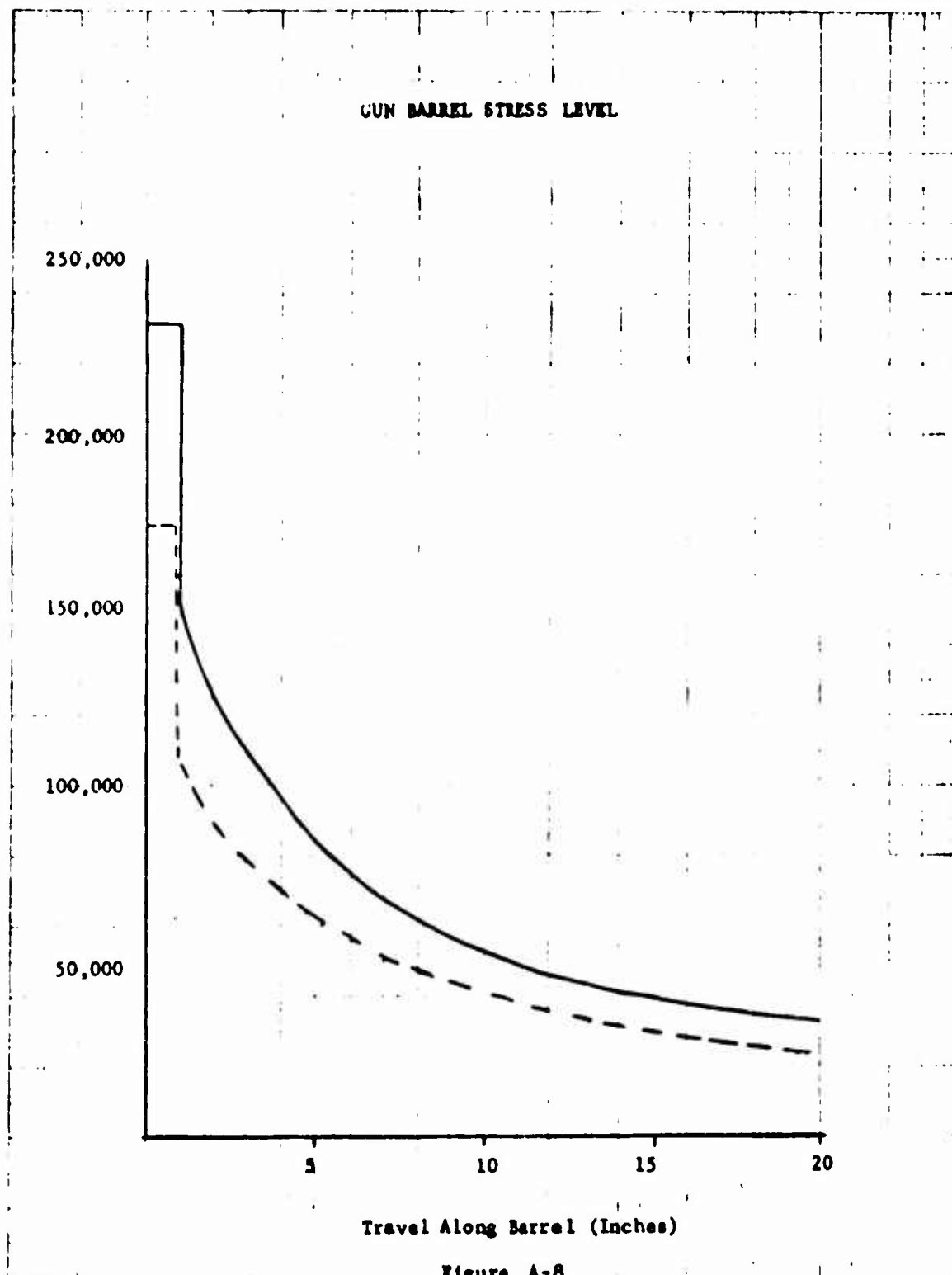


Figure A-8

$$\begin{aligned}
 S_s &= \frac{P \frac{\pi}{4} [D_o^2 - D_i^2]}{\pi D L} \\
 &= \frac{80,000 \frac{\pi}{4} [.438^2 - .220^2]}{.5 \times \pi \times .391 \times .422} \\
 &= \frac{80,000 [.1507 - .0380]}{.259} \\
 &= 34,800 \text{ psi}
 \end{aligned}$$

The margin of safety is,

$$M.S. = \frac{85,000}{34,800} - 1 = 1.44$$

The margin of safety for the proof round is,

$$M.S. = \frac{255,000}{170,000} - 1 = .5$$

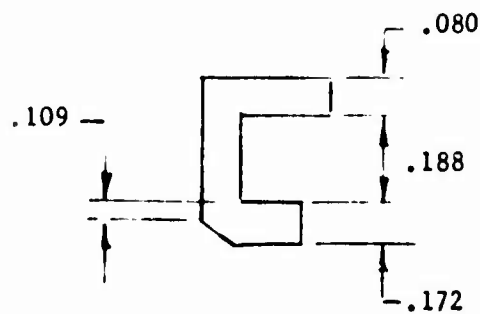
Receiver

The neutral axis of the receiver is:

$$\bar{y} = .085 \text{ in.}$$

The bending moment of inertia is,

$$I = 1.91 \times 10^{-4} \text{ in.}^4$$





Corporation

The bending moment for the proof round is,

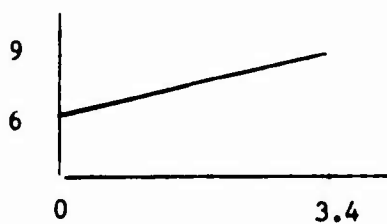
$$M = 176 \text{ in-lb}$$

Using these values, the maximum combined stress is,

$$\begin{aligned} S &= \frac{mc}{I} + \frac{F}{A} \\ &= \frac{176 \times .103}{1.91 \times 10^{-4}} + \frac{4120}{.0545} \\ &= 170,000 \text{ psi} \end{aligned}$$

4. Drive Spring Analyses

The drive spring presently employed exhibits the following force-stroke curve.



The spring rate K is determined to be,

$$K = \frac{F_2 - F_1}{\Delta L} = \frac{3}{3.4} = .88 \text{ lb/in}$$

The preload deflection is,

$$x = \frac{8}{1.17} = \frac{6}{.88} = 6.80 \text{ in.}$$

The free length is,

$$F.L. = 8.35 + 6.80 = 15.15 \text{ in}$$

The maximum possible force is when the spring is compressed to 3.4 inches.

The deflection is,

$$15.15 - 4.10 = 11.75 \text{ in.}$$

The force at this deflection is,

$$F = Kx = (.88)(11.75) = 10.35$$

The maximum shear stress is

$$\begin{aligned} S_s &= \frac{8FD}{\pi d^3} \quad f s \\ &= \frac{(8)(10.35)(.390)(1.2)}{\pi (.047)^3} \\ &= 118,000 \text{ psi} \end{aligned}$$



Corporation

STRESS SUMMARY AND LIFE EXPECTANCY

PART	MAXIMUM STRESS AT 60,000 PSI OPERATING PRESSURE	MATERIAL	LIFE EXPECTANCY (Cycles)
Chamber	$S_h = 167,000$	18% Nickel Maraging Steel	8×10^4
Barrel	$S_h = 82,000$	4140, RC30	Infinite
Chamber-Barrel Threads	$S_s = 26,000$	4140, RC30	Infinite
Receiver Sides	$S_b = 132,000$	18% Nickel Maraging Steel	5×10^5
Bolt Lugs	$S_{br} = 127,000$	18% Nickel Maraging Steel	5×10^5
Firing Spring	$S_s = 118,000$	National Standard N.S.355	1×10^6
Firing Pin	$S_{br} = 80,000$	18% Nickel Maraging Steel	Infinite

F. Weight Analysis

1. Total Weight of Weapon

The following is the most recent weight analyses for the AAI concept of the Individual Shoulder Fired Weapon capable of firing caseless ammunition.

TABLE A-7

<u>COMPONENT</u>	<u>WEIGHT IN POUNDS</u>
Plastic Stock Assembly	1.30
Bolt and Firing Pin	.34
Barrel and Receiver	1.52
Drive Spring and Slide Assembly	.33
Trigger Group	.38
Flash Suppressor	.22
Buffer Assembly	.24
Magazine, 20 round	.16
Sling, Light Weight	.15
Heat Sink	.60
Foregrip	.40
Ejector	.08
Empty Weight - - - - -	5.72
20 each 5.56mm Cartridges	.24
Loaded Weight - - - - -	5.96

2. Center of Gravity of Weapon

The following analysis was used to determine the center of gravity of the loaded weapon.

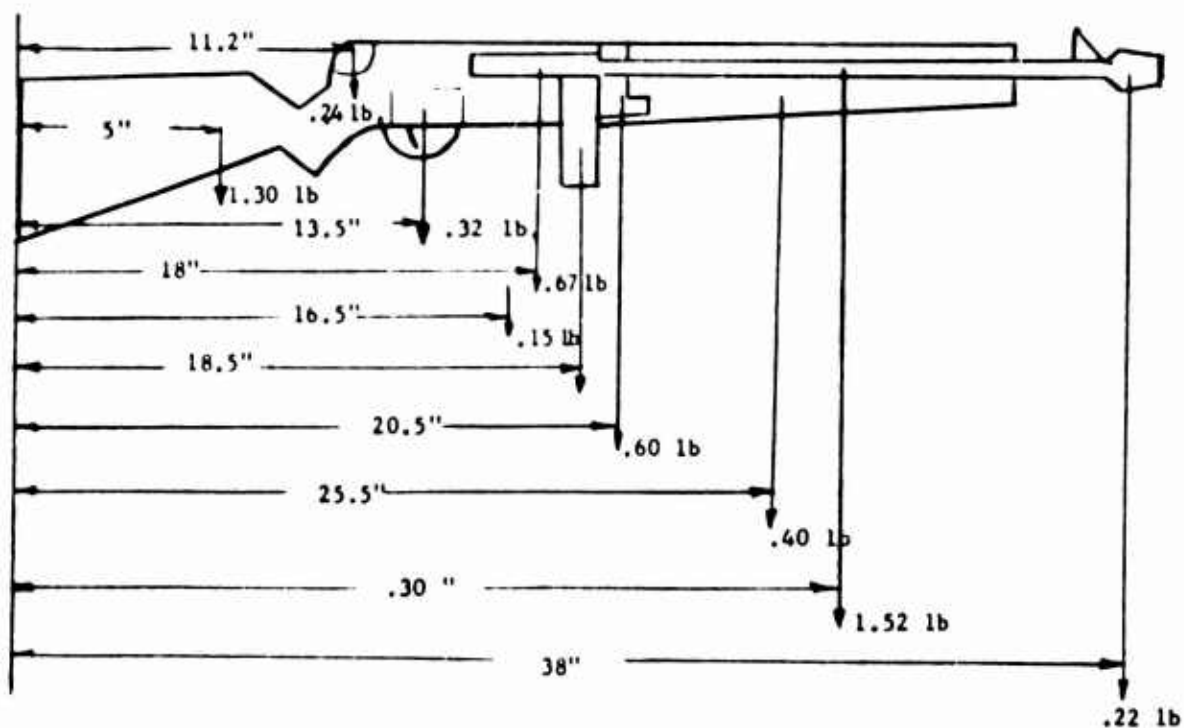


Figure A-9

$$C.G. = \frac{\Sigma ML}{\Sigma M}$$

$$\begin{aligned}
 &= (130)(15) + (.24)(11.2) + (.38)(13.5) + (.67)(18) \\
 &\quad + (.15)(16.5) + (.40)(18.5) + (.60)(20.5) + (.40)(25.5) \\
 &\quad + (1.52)(30) + (.22)(38) \\
 &\quad \underline{\hspace{10em}} \\
 &\quad \quad \quad 5.96
 \end{aligned}$$

$$= \frac{112.58}{5.96}$$

$$= 18.8 \text{ inches from back}$$